

UC Santa Barbara

UC Santa Barbara Electronic Theses and Dissertations

Title

Activation of a Type VI Secretion System Phospholipase Effector via Immunity-dependent Advanced Glycation End-product Crosslinking

Permalink

<https://escholarship.org/uc/item/9z18j6q4>

Author

Jensen, Steven James

Publication Date

2024

Peer reviewed|Thesis/dissertation

UNIVERSITY OF CALIFORNIA

Santa Barbara

Activation of a Type VI Secretion System Phospholipase Effector via
Immunity-dependent Advanced Glycation End-product Crosslinking

A dissertation submitted in partial satisfaction of the
requirements for the degree Doctor of Philosophy
in Molecular, Cellular, and Developmental Biology

by

Steven James Jensen

Committee in charge:

Professor Christopher S. Hayes, Chair

Professor David Low

Professor Chris Richardson

September 2024

The dissertation of Steven James Jensen is approved.

David Low

Chris Richardson

Christopher S. Hayes, Committee Chair

September 2024

Activation of a Type VI Secretion System Phospholipase Effector via
Immunity-dependent Advanced Glycation End-product Crosslinking

Copyright © 2024

By

Steven James Jensen

Acknowledgements

I would like to express my gratitude to those who supported me over the course of earning my doctorate degree, as I certainly could not have done it alone. I would first like to thank my advisor, Chris Hayes, for his continued guidance during my time in his lab. Chris provided scientific expertise and ingenuity that helped me clear numerous obstacles in my research, but also showed patience with me during the times where I did end up running into pitfalls. Our shared enthusiasm for basic research fueled this project in its early stages and I think we are both thrilled with the results. I would also like to thank the current and former members of my committee, David Low, Chris Richardson, and Carolina Arias, for their advice and encouragement.

I would also like to offer my thanks to all the current and former members of the Hayes lab. Sonya Donato was my mentor when I first joined the lab and continued to be an exemplary scientist and dependable source of advice. Zachary Ruhe, whose initial experiments served as the foundation of this dissertation, was very cooperative as I began to get involved with this project. Kiho Song, my benchmate for the first two years, might just be the friendliest neighbor I will ever have. Micheal Costello was always willing to talk shop, thanks to his passion for science that is second only to Chris. I consider Quan Nhan to be my lab brother, not just for his kindness and dependability, but because of our esoteric conversations about TV shows and video games. Fernando 'Docty' Garza-Sánchez is someone who I cannot thank enough. Docty was always willing to offer his advice, reagents, and even his

hands with experiments. But most importantly he was my fellow night owl in the lab, and I appreciate him keeping me company over the years. I would also like to thank the bright and eager undergraduate assistants that I got to work with: Cole Costello, Kristen Barlow, Drue Wigton, Joyce Kwan, and Lizhen Chen.

I finally want to thank my family for their love and support that helped me throughout graduate school. Even after nearly nine years you kept the needling over finishing to a minimum, and I am very appreciative of that.

Vita of Steven James Jensen

Education

PhD in Molecular, Cellular, and Developmental Biology 2015-Present

University of California, Santa Barbara, CA

GPA: 3.99/4.00

Bachelor of Science in Biochemistry 2010-2014

California Polytechnic State University, San Luis Obispo, CA

GPA: 3.89/4.00

Research Experience

Graduate Student Researcher 2016-Present

University of California, Santa Barbara

Department of Molecular, Cellular, and Developmental Biology

Advisor: Christopher Hayes

- Used genetic engineering and biochemical assays to identify activation of a bacterial phospholipase required the formation of an advanced glycation end product (AGE) cross-link
- Purified proteins with introduced disulfide bonds via oxidative refolding, then assessed disulfide formation via SDS-PAGE and activity assays
- Assessed Type VI Secretion System (T6SS) activity of *Enterobacter cloacae* mutants via fluorescence microscopy and co-culture growth competition

Undergraduate Student Researcher 2013-2014

California Polytechnic State University, San Luis Obispo, CA

Advisor: Kenneth Hillers

- Produced mutant yeast strains via electroporation transformation, selective mating, and tetrad dissection

Publications

1) Jensen SJ, Cuthbert BJ, Garza-Sánchez F, Goulding CW, Hayes CS. Advanced glycation end product (AGE) crosslinking as a bona fide post-translational modification. *Under review*.

2) Jensen SJ, Ruhe ZC, Williams AF, Nhan DQ, Garza-Sánchez F, Low DA, Hayes CS. Paradoxical Activation of a Type VI Secretion System Phospholipase Effector by Its Cognate Immunity Protein. *J Bacteriol.* 2023 Jun 27;205(6):e0011323
PMCID: PMC10294671.

3) Donato SL, Beck CM, Garza-Sánchez F, **Jensen SJ**, Ruhe ZC, Cunningham DA, Singleton I, Low DA, Hayes CS. The β -encapsulation cage of rearrangement hotspot (Rhs) effectors is required for type VI secretion. *Proc Natl Acad Sci U S A*. 2020 Dec 29;117(52):33540-33548. PMID: PMC7777165.

Honors and Awards

Graduate

- Storke Award for Highest GPA in 1st year courses (2015-2016)
- Doctoral Student Travel Grant (2022)

Undergraduate

- Senior Recognition Award: Outstanding Biochemistry Major (2013-2014)
- Dean's List (11 quarters)

Presentations

Oral: **Jensen SJ** and Hayes CS. "Intramolecular Methylglyoxal Cross-Linking Activates a Type VI Secretion System Lipase Effector Protein"
Molecular Genetics of Bacteria and Phage Meeting. Madison, WI, August 2022.

Poster: **Jensen SJ et al.** "Activation of a Bacterial Phospholipase via AGE cross-linking"
Molecular Genetics of Bacteria and Phage Meeting. Madison, WI, August 2024.

Poster: **Jensen SJ** and Hayes CS. "A Type VI Secretion System immunity protein is required for delivery of its cognate lipase effector in *Enterobacter cloacae*"
Molecular Genetics of Bacteria and Phage Meeting. Madison, WI, August 2019.

Teaching Experience

Teaching Assistant University of California, Santa Barbara

- | | |
|---|------------------|
| • Microbiology Lab (MCDB131L) | Fall 2019-2022 |
| • Bacterial Genetics (MCDB101A) | Winter 2017-2021 |
| • Microbiology (MCDB131) | Fall 2018 |
| • Introduction of Biology Lab (MCDB1AL) | Fall 2015 |

Abstract

Activation of a Type VI Secretion System Phospholipase Effector via
Immunity-dependent Advanced Glycation End-product Crosslinking
by

Steven James Jensen

Bacteria employ various mechanisms to inhibit the growth of competitors in their environment. One example of this is the Type VI secretion system (T6SS), a multiprotein nanomachine that propels a spear-like structure to pierce the envelopes of adjacent target cells and enable delivery of toxic T6SS-associated effector proteins. Many T6SS-deploying bacteria utilize Type VI lipase effector (Tle) proteins to destabilize the phospholipid bilayers of target cells, while simultaneously synthesizing Type VI lipase immunity (Tli) proteins to neutralize Tle delivered from kin.

My thesis focuses on a Tle-Tli pair from the coliform species *Enterobacter cloacae*. In Chapter II, I show that Tle is inactive when delivered by inhibitor cells that do not express its cognate Tli protein. This is the first described instance of a T6SS effector that is activated by its immunity protein. I present further data in Chapter III showing that the nature of this activation is a cross-link that forms when a specific arginine-lysine pair within Tle reacts with the alpha-dicarbonyl compound methylglyoxal. The resulting cross-link is an example of an advanced glycation end-product (AGE). The

formation of AGEs in proteins is known to be a slow, spontaneous process and has previously been associated with numerous degenerative diseases including atherosclerosis and type 2 diabetes. In Chapter IV, I show evidence that similar activation mechanisms occur in Tle homologs from *Serratia marcescens* and *Dickeya dadantii*. The AGE crosslink responsible for activating Tle forms with a speed and specificity that is atypical for these reactions and is the first example of an AGE structure being necessary for protein function. Therefore, the Tli-dependent activation of Tle in *E. cloacae* and its homologs may serve to deepen the current understanding of AGEs.

TABLE OF CONTENTS

Chapter I: Introduction	1
A. Structure and mechanism of the T6SS.....	1
B. T6SS Regulation.....	3
C. T6SS Effectors and Immunity proteins.....	5
D. Phospholipase A Activity and Structure.....	8
E. Type VI Lipase Effectors (Tles).....	9
F. Figures.....	12
Chapter II: Paradoxical Activation of a Type VI Secretion System	
Phospholipase Effector by Its Cognate Immunity Protein	14
A. Introduction.....	15
B. Results.....	18
C. Discussion.....	24
D. Acknowledgements.....	30
E. Materials and Methods.....	31
F. Figures and Tables.....	39
Chapter III: Advanced Glycation End-product (AGE) Crosslinking Activates a	
Type 6 Secretion System Phospholipase Effector Protein	60
A. Introduction.....	61
B. Results.....	62

C. Discussion.....	72
D. Acknowledgements.....	75
E. Materials and Methods.....	76
F. Figures and Tables.....	87
Chapter IV: Chapter IV: Characterization of ECL Tle-Tli homologs.....	106
A. Introduction.....	106
B. Results.....	108
C. Discussion.....	112
D. Materials and Methods.....	116
E. Figures and Tables.....	120
Chapter V: Concluding Remarks.....	129
References.....	131

Chapter I: Introduction

Bacteria must adjust and respond to various environmental stresses to thrive. One such obstacle is the presence of other bacterial species competing for limited resources. In response bacteria have evolved various mechanisms to inhibit the growth of competitors in their vicinity. The Type VI secretion system (T6SS) is a multiprotein nanomachine that propels a spear-like structure with enough force to pierce the membranes of cells immediately adjacent to the secreting cell (Cherrak et al., 2019). This allows for the direct transfer of toxic effector proteins into recipient 'target' cells. First discovered in *Vibrio cholerae*, an estimated 25% of Proteobacteria species utilize the T6SS for interbacterial competition and/or anti-host activity (Pukatzki et al., 2006; Boyer et al., 2009). This introduction will provide further details on the structure, mechanism, and regulation of the T6SS, followed by a summary of the various effectors delivered through this system. Finally, as this thesis revolves around a T6SS effector protein with phospholipase A activity, there will be an overview on the structure and activity of phospholipases, including those deployed by the T6SS.

Structure and mechanism of the T6SS

The T6SS is an assembly made from 14 core proteins and takes the form of a hollow tube, or tail, surrounded by a contractile sheath built upon a baseplate structure (**Fig. 1**) (Cherrak et al., 2019; Cianfanelli, Monlezun, et al., 2016; Coulthurst, 2019). These features are structurally homologous to the tails of *Myoviridae* bacteriophage; in the T6SS these structures are anchored in place with a membrane complex (Brackmann et al., 2017; Cherrak et al., 2018; Ge et al., 2015;

Taylor et al., 2016). The membrane complex is the first structure to be assembled and is comprised of three transmembrane proteins: TssJ resides in the outer membrane while TssL and TssM are in the inner membrane (Durand et al., 2015). TssM interacts with TssJ to form a complex that spans both membranes. The base plate structure is assembled at the cytoplasmic surface of the membrane complex through the aggregation of TssE-TssF-TssG-TssK subunits (Brunet, Zoued, et al., 2015). Six of these subunits form a ring structure while interactions between TssK and the membrane complex anchor the base plate in place (Nazarov et al., 2018). An additional protein complex, comprised of a VgrG trimer and a PAAR repeat protein, is bound to the center of the baseplate ring; this serves as the tip of the secreted tube structure (Shneider et al., 2013). The tube is built upon the tip by stacking hexameric rings of hemolysin co-regulated protein (Hcp) until the polymerizing tail is long enough to reach the membrane on the opposite side of the cell (Basler et al., 2012; Douzi et al., 2014). As the tube elongates, a contractile sheath made from TssB/TssC dimers forms around the tube (Kudryashev et al., 2015). The conformation of the sheath in this pre-firing state holds the potential energy used to propel the inner tube during secretion (J. Wang et al., 2017).

Secretion appears to be initiated by a conformational change in the base plate, causing the sheath subunit structures to collapse within the span of a few milliseconds (Kudryashev et al., 2015; J. Wang et al., 2017). The inner tube, including the VgrG-PAAR tip, is fired out of the sheath, through the baseplate and membrane complex, and outside the cell. Estimations for the energy associated with a single T6SS contraction event range from 18,000 to 44,000 kcal/mol (Basler et al.,

2012; J. Wang et al., 2017). When fired directly into an adjacent cell, it is believed that most tubes will puncture the outer membrane and disassemble in the target cell periplasm (Mariano et al., 2018). T6SS effectors with periplasmic molecular targets have immediate access to their substrates; meanwhile cytoplasmic-acting effectors, such as nucleases, rely on transmembrane domains to breach the inner membrane and enter the target cell cytoplasm (Quentin et al., 2018).

Following secretion, inhibitor cells begin to disassemble the T6SS complex from its post-firing state. The AAA+ ATPase ClpV disassembles contracted sheaths by binding and unfolding TssC subunits (Bönemann et al., 2009; Kapitein et al., 2013). ClpV specifically targets the sheath in its post-firing state by binding to an N-terminal helix of TssC that is only exposed in its contracted conformation (Douzi et al., 2016; Pietrosiuk et al., 2011). *V. cholerae* inhibitors lacking ClpV have TssB/TssC sheaths that remain in their post-contraction state and block the formation of new T6SS complexes, suggesting that the disassembly and re-use of TssB/TssC subunits is an essential step for successive secretion events (Basler et al., 2012a).

T6SS Regulation

Like other secretion systems, Type VI secretion is a form of active transport and requires energy. The tube structure, which is estimated to consist of 700 Hcp subunits, is released from the inhibitor cell and needs to be resynthesized during each secretion cycle (Basler, 2015). And while contractile sheath proteins may be recycled between firing events, disassembly of the ~1500 subunit structure is ATP-dependent. Thus, it is natural that different bacteria species have evolved myriad

regulatory pathways to control T6SS activity in response to various environmental stimuli.

Many bacteria suppress their T6SS activity until they detect specific environmental signals. Such signals can be abiotic factors such as temperature, pH or ion concentrations (Hespanhol et al., 2023). These signals can serve as indicators that bacteria are in environments where T6SS activity will be beneficial. For example, in the squid symbiote *Vibrio fischeri* T6SS activity increases when cells are grown on a medium that is viscous and slightly acidic (Speare et al., 2021). These are conditions present inside the bacteria's host, and thus T6SS activity will be upregulated as *V. fischeri* competes with other bacteria for colonization. Some bacteria will only activate their T6SS if specific threats are detected, as seen in the 'tit-for-tat' system observed in *Pseudomonas aeruginosa* (Basler et al., 2013). In this defensive system the T6SS is only deployed after receiving a T6SS attack from an adjacent cell. The outer membrane protein TagQ detects a currently unknown signal of membrane instability after being fired upon, setting off a phosphorylation cascade that ends with the phosphorylated Fha1 protein initiating T6SS assembly at the vicinity of the initial attack (Casabona et al., 2013). It has been shown that other sources of membrane perturbation, such as polymyxin B, also induce this response (L. Hu et al., 2021). Regulations such as these can limit T6SS activity to times when a competitor cell is likely to be in proximity and may allow the apparatus to be aimed directly at an adjacent target.

Other bacteria appear to have a more offensive strategy for T6SS deployment. Species such as *Serratia marcescens*, *Vibrio cholerae*, and

Enterobacter cloacae do not require cell contact as a signal for T6SS activity and have been shown to be active even in liquid culture, where direct cell-to-cell contact is less likely to occur than on solid surfaces. (Basler et al., 2013; Donato et al., 2020; Gerc et al., 2015). Offensive T6SSs can still be regulated for greater efficiency. In *V. cholerae* T6SS secretion is under control of the quorum sensing regulator LuxO to repress secretion in low density liquid cultures (Zheng et al., 2010). In *S. marcescens* phosphorylation/dephosphorylation of Fha allows the T6SS to be re-positioned between firings; the ability to shift the direction of secretion has been shown to increase inhibition of target bacteria in co-culture competitions (Ostrowski et al., 2018).

T6SS Effectors and Immunity proteins

The T6SS fires a spear complex that breaches the cell envelope of target cells, yet the breach itself is not believed to cause significant harm to these targets (L.-S. Ma et al., 2014). Inhibition of targets cells is instead achieved through the activity of the effector proteins delivered through the T6SS.

Effector proteins fall into one of two groups, cargo effectors and specialized effectors, based on how they are incorporated into the T6SS apparatus. Specialized effectors are any components of the secreted spear (Hcp, VgrG, and PAAR) that have an additional domain with effector activity, typically located at their C-terminus (Brooks et al., 2013; J. Ma et al., 2017; Whitney et al., 2014). T6SS-carrying bacteria often have multiple unique specialized effectors for each core component, allowing modular variation of which effectors are deployed in each firing event (Hachani et al., 2014). In contrast, cargo effectors are proteins separate from the T6SS core and rely

on non-covalent interactions with one of the three spear proteins to be 'loaded' into the secretion structure (Durand et al., 2014). Cargo effectors are usually genetically adjacent to the T6SS component they associate with (Boyer et al., 2009; Cherrak et al., 2019). Some effector proteins, be they cargo or specialized, require chaperone proteins known as effector-associated genes (Eag) for proper delivery. In *P. aeruginosa* the cargo effector Tse6 requires EagT6 to bind with VgrG, while the specialized RhsA effectors in *S. marcescens* and *E. cloacae* are stabilized by their own Eag_{RA} proteins (Alcoforado Diniz & Coulthurst, 2015; Donato et al., 2020; Quentin et al., 2018). A given T6SS spear can contain both cargo and specialized effectors, each with their own biochemical activity serving to inhibit growth of target cells.

The majority of currently identified T6SS effectors have anti-bacterial activities (Coulthurst, 2019). Many of these effectors target common features of the prokaryotic cell envelope. Effectors with amidase or muramidase activity can degrade peptidoglycan in the cell wall to cause target cell lysis (Russell et al., 2012; Whitney et al., 2013). Phospholipase effectors destabilize the cell membrane through hydrolysis of the phospholipid bilayer (Russell et al., 2013). Phospholipases will be described in further detail in the following section. Bacterial inhibition can also be achieved via T6SS effectors that act in the cytoplasm. Species such as *Dickeya dadantii* 3937 deploy a pair of specialized PAAR Rhs proteins with C-terminal DNase domains to degrade DNA in target cells (Koskiniemi et al., 2013). Effectors with NADase domains inhibit targets by decreasing the amount of NAD⁺ and NADP⁺ available (Whitney et al., 2015). The Tre effector in *Serratia proteamaculans* has

been shown to ADP-ribosylize FtsZ monomers and inhibit target cell division (Ting et al., 2018).

Alongside its interbacterial function, some pathogens utilize the T6SS to deliver anti-eukaryotic virulence factors during host colonization (Monjarás Feria & Valvano, 2020). Phospholipase effectors can play a role here by destabilizing host cell membranes and facilitating bacteria internalization (Jiang et al., 2014). The PldA phospholipase in *P. aeruginosa* has even been shown to act on both prokaryotic and eukaryotic substrates (Bleves et al., 2014). Other effectors specifically target molecules only present in host cells. VgrG1 in *Vibrio cholerae* is a specialized effector with an actin cross-linking domain and has been shown to cause host cell death and prevent macrophage phagocytosis (A. T. Ma et al., 2009; Pukatzki et al., 2007). The *Burkholderia cenocepacia* amidase effector TecA targets a specific arginine residue in Rho GTPases to disorganize the actin cytoskeleton of macrophages (Aubert et al., 2016).

Pathogens can express eukaryote-specific effectors without any detriment to their viability, but bacteria that secrete anti-prokaryotic effectors need to prevent self-inhibition from occurring when they are received from sibling cells. For this reason, all anti-bacterial T6SS effectors are co-expressed with an associated immunity protein encoded directly downstream (Ting et al., 2018). Immunity proteins will specifically bind to their corresponding effectors and neutralize their activity (Benz et al., 2012). While immunity proteins typically function by occluding the active site of the bound effector, it has been shown that the DNA binding site of the nuclease effector Tde1 from *Agrobacterium tumefaciens* becomes disordered when bound to

its immunity protein, demonstrating that effector neutralization is not limited to restricting access to the active site (Bosch et al., 2023). Immunity proteins need to be present where their effectors are active, therefore immunity proteins associated with periplasmic amidase and phospholipase effectors contain membrane-localization signals (Russell et al., 2013; H. Zhang et al., 2013). Effectors may be paired with multiple copies of an immunity protein, which has been thought to accelerate the rate of effector diversification. (Kirchberger et al., 2017). Bacterial genomes may also contain clusters of T6SS immunity genes for effectors they do not encode. Carrying these orphan immunity genes can provide defense against non-self T6SSs, and they are believed to be acquired from horizontal gene transfer events between close or distantly related species (Kirchberger et al., 2017; Russell et al., 2012).

Phospholipase A Activity and Structure

Phospholipases are enzymes that hydrolyze ester bonds of phospholipid substrates (Istivan & Coloe, 2006). These enzymes target specific esters of the phospholipid core and are classified by which bond(s) they act on (**Fig. 2A**). Phospholipase A enzymes (PLAs) act on the acyl ester bonds of the phospholipid: phospholipase A₁ enzymes (PLA₁s) cleave the *sn1* fatty acid tail of the substrate while those with phospholipase A₂ activity (PLA₂s) remove the *sn2* tail. Some PLAs are capable of both A₁ and A₂ activity; these enzymes are also known as phospholipase B's (PLBs). Along with substrate specificity, PLAs are also characterized by their structural features. Many PLAs are α/β hydrolases, such as mammalian pancreatic lipase-related protein 2 (PLRP2) (**Fig. 2B**) (Eydoux et al.,

2008). These hydrolases have the structure of a β -sheet surrounded by interspersed α -helices; the active site is a catalytic triad of Ser/(Asp or Glu)/His residues. The catalytic serine is located on a loop with a GX SXG motif, forming a characteristic nucleophilic 'elbow' (Derewenda & Sharp, 1993). There are also several taxa-specific families of PLAs that are not α/β hydrolases, such as the mammalian secreted phospholipase A₂ (sPLA₂) and outer membrane phospholipase A (OMPLA) found in Gram-negative bacteria (Istivan & Coloe, 2006; Murakami et al., 2011).

Another structural component present in some PLAs and lipases is the lid domain (Khan et al., 2017). The lid is an amphipathic α -helix or loop that is positioned near the active site (**Fig. 2B**). This domain can switch conformations from a closed state, where the active site is occluded by the lid, and an open state that leaves the active site open (Brocca et al., 2003). It is thought that the lid enters the open conformation when the enzyme is present in a lipid-water phase interface (Reis et al., 2009). This is believed to be the mechanism behind interfacial activation: the observed phenomenon that the activity of many lipases significantly increases once its substrate has reached critical micellar concentration (Cambillau, 1996). Contact with micelle surfaces may stabilize the open lid conformation, exposing its hydrophobic face in a position that facilitates binding with lipid substrates and allows them to access the open active site (Yang & Lowe, 2000).

Type VI Lipase Effectors (Tles)

Many T6SS-carrying bacteria use the system to deploy phospholipase effectors that destabilize target cell membranes. These Type VI lipase effector (Tle)

proteins were first characterized by Russell et al., wherein they demonstrated that these effectors have phospholipase activity and cause permeabilization and growth inhibition of target cells in a T6SS-dependent manner (Russell et al., 2013). They directly studied Tle proteins from *Vibrio cholerae*, *Burkholderia thailandensis*, and *Pseudomonas aeruginosa*, but also showed predicted Tle genes present in a broad range of Gram-negative genomes and classified them into 5 Tle families; Tle1-4 contain predicted phospholipase A's while the Tle5 family has Tle proteins with phospholipase D motifs. Like all other anti-bacterial T6SS effectors Tle genes have downstream immunity genes, referred to as Type VI lipase immunity (Tli) genes. Tli genes encode lipoproteins with periplasmic localization signals, leading to the assumption that Tle effectors are active in the periplasm. Many Tle-deploying species have multiple copies of Tli genes, likely stemming from gene duplication events. Lu et al. reported a Tle4-Tli4 complex from *P. aeruginosa* that suggests Tli proteins neutralize their cognate Tle effectors by binding to their lid domain, thereby preventing interfacial activation from occurring. (Lu et al., 2014). In terms of the core T6SS constituents, Tle proteins are frequently associated with the VgrG tip protein. Tle genes are often located adjacent to VgrG within T6SS loci, and in enteroaggregative *Escherichia coli* Tle1 binds to a C-terminal adaptor domain of VgrG to attach itself to the trimeric tip structure (Flaughnatti et al., 2020).

This thesis is focused on research pertaining to a previously uncharacterized Tle from *Enterobacter cloacae* ATCC 13047 (ECL). Chapter II details a study that uncovers a unique relationship between ECL Tle and its cognate Tli, wherein the effector requires the co-expression of its immunity for proper deployment. In Chapter

III the molecular nature of Tle activation is shown to be the formation of a particular advanced glycation end-product (AGE) crosslink within its structure. Chapter IV investigates this activation in homologous lipase effectors to identify common trends seen in Tli-dependent Tle activation.

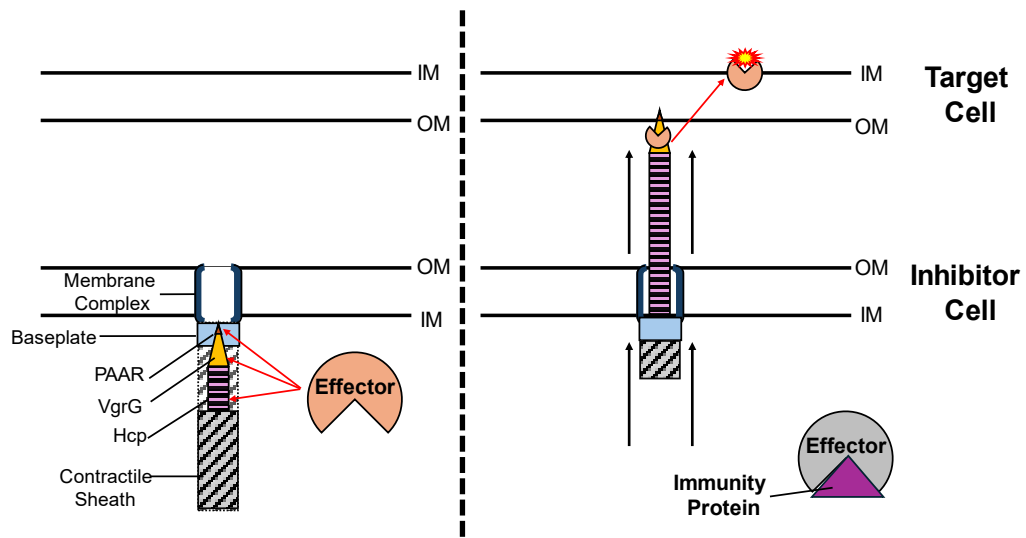


Figure 1 The type VI secretion system (T6SS)

Diagram showing the structure of the T6SS in pre-firing (left) and post-firing (right) states.

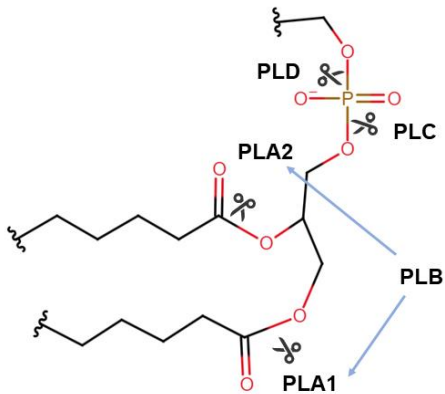
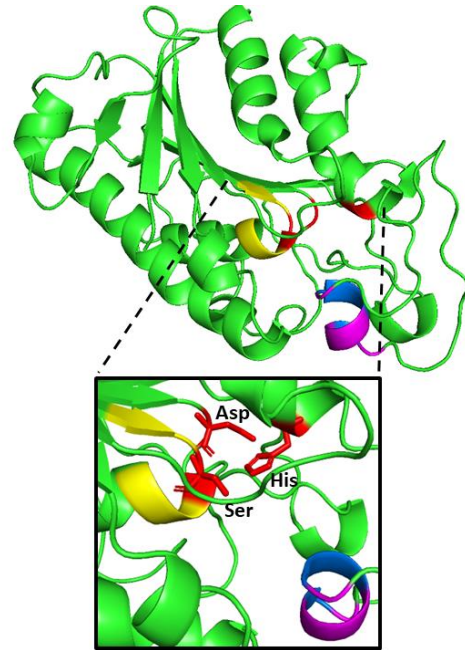
A**B**

Figure 2 Phospholipase specificity and structure

A) Diagram showing the phospholipid ester bonds hydrolyzed by different phospholipase classes (PLA1, PLA2, PLB, PLC, and PLD). PLBs have both PLA1 and PLA2 activity.

B) The structure of rat pancreatic lipase-related protein 2 (PLPR2). Inset shows the active site and lid domain. The nucleophilic elbow is colored yellow, the Ser-Asp-His catalytic triad is in red, the hydrophobic face of the lid is in blue, and the hydrophilic face of the lid is in purple.

Chapter II: Paradoxical Activation of a Type VI Secretion System Phospholipase Effector by Its Cognate Immunity Protein

Note: The research in this chapter was originally published in *Journal of Bacteriology*. The manuscript was originally written by Christopher Hayes and Zachary Ruhe and has been reprinted in the format of this thesis. Zachary Ruhe and I made equal contributions to this study.

Jensen, S. J., Ruhe, Z. C., Williams, A. F., Nhan, D. Q., Garza-Sánchez, F., Low, D. A., & Hayes, C. S. (2023). Paradoxical Activation of a Type VI Secretion System Phospholipase Effector by Its Cognate Immunity Protein. *Journal of Bacteriology*, 205(6), e0011323. <https://doi.org/10.1128/jb.00113-23>

Introduction

Research over the past 20 years shows that bacteria commonly deliver growth-inhibitory toxins directly into neighboring competitors ((Ruhe et al., 2020a)). This phenomenon was first described as contact-dependent growth inhibition (CDI) in *Escherichia coli* isolate EC93 (Aoki et al., 2005). CDI is mediated by a specialized type V secretion system (T5SS) composed of CdiB and CdiA proteins. CdiB is an Omp85 family β -barrel protein responsible for transport of the CdiA effector protein to the cell surface (Ruhe et al., 2018). Upon binding a receptor on a neighboring bacterium, CdiA delivers its C-terminal toxin domain into the target cell to inhibit growth. CDI⁺ strains protect themselves from autoinhibition by producing immunity proteins that specifically neutralize the toxin domain. Shortly after the discovery of T5SS-mediated CDI, two reports demonstrated that type VI secretion systems (T6SSs) are also potent mediators of interbacterial competition (Hood et al., 2010; MacIntyre et al., 2010). T6SSs are dynamic multiprotein machines related in structure and function to the contractile tails of *Myoviridae* bacteriophages. The T6SS duty cycle begins with the assembly of a phage-like baseplate complex around trimeric VgrG, which is homologous to the β -tailspike protein of coliphage T4 (Leiman et al., 2009). The baseplate then docks onto the cytosolic face of the transenvelope complex, which forms a secretion conduit across the cell envelope (Brunet, Zoued, et al., 2015). The latter assembly nucleates the polymerization of a contractile sheath surrounding a central tube of Hcp proteins. Toxic effector proteins are typically linked to the VgrG β -spike (Pukatzki et al., 2007; Shneider et al., 2013)

and can also be packaged within the lumen of the Hcp tube (Silverman et al., 2013). Once the sheath has grown to span the width of the cell, it contracts to expel the VgrG-capped tube through the transenvelope complex. The ejected projectile perforates neighboring bacteria and releases its toxic payload to inhibit target cell growth. As with toxic CdiA proteins, antibacterial T6SS effectors are encoded with cognate immunity proteins that protect the cell from intoxication by its isogenic siblings (Hernandez et al., 2020; Ruhe et al., 2020). In this manner, T5SSs and T6SSs confer a competitive fitness advantage to bacteria, and their effector-immunity protein pairs play an important role in self/nonself discrimination. Given that T5SS- and T6SS-mediated competition relies on cell-to-cell contact, the systems are often only deployed under conditions that favor productive effector delivery. Several regulatory strategies have been described for T6SSs, which are controlled at all levels of gene expression. T6SS loci are commonly subject to H-NS-mediated transcriptional silencing (Bernard et al., 2010; Brunet, Khodr, et al., 2015; Caro et al., 2020; J. Ma et al., 2018; Storey et al., 2020), and many require specific bacterial enhancer proteins to initiate transcription in conjunction with σ^{54} (Bernard et al., 2010; Pukatzki et al., 2006). Environmental signals also influence T6SS transcription through quorum sensing and two-component regulatory signaling pathways (Bernard et al., 2010; Majerczyk et al., 2016; Sana et al., 2012). In *Pseudomonas aeruginosa*, the stability and translation of T6SS transcripts are modulated by small noncoding RNAs (Bernard et al., 2011). Finally, assembly of the secretion apparatus is subject to posttranslational control by a serine/threonine kinase and phosphatase (Mougous et al., 2007). There are fewer studies on the

regulation of antibacterial T5SSs. The originally identified *cdiBAI* locus from *E. coli* EC93 is expressed constitutively (Aoki et al., 2005; Wäneskog et al., 2021), but systems from other species are strictly regulated. The CDI system of *Burkholderia thailandensis* E264 is activated through a quorum sensing pathway (Majerczyk et al., 2014), and the loci of *Dickeya dadantii* EC16 and 3937 are expressed only when these bacteria are grown on plant hosts (Aoki et al., 2010; Rojas et al., 2002, 2004). The latter observations suggest that CDI promotes host colonization and pathogenesis, although the T5SS effector domains deployed by these phytopathogens are clearly antibacterial (Aoki et al., 2010; Beck et al., 2014).

We previously reported that the CDI system of *Enterobacter cloacae* ATCC 13047 (ECL) is not active under laboratory conditions, although it is functional when expressed from a heterologous promoter (Beck et al., 2014). The wild-type *cdiBAI*^{ECL} operon appears to be transcribed from a single promoter with possible operator sites for PurR and Fnr. These predictions suggest that *cdi* transcription may be repressed when ECL is grown in standard culture media. In an attempt to identify transcriptional regulators, we generated an ECL strain that harbors the *gusA* reporter gene under the control of the *cdi* promoter and then screened it for transposon mutants that exhibit increased β -glucuronidase activity. Surprisingly, the recovered mutations have no effect on *cdi* transcription and instead act to increase cell permeability to the chromogenic β -glucuronidase substrate. We identified multiple insertions in *tli*, which encodes a previously described immunity protein that neutralizes the T5SS phospholipase effector Tle (Whitney et al., 2014). Thus, cell envelope integrity is disrupted by unrestrained

phospholipase activity in these mutants. Increased permeability is T6SS dependent, indicating that *tli* mutants are intoxicated by Tle delivered from neighboring siblings rather than internally produced phospholipase. Notably, we find that Δtli mutants are not hyperpermeable because they fail to deploy active Tle. Taken together, our findings indicate that Tli has distinct functions, depending on its subcellular localization. In addition to its established role as a periplasmic immunity factor, we propose that a cytosolic pool of Tli is required to activate the Tle phospholipase prior to T6SS-dependent export.

Results

Disruption of tli increases cell permeability.

We initially sought to identify regulators of the *cdiBAI* gene cluster in *Enterobacter cloacae* ATCC 13047 (ECL) using a β -glucuronidase (*gusA*) reporter to monitor expression. We fused the *E. coli gusA* gene to the *cdiB* (ECL_04452) promoter region and placed the construct at the ECL *glmS* locus using Tn7-mediated transposition. The resulting *cdi-gusA* reporter strain was subjected to transposon Tn5-mediated mutagenesis, and >25,000 insertion mutants were screened on agar medium supplemented with the chromogenic β -glucuronidase substrate X-Gluc (5-bromo-4-chloro-1H-indol-3-yl- β -D-glucopyranosiduronic acid). Nine different transposon insertion sites were identified from 17 mutants that formed pigmented colonies on indicator medium. One insertion is located within *tle* (ECL_01553), and the other eight disrupt the downstream *tli* cistron (ECL_01554) (**Fig. 1A**).

The *tle* gene encodes a toxic phospholipase effector deployed by the type VI secretion system 1 (T6SS-1) of ECL, and *tli* encodes an ankyrin repeat immunity

protein that neutralizes Tle activity (Donato et al., 2020). We transferred the transposon mutations into the original parental reporter strain using Red-mediated recombineering and found that all of the reconstructed mutants, except the *tle-1106* strain, recapitulate the original phenotype on indicator medium (**Fig. 1B**). Quantification of β -glucuronidase activity in cell lysates from a subset of mutants revealed that each has the same specific activity as the parental reporter strain (**Fig. 1C**). These data indicate that *cdi* transcription is unaffected by the *tli* mutations. Moreover, immunoblot analyses showed that none of the mutants exhibits increased production of CdiB (**Fig. 1D**) or CdiA (**Fig. 1E**). Given these results, we hypothesized that the loss of Tli immunity function leads to unopposed Tle phospholipase activity, which in turn degrades cell membranes to increase permeability to X-Gluc. Consistent with this model, parental reporter cells grown on indicator medium become pigmented after treatment with SDS solution (**Fig. 2A**). Moreover, complementation with plasmid-borne *tli* suppresses pigment conversion (**Fig. 2B**), but it has little effect on specific β -glucuronidase activities (**Fig. 2C**). Together, these results indicate that diminished immunity function leads to increased cell permeability.

Increased cell permeability is dependent on T6SS-1 activity.

Two scenarios could account for hyperpermeability: the *tli* mutants could be permeabilized by internally produced phospholipase, or they could be intoxicated by Tle delivered from neighboring sibling cells. These models are not exclusive, and the phenotype may reflect a combination of external and internal phospholipase activities. To eliminate the contribution from T6SS-delivered effector, we

deleted *tssM* (**Fig. 3A**), which encodes a critical component of the transenvelope complex required for secretion. The resulting *tli* Δ *tssM* cells do not secrete Hcp into culture supernatants (**Fig. 3B**), confirming that T6SS-1 is inactivated.

The *tli* Δ *tssM* strains also exhibit less pigmentation when grown on X-Gluc indicator medium (**Fig. 3C**, top row). To ensure that the Δ *tssM* mutation does not abrogate *tIe* expression, we showed that complementation with plasmid-borne *tssM* restores Hcp secretion and hyperpermeability phenotypes to each strain (**Fig. 3B** and **C**, bottom row). These data indicate that increased cell permeability is largely due to T6SS-1-dependent exchange of phospholipase toxin between sibling cells.

Although *tli* is disrupted in each mutant, most retain the capacity to produce a truncated form of the immunity protein. Insertions in the lipoprotein signal sequence (*tli-17*, *tli-21*, *tli-31*, *tli-57*, and *tli-64*) should allow cytosolic Tli to be synthesized using Met10, Met16, or Met24 as alternative translation initiation codons (**Fig. 1A**). Furthermore, the *tli-663* and *tli-673* alleles are predicted to produce secreted Tli lipoproteins that carry transposon-encoded residues fused at Asp221 and Lys224, respectively (**Fig. 1A**). Immunoblotting revealed that the *tli-17*, *tli-21*, *tli-57*, and *tli-64* mutants accumulate Tli to about the same level as the parental *tli*⁺ strain, but we were unable to detect antigen in *tli-231*, *tli-663*, and *tli-763* cell lysates (**Fig. 4A**). We next asked whether truncated Tli provides any protection against Tle delivered from wild-type ECL inhibitor cells. Because the *tli* mutants also deploy Tle to intoxicate their siblings, we examined immunity function in a Δ *tssM* background to ensure that the mutants act only as target cells during coculture. The *tli* Δ *tssM* target cells are

outcompeted between 50- and 100-fold by wild-type ECL, but they show no fitness disadvantage when cocultured with ECL $\Delta tssM$ mock inhibitor cells (**Fig. 4B**). This level of growth inhibition is comparable to that observed with $\Delta tle \Delta tli$ target cells (**Fig. 4B**), which harbor a true null allele of *tli*. Thus, the transposon insertions completely abrogate immunity to Tle. Given that cytosolic immunity protein fails to protect, these results also indicate that Tli must be localized to the periplasm to neutralize toxic phospholipase activity. **ECL Δtli mutants fail to deploy active Tle.**

Although the *tli* disruptions behave as null mutations in competition cocultures, we noted that the *tli-231* insertion induces a modest permeability phenotype compared to the other alleles. This observation is curious because *tli-231* is arguably the most disruptive to Tli structure and is therefore expected to cause a more profound phenotype. To explore this issue, we asked whether a Δtli null strain phenocopies the transposon mutants on X-Gluc indicator medium and surprisingly found that Δtli cells are not hyperpermeable (**Fig. 5A**). This result could reflect the acquisition of an inactivating mutation in *tle* during construction of the Δtli strain. However, the hyperpermeable phenotype is restored when truncated Tli proteins lacking the N-terminal 23 (Tli- $\Delta 23$) and 51 (Tli- $\Delta 51$) residues are expressed from a plasmid in Δtli cells (**Fig. 5A**). Further truncation of the immunity protein to Tli- $\Delta 75$, which approximates the fragment produced by the *tli-231* allele, does not induce autopermeabilization (**Fig. 5A**). These data suggest that Δtli cells do not deploy active Tle. Accordingly, we found that *tle*⁺ Δtli cells behave like $\Delta tssM$ mock inhibitors when competed against $\Delta tle \Delta tli$ target cells (**Fig. 5B**). The competitive fitness of the *tle*⁺ Δtli strain is restored to wild-type levels when the cells express wild-type Tli

or Tli- Δ 23, but not the Tli- Δ 51 or Tli- Δ 75 truncations (**Fig. 5B**). Although Tli- Δ 51 fails to confer a competitive advantage (**Fig. 5B**), target cell growth in these cocultures is suppressed compared to that in experiments with *tle*⁺ *Δtli* inhibitors that harbor an empty vector plasmid (**Fig. 5C**). Quantification of viable Tli- Δ 51-producing cells shows that their growth is also inhibited (**Fig. 5D**), indicating that intersibling intoxication obviates any competitive advantage gained by Tle delivery. This autoinhibition is not observed with Tli- Δ 23-producing cells (**Fig. 5D**), although they exhibit a similar hyperpermeable phenotype on indicator medium (**Fig. 5A**).

To test whether the ECL *Δtli* strain deploys other T6SS-1 effectors, we performed competition assays with *E. coli* target bacteria, which have previously been shown to be inhibited by ECL *Δtle* mutants (Donato et al., 2020b). Wild-type ECL outcompetes *E. coli* almost 10⁶-fold on agar medium, and most of this growth advantage is lost when T6SS-1 is inactivated with the *ΔtssM* mutation (**Fig. 5E**). ECL *Δtli* mutants retain most of this inhibition activity against *E. coli* target cells (**Fig. 5E**), demonstrating that *tli* is not required to deliver other T6SS-1 effectors. Together, these results indicate that Tle-mediated growth inhibition depends on a cytosolic pool of Tli.

Tli is required for the toxic activity of Tle.

Tli could be required to stabilize Tle, or perhaps the immunity protein acts as a chaperone to load effector into the T6SS-1 apparatus. We first asked whether Tli stabilizes the lipase effector, but were unable to detect Tle antigen in either wild-type (*tle*⁺ *tli*⁺) or *Δtli* cell lysates (**Fig. 6A**). Given the low endogenous level of Tle, we expressed *tle* and *tle-tli* from plasmid vectors (pTle and pTle-Tli) in ECL *Δtle Δtli* cells

to examine effector stability. Immunoblotting showed that full-length Tle is produced from both constructs, though some minor degradation products are apparent in the absence of Tli (**Fig. 6A**). Despite producing detectable lipase, cells harboring the pTle plasmid have no inhibition activity against $\Delta tle \Delta tli$ target bacteria (**Fig. 6B**). In contrast, the pTle-Tli construct confers a significant growth advantage under the same conditions (**Fig. 6B**). We also tested whether Tli is required for effector secretion, but were unable to detect Tle antigen in culture supernatants even when expressed from a plasmid vector. Therefore, we asked whether Tli is still required for growth inhibition activity when phospholipase export is ensured by fusion to the VgrG β -spike protein. The ECL T6SS-1 locus encodes two VgrG proteins (VgrG1 and VgrG2) (**Fig. 3A**), each of which is sufficient to support secretion activity (Donato et al., 2020). We reasoned that the lipase domain could be fused to VgrG2, because other *Enterobacter* strains encode “evolved” VrgG2 homologs that carry effector domains at their C termini (see **Fig. S1** in the supplemental material). AlphaFold2 modeling indicates that Tle is composed of two domains connected by a flexible linker (**Fig. 7A**). The novel N-terminal domain of Tle is presumably required for T6SS-mediated export, and its C-terminal domain adopts an α/β -hydrolase fold that resembles neutral lipases from fungi. Using the AlphaFold2 model as a guide, we fused the linker region and phospholipase domain of Tle to VgrG2 (**Fig. 7B**), then asked whether the VgrG2-lipase chimera restores growth inhibition activity to a VgrG-deficient mutant. Because ECL $\Delta tle-tli-vgrG1-vgrG2$ cells do not produce functional VgrG, they cannot assemble the T6SS-1 apparatus (Donato et al., 2020) and do not kill *E. coli* target bacteria during coculture (**Fig. 7C**). Complementation of

Δtle-tli-vgrG1-vgrG2 cells with the VgrG2-lipase construct restores growth inhibition activity against *E. coli* target cells (**Fig. 7C**). Moreover, this inhibition activity is quantitatively similar to that of an ECL *ΔvgrG1* inhibitor strain (**Fig. 7C**), which produces VgrG2 and Tle as separate polypeptides. These results suggest that the VgrG2-lipase chimera supports the same T6SS-1 activity as wild-type VgrG2. However, the VgrG2-lipase construct has no growth inhibition activity against ECL *Δtle Δtli* target cells (**Fig. 7D**), indicating that the fused lipase domain is inactive. We next tested whether addition of the *tli* gene to the fusion construct promotes phospholipase activity (**Fig. 7B**). Although the resulting pVgrG2-lipase/Tli construct is somewhat less effective against *E. coli* target cells (**Fig. 7C**), it inhibits the growth of ECL *Δtle Δtli* target cells to the same extent as an ECL *ΔvgrG1* inhibitor strain (**Fig. 7D**). We also showed that mutation of the predicted catalytic Ser341 residue in the lipase domain abrogates growth inhibition activity against ECL *Δtle Δtli* cells (**Fig. 7D**), but not *E. coli* target cells (**Fig. 7C**), indicating that the VgrG2-lipase fusion supports the delivery of other T6SS-1 effectors. Together, these results demonstrate that the Tle phospholipase domain is only active when coproduced with its cognate immunity protein.

Discussion

Here, we identify ECL transposon mutants that exhibit increased permeability to a chromogenic β -glucuronidase substrate. The transposon insertions disrupt *tli*, which encodes an immunity protein that neutralizes the previously described Tle phospholipase effector (Donato et al., 2020). Thus, unmitigated Tle activity damages cellular membranes, allowing chromogenic substrate to enter the cytosol and/or β -

glucuronidase to escape into the extracellular medium. This hyperpermeability is dependent on T6SS-1 activity, indicating that the mutants are intoxicated by Tle delivered from neighboring siblings rather than their own internally produced phospholipase. This phenomenon is similar to the observations of Russell et al., who found that deletion of the *tli5*^{PA} (PA3488) immunity gene from *Pseudomonas aeruginosa* PAO1 leads to increased cell permeability through unopposed PldD^{PA} phospholipase activity (Russell et al., 2013). Moreover, *P. aeruginosa* autointoxication requires a functional H2-T6SS locus (Russell et al., 2013), indicating that the phenotype is due to intersibling exchange of phospholipase. However, in contrast to *P. aeruginosa*, ECL Δtli null mutants fail to deploy active phospholipase and consequently do not exhibit hyperpermeability. Instead, the strongest phenotypes are associated with mutations that prevent targeting of Tli to the periplasm, yet still allow the immunity protein to accumulate to wild-type levels. These findings indicate that Tli has different functions, depending on its subcellular localization. Tli in the periplasm acts to neutralize incoming phospholipase effectors, whereas cytoplasmic Tli produced from alternative translation initiation sites is required for the activation and/or export of Tle. Because we cannot ascertain whether Tle is secreted from Δtli mutants, it is possible that cytosolic Tli acts a chaperone to load the effector into the T6SS apparatus. However, the immunity protein probably has another function because growth inhibition activity remains *tli*-dependent when phospholipase delivery is achieved through fusion to VgrG2. We propose that Tli activates the effector domain prior to T6SS-mediated export. AlphaFold2 modeling suggests that the lipase catalytic core is not altered

upon binding to Tli, although dramatic conformational changes are predicted for lipase helices $\alpha 5$, $\alpha 10$, and $\alpha 11$ (see Fig. S2A and B in the supplemental material). Helix $\alpha 5$ is pulled away from the lipase domain through predicted interactions with the first ankyrin repeat of Tli, allowing $\alpha 10$ and $\alpha 11$ to migrate into the vacated position (**Fig. S2A and B**). In the absence of Tli, helix $\alpha 5$ forms a “lid” that covers the active site and precludes access to solvent (**Fig. S2A and B**). Similar lid structures are found in many other lipases, and these helices are typically displaced to expose the active site upon binding to membranes in a process termed “interfacial activation” (Khan et al., 2017). Thus, the predicted conformational changes in the lid could underlie lipase activation, but because Tli blocks lipase activity, the model may correspond to the neutralized conformation. We also modeled lipase interactions with immunity proteins produced from the various *tli* alleles identified in this study. Lipase interactions with Tli-64, Tli-663, and Tli-673 are nearly identical to those with wild-type Tli (**Fig. S2C, E, and F**), but Tli-231, which lacks N-terminal ankyrin repeats, does not displace helix $\alpha 5$ of the lipase domain (**Fig. S2D**). The implications of the latter model for lipase activation are not clear given that we are unable to detect Tli antigen in *tli-231* mutants. Though the mechanism remains unknown, it seems likely that Tle activation requires direct binding interactions with cytosolic Tli. Because presumably only the effector protein is exported, this model implies that there must be an additional mechanism to dissociate the Tle-Tli complex prior to loading into the T6SS apparatus.

Russell et al. first described and delineated five families of T6SS phospholipase effectors, which they designated Tle1 through Tle5 (Russell et al., 2013). Although

not identified in that study, Tle^{ECL} from ECL contains the GxSxG catalytic motif found in the Tle1, Tle2, Tle3, and Tle4 effector families. AlphaFold2 modeling suggests that Tle^{ECL} adopts an α/β -hydrolase fold, with the GxSxG sequence forming a classic nucleophilic “elbow” in the turn between β 4 and α 7. A DALI server search indicates that Tle^{ECL} is not closely related to known T6SS effectors and instead is most similar to a family of neutral lipases secreted by fungi (Brady et al., 1990; Lan et al., 2017; Lou et al., 2010). This conclusion is supported by direct comparisons of the Tle^{ECL} model with the crystal structures of Tle1^{PAO1} and Tle4^{PAO1} from *Pseudomonas aeruginosa* PAO1. Superimposition of core α/β -hydrolase domains reveals that the flanking secondary elements are distinct between the effectors (**Fig. S3**). Moreover, Tle1^{PAO1} and Tle4^{PAO1} have modules that are absent from Tle^{ECL}. Tle1^{PAO1} contains a putative membrane-anchoring domain (H. Hu et al., 2014), and the α/β -hydrolase core of Tle4^{PAO1} is interrupted by three inserted segments that form a cap domain to cover the active site (Lu et al., 2014). We note that the Tle^{ECL} model also differs substantially from AlphaFold2 predictions for Tle2 (VasL) from *Vibrio cholerae* and Tle3 from *Burkholderia thailandensis* E264. Database searches reveal that Tle^{ECL} is commonly encoded by *Enterobacter* and *Cronobacter* T6SS loci, and it shares significant sequence identity with the Slp effector from *Serratia marcescens* (see **Table S1** in the supplemental material) (Cianfanelli, Alcoforado Diniz, et al., 2016). Homologous lipase domains are more broadly distributed across *Erwinia*, *Dickeya*, *Burkholderia*, and *Vibrio* species, where they are fused to predicted VgrG, PAAR, and DUF4150 domain proteins (**Table S1**). Related lipase domains also form the C termini of rearrangement hot spot (Rhs) proteins in

various *Pseudomonas* and *Vibrio* isolates. Rhs proteins constitute another important class of T6SS effectors that carry variable C-terminal toxin domains (Alcoforado Diniz & Coulthurst, 2015; Koskiniemi et al., 2013; Ruhe et al., 2020; D. Zhang et al., 2012). Finally, a handful of *Deltaproteobacteria* encode predicted CdiA proteins with similar lipase domains (**Table S1**), indicating that this effector family can also be delivered through the T5SS pathway. Notably, these lipase sequences are linked to putative immunity genes that encode ankyrin repeat proteins (**Table S1**), raising the possibility that all of these effectors are activated by their cognate immunity proteins. Although it remains to be determined whether other lipases require activation, a similar phenomenon has been reported for the PAAR domain-containing PefD effector of *Proteus mirabilis* HI4320. Mobley and coworkers found that disruption of the corresponding *pefE* immunity gene, which encodes a predicted β -propeller protein, abrogates the growth inhibition activity of PefD in cocultures (Alteri et al., 2017). PefD function is also dependent on *pefF* and *pefG*, which encode an armadillo repeat protein and a thioredoxin-like oxidoreductase, respectively (Alteri et al., 2013, 2017). AlphaFold2 indicates that PefD contains an intricate array of six disulfide bonds (<https://www.uniprot.org/uniprotkb/B4EVA8/entry#structure>), suggesting that PefE and PefF could be chaperones that hold the effector in the proper conformation for PefG-catalyzed disulfide bond formation. However, PefD and the related Tse7 effector from *P. aeruginosa* are toxic DNases that must be transferred into the cytoplasm to inhibit growth (Alteri et al., 2017; Pissaridou et al., 2018). Given that any disulfides would likely be reduced by glutathione and thioredoxin after delivery into the target cell, perhaps these bonds promote export

rather than enzymatic activity. Proper disulfide formation is clearly important for other T6SS effectors that function in the periplasm. Peptidoglycan amidase and pore-forming effectors from *Serratia marcescens* both depend on DsbA (Mariano et al., 2018), which is a highly conserved oxidoreductase that catalyzes disulfide formation in the periplasm of most Gram-negative bacteria (Collet et al., 2020a). T5SS/CdiA effector domains are also known to exploit target cell proteins to promote toxicity. CdiA from uropathogenic *E. coli* delivers a novel tRNA anticodon nuclease domain that is only active when bound to the cysteine biosynthetic enzyme CysK (Aoki et al., 2010; Diner et al., 2012; Johnson et al., 2016). Other CdiA proteins carry BECR-fold RNases that interact with elongation factor Tu (EF-Tu) to cleave the 3'-acceptor stems of specific tRNA molecules (Gucinski et al., 2019; Jones et al., 2017; Michalska et al., 2017; J. Wang et al., 2022).

Given that our screen ultimately selected for hyperpermeable cells, it is perhaps surprising that we did not recover other mutations that are known to disrupt the cell envelope. The first “leaky” mutants were isolated in screens for *E. coli* and *Salmonella enterica* serovar Typhimurium cells that release periplasmic RNase I and alkaline phosphatase into culture media (Amouroux et al., 1991; Lazzaroni & Portalier, 1981; Lopes et al., 1972; Weigand & Rothfield, 1976). These early studies uncovered a critical role for TolA in Gram-negative cell envelope integrity (Amouroux et al., 1991). Later, *E. coli lamB* cells were used to identify mutations in *ompC* and *ompF* that allow high-molecular-weight maltodextrins to enter the periplasm (Benson et al., 1988; Benson & Decloux, 1985). The same strategy also led to the discovery of *lptD* (Sampson et al., 1989), which encodes an essential β -barrel

protein that inserts lipopolysaccharide into the outer membrane (H. Dong et al., 2014; Gu et al., 2015; Li et al., 2015; Qiao et al., 2014). More recently, Bernhardt and coworkers used a cell-impermeable β -galactosidase substrate to identify over 100 *E. coli* genes that contribute to envelope integrity (Paradis-Bleau et al., 2014). Although the approach taken by Paradis-Bleau et al. is essentially the same as in our study, they note that disruption of outer membrane integrity alone is probably sufficient for substrate entry in their screen (Paradis-Bleau et al., 2014). In contrast, ECL lacks outer and inner membrane transporters for β -glucuronides (Liang et al., 2005), and therefore both membranes must be permeabilized for substrate entry. These observations suggest that T6SS-delivered Tle damages the outer and inner membranes of target bacteria and that the loss of Tli immunity function produces the most striking phenotype on indicator media.

Acknowledgements

We thank Stephanie Aoki for the construction of plasmid pDAL6480 and Jiang Xiong for technical assistance.

This work was supported by grants GM117930 (C.S.H.) from the National Institutes of Health and MCB 1545720 (D.A.L. and C.S.H.) from the National Science Foundation. Z.C.R. was supported by the Tri-Counties Blood Bank Postdoctoral Fellowship.

Conceptualization, S.J.J., Z.C.R., D.A.L., and C.S.H.; Funding Acquisition, D.A.L. and C.S.H.; Investigation, S.J.J., Z.C.R., A.F.W., D.Q.N., and F. G.-S.; Methodology, Z.C.R. and C.S.H.; Supervision, D.A.L. and C.S.H.; Validation, S.J.J., D.Q.N., and

F.G.-S.; Visualization, Z.C.R. and C.S.H.; Writing – Original Draft, Z.C.R. and C.S.H.;
Writing – Review & Editing, S.J.J., D.A.L., and C.S.H.

Materials and Methods

Bacterial strain and plasmid constructions.

The bacterial strains and plasmids used in this study are listed in **Table 1** and **Table 2**, respectively, and oligonucleotides are listed in Table S2 in the supplemental material. All bacteria were grown at 37°C in lysogeny broth (LB): 1% tryptone, 1% yeast extract, and 0.5% NaCl. Media were supplemented with antibiotics at the following concentrations: ampicillin (Amp), 150 µg/mL; gentamicin (Gent), 12 µg/mL; kanamycin (Kan), 50 µg/mL; rifampin (Rif), 200 µg/mL; spectinomycin (Spec), 15 µg/mL; tetracycline (Tet), 100 µg/mL; and trimethoprim (Tmp), 100 µg/mL (where indicated). The ECL *cdi-gusA* reporter strain ZR71 was constructed by Tn7-mediated transposition. *E. coli gusA* was amplified with oligonucleotide primers CH3025/CH3026 and ligated to pUC18T-mini-Tn7T-Gm (Choi et al., 2008) using EcoRI/SacI restriction sites to generate plasmid pZR42. The ECL *cdiB* promoter region was amplified with CH3146/CH3147 and ligated to pZR42 using KpnI/EcoRI restriction sites to generate pCH3468. pCH3468 and pTNS2 (Choi et al., 2005) were introduced into wild-type ECL by conjugation, and gentamicin-resistant (Gent^r) clones were screened for *cdi-gusA* transposition into the *glmS* locus. The same mating procedure was used to generate strain CH3469 (ECL Δtli *glmS::cdi-gusA*) from strain CH14588. The $\Delta tssM1::kan$ allele (from pCH11050) was introduced into ECL strains carrying plasmid pKOBEG using Red-mediated recombination as described previously (Beck et al., 2014; Donato et al., 2020). ECL

$\Delta tli::kan$ (CH14587) and $\Delta tle-tli-vgrG1-vgrG2::kan$ (CH1360) mutants were constructed using pCH371, which is a pRE118 (Edwards et al., 1998) derivative that carries the *pheS(A294G)* counterselectable marker instead of *sacB*.

The *pheS(A294G)* allele was first amplified with DL2217/DL2194 and fused to the *tet* promoter in pBR322 using EcoRV/SphI restriction sites to generate plasmid pDAL912. The P_{tet} -*pheS(A294G)* fragment was then amplified with DL2195/DL2196 and combined with pRE118-derived fragments generated with DL2197/DL2198 and D2199/DL1667 using overlap extension PCR (OE-PCR). The final PCR product was introduced into pRE118 using Red-mediated recombination to generate plasmid pDAL6480. A chloramphenicol resistance (Cm^r) cassette was amplified with CH5269/CH5270, digested with XbaI/NsiI, and ligated to XbaI/SbfI-digested pDAL6480 to generate plasmid pCH377. The FLP recombination target (FRT)-flanked Kan^r cassette from pKAN/pCH70 (Hayes & Sauer, 2003) was subcloned into pCH377 via SacI/KpnI restriction sites to generate pCH371. The pCH1359 $\Delta tle-tli-vgrG1-vgrG2$ knockout construct was generated by sequential cloning of CH3373/CH3374 (SacI/BamHI) and CH3197/CH3198 (XhoI/KpnI) fragments into pCH371. The pCH3884 $\Delta tli::kan$ knockout construct was generated by sequential cloning of ZR39/ZR40 (SacI/BamHI) and CH3377/CH3378 (XhoI/KpnI) fragments into pCH371. Plasmids pCH1359 and pCH3884 were introduced into ECL by conjugation, followed by selection for Kan^r Cm^r exconjugants. Clones were cultured in M9 minimal medium supplemented with 0.4% d-glucose, 2 mM d/l-chlorophenylalanine, and 50 μ g/mL kanamycin and then screened for Kan^r Cm^s clones that had lost the *pheS(A294G)* marker through homologous

recombination. The Kan^r cassette was removed from CH14587 using the FLP recombinase encoded on pCP20 (Cherepanov & Wackernagel, 1995) to generate strain CH14588.

The Tn5 delivery vector pLG99 (Gallagher et al., 2013) was modified to introduce a spectinomycin resistance (Spec^r) cassette. An EcoRV/SpeI fragment from pSPM/pCH9384 (Whitney et al., 2014) was ligated to a pLG99 vector prepared by NsiI (followed by end-filling with T4 DNA polymerase) and AvrII digestion. The ECL *tli* coding sequence was amplified with primer pairs, CH3418/CH3419 (wild-type *tli*), CH3719/CH3419 (*tli*-Δ23), CH5137/CH3419 (*tli*-Δ51), and CH5318/CH3419 (*tli*-Δ75), and the products were ligated to pCH450K (Hayes & Sauer, 2003) using KpnI/XhoI restriction sites to generate plasmids pCH494, pCH495, pCH5036, and pCH5037, respectively. ECL *t/e* was amplified with primers CH4469/ZR248 and ligated to pCH450 using EcoRI/XhoI restriction sites to generate plasmid pCH14212. *tli* was then amplified with CH4762/CH3419 and ligated via BstXI/XhoI to pCH14212 to generate plasmid pCH3128. Primers CH3719/CH4154 were used to amplify *tli*-Δ23 for ligation into pET21K via KpnI/XhoI to generate pCH3291, which overproduces cytosolic Tli with a C-terminal His₆ epitope. Primers CH5087/ZR248 were used to amplify the lipase domain coding region of *t/e* for ligation into pSH21P via SpeI/XhoI to generate plasmid pCH15269, which overproduces the domain with an N-terminal His₆ epitope. ECL *tssM* was amplified with CH3023/CH3024 and ligated to pCH450 using NcoI/XhoI restriction sites to generate plasmid pCH11198. The *cdiB* gene from *E. coli* STEC_O31 was amplified with ZR443/ZR444 and ligated to pET21b using EcoRI/XhoI restriction sites to generate plasmid pCH6118.

To construct the VgrG2-lipase fusion, *vgrG2* from ECL was amplified with CH4452/CH5205 and ligated to pCH450 using EcoRI/KpnI restriction sites. *vgrG-CT/vgrI* sequences were amplified from *Enterobacter hormaechei* ATCC 49162 using CH5203/CH5204 and appended to the *vgrG2* construct using KpnI/PstI restriction sites to generate pCH417. Plasmid pCH417 was amplified with CH4452/CH5770 to add a SacI linker, and lipase domain/*tli* modules from CH5772/ZR248 and CH5772/CH3419 amplifications were ligated via SacI/XhoI to generate plasmids pCH9063 and pCH9062, respectively. The Ser341Ala substitution was introduced into the lipase domain by OE-PCR using primers CH4762/CH4763 in conjunction with CH5772/CH3419 to generate plasmid pCH3763.

Transposon mutagenesis and mutant screening.

Plasmid pLG99::*spec* was introduced into ECL strain ZR71 cells via conjugation, and *Spec^r* clones were selected on tryptone broth agar (1% tryptone, 0.5% NaCl, 1.5% agar) supplemented with 100 µg/mL *Spec* and 100 µg/mL of 5-bromo-4-chloro-1H-indol-3-yl β-d-glucopyranosiduronic acid (X-Gluc). Transposon insertion sites were identified by arbitrarily primed PCR. The Tn5 right arm was amplified with Tn5-Right1/CH2020 or Tn5-Right1/CH2022. Products were reamplified using nested primers Tn5-Right2/CH2021. The Tn5 left arm was amplified using primers Tn5-Left1/CH2020 and Tn5-Left1/CH2022. The resulting reactions were amplified with nested primers Tn5-Left2/CH2021. Second-round reactions were sequenced using oligonucleotides Tn5-Right3 and Tn5-Left3 as primers.

X-Gluc permeability and β-glucuronidase assays.

β -Glucuronidase activity was quantified as described by Miller (Miller, 1972). Cells were harvested from tryptone broth (TB) agar and suspended in 100 mM sodium phosphate (pH 7.0) at an optical density at 600 nm (OD_{600}) of 1.0. A drop of toluene and a drop of 0.1% SDS were added to 100 μ L of the cell suspension, followed by vortexing for 15 s. The suspension was then incubated at 37°C for 90 min without caps to allow evaporation of toluene. Cell suspensions and substrate solution (1 mg/mL *p*-nitrophenyl β -d-glucuronide in 100 mM sodium phosphate [pH 7.0] and 5 mM β -mercaptoethanol) were equilibrated to 28°C. Cell lysate (100 μ L) was added to 600 μ L of substrate solution and incubated at 28°C for 30 min. Reaction mixtures were quenched with 700 μ L of 1 M sodium carbonate. Quenched reaction mixtures were centrifuged at 14,000 $\times g$ for 10 min, supernatant was removed, and absorbance was measured at 420 nm. β -Glucuronidase activity was quantified in Miller units, where enzyme units = 1,000 (A_{420})/(OD_{600} of 1.0 at 0.1 mL for 30 min). Overnight cultures were adjusted to an OD_{600} of 3.0, and 10 μ L was spotted onto TB agar supplemented with 100 μ g/mL X-Gluc and incubated overnight at 37°C. Culture plates were imaged using a light scanner.

Competition cocultures.

Inhibitor and target cells were grown overnight in LB and then diluted 1:50 into fresh LB and grown at 37°C to mid-log phase. Cells were harvested by centrifugation at 3,400 $\times g$ for 2 min, resuspended to an optical density at 600 nm (OD_{600}) of 3.0, and mixed at a 10:1 ratio of inhibitor to target cells. Cell mixtures (10 μ L) were spotted onto LB agar (supplemented with 0.4% l-arabinose when using strains with arabinose-inducible constructs) and incubated at 37°C. A portion of each cell mixture

was serially diluted into $1 \times$ M9 salts and plated onto antibiotic-supplemented LB agar to enumerate inhibitor and target cells as CFU at $t = 0$ h. For the competition in **Fig. 4B**, inhibitor strains were scored using Tmp^r (conferred by plasmid pSCBAD) (Koskiniemi et al., 2015a), and targets were scored by Spec^r . For all other competitions, inhibitors were scored by Tet^r (conferred by pCH450 derivatives), and *E. coli* and ECL target cells were enumerated by Rif^r . After 4 h of coculture, cells were harvested from the agar surface with polyester-tipped swabs and resuspended in 800 μL of $1 \times$ M9 salts. The cell suspensions were serially diluted in $1 \times$ M9 salts and plated as described above to quantify endpoint CFU. Competitive indices were calculated as the final ratio of inhibitor to target cells divided by the initial ratio of inhibitor to target cells.

Hcp secretion.

Overnight cultures of ECL were diluted 1:50 into 3 mL LB and grown to an OD_{600} of ~ 1.0 at 37°C . The cultures were then supplemented with 0.4% l-arabinose and incubated for 45 min. The cultures were centrifuged at $3,400 \times g$ for 5 min, and the cell pellets were resuspended in 100 μL of urea lysis buffer (8 M urea, 150 mM NaCl, 20 mM Tris-HCl [pH 8.0]) for lysis. Supernatants were collected and centrifuged for an additional 5 min to remove any remaining cells. Supernatants were then passed through a 0.22- μm -pore low-binding polyvinylidene fluoride (PVDF) filter. The filtered culture supernatants were adjusted to 10% trichloroacetic acid and incubated on ice for 1 h. Samples were centrifuged at $21,000 \times g$ for 10 min. Precipitates were resuspended twice in 1 mL ice-cold acetone and recollected by centrifugation at $21,000 \times g$ for 5 min. Precipitates were air-dried at ambient temperature and then

dissolved in 50 μ L urea lysis buffer. Protein concentrations were estimated by Bradford assay, and \sim 5 μ g was loaded onto 10% polyacrylamide SDS gels for electrophoresis and immunoblot analysis.

Antiserum generation and immunoblotting.

His₆-tagged variants of Tli- Δ 23 and the Tle lipase domain from ECL, and CdiB from *E. coli* STEC_O31 were overproduced in *E. coli* strain CH2016 from plasmids pCH3291, pCH15269, and pCH6118, respectively. Overnight cultures were diluted 1:100 in fresh LB supplemented with Amp and grown to mid-log phase at 37°C in a baffled flask. Expression was then induced with isopropyl β -d-1-thiogalactopyranoside at a final concentration of 1.5 mM for 90 min. Cultures were harvested by centrifugation and cell pellets frozen at -80°C . Cells were broken by freeze-thaw in urea lysis buffer supplemented with 0.05% Triton X-100 and 20 mM imidazole as described previously (Garza-Sánchez et al., 2006a). Proteins were purified by Ni²⁺-affinity chromatography under denaturing conditions in urea lysis buffer, followed by elution in urea lysis buffer supplemented with 25 mM EDTA. The purified proteins were dialyzed against water and lyophilized to be used as antigens to generate rabbit polyclonal antisera (Cocalico Biologicals, Inc., Reamstown, PA).

Samples were analyzed by SDS-PAGE using Tris-tricine-buffered gels run at 110 V. For Hcp, CdiB, and Tle immunoblots, samples were run on 10% polyacrylamide gels for 1 h. Tli samples were run on 10% polyacrylamide gels for 2 h 15 min, and CdiA samples were run on 6% polyacrylamide gels for 3.5 h. Gels were soaked for 10 min in transfer buffer (25 mM Tris, 192 mM glycine [pH 8.6], 20% methanol [10% methanol for CdiA gels]) before electroblotting to PVDF membranes using a semidry

transfer apparatus run at 17 V for 30 min. For CdiA, gels were electroblotted for 1 h. Membranes were blocked with 4% nonfat milk in 1 × phosphate-buffered saline (PBS) for 45 min at ambient temperature and then incubated with primary antibodies in 1 × PBS with 4% nonfat milk overnight. Rabbit polyclonal antisera for Hcp (Donato et al., 2020b), Tle, Tli, CdiA (Ruhe et al., 2015) and CdiB were used at dilutions of 1:10,000, 1:5,000, 1:5,000, 1:10,000, and 1:12,500, respectively. After three 10-min washes in 1 × PBS, the membranes were incubated with IRDye 800CW-conjugated goat anti-rabbit IgG (1:125,000 dilution) (Li-Cor) in 1 × PBS for 45 min. Immunoblots were visualized using a Li-Cor Odyssey infrared imager.

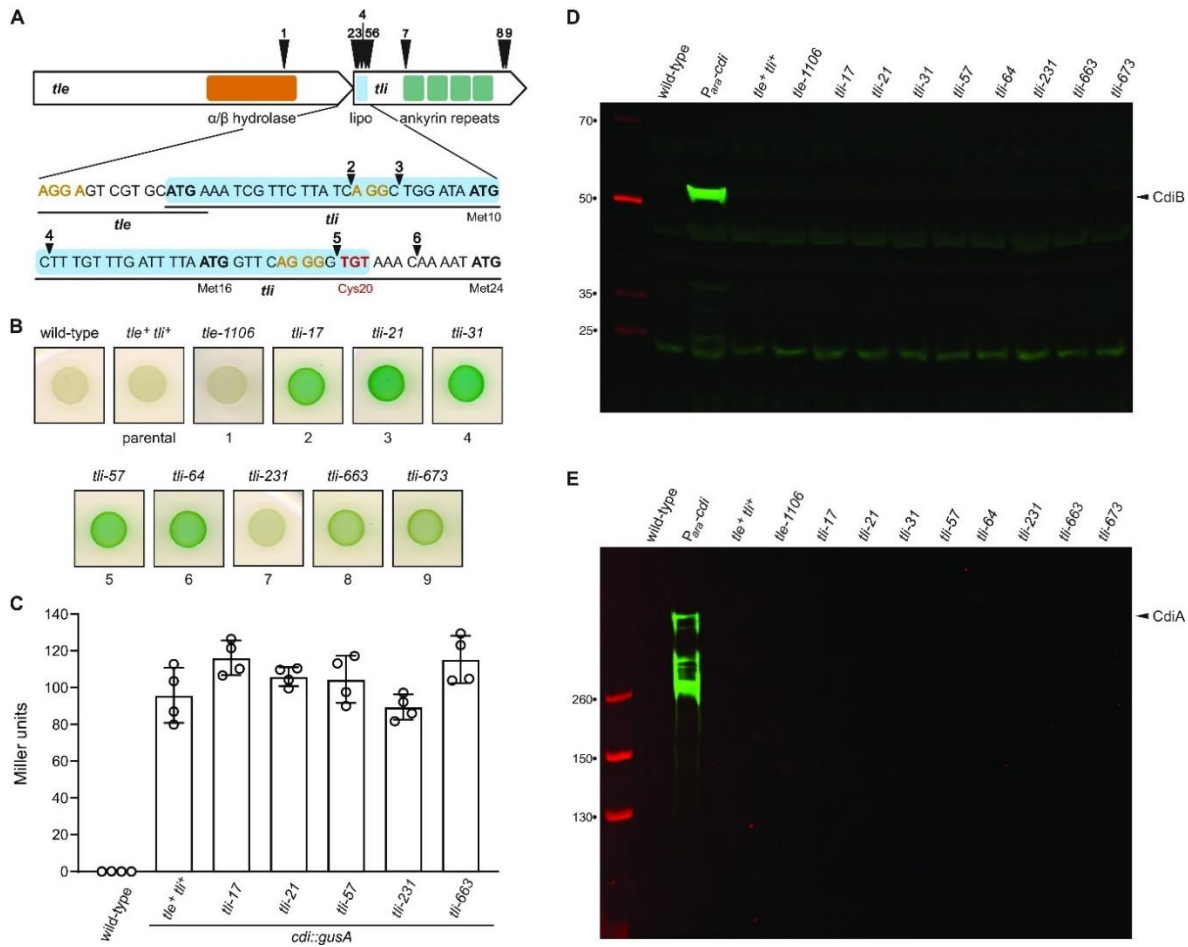


Figure 1 Identification of Tn5 insertions in the *tli* immunity gene.

(A) Schematic of Tn5 insertion sites in *tle* and *tli*. Regions encoding the predicted α/β -hydrolase domain of Tle and the Tli lipoprotein signal peptide (lipo) and ankyrin repeats are depicted. Alternative translation initiation codons (Met10, Met16, and Met24) are indicated, and possible ribosome-binding sites are shown in orange font. The codon for the lipidated Cys20 residue is shown in red font. (B) Wild-type ECL, the parental *cdi-gusA* reporter strain (*tle*⁺ *tli*⁺), and *tli* mutants were grown on LB agar supplemented with X-Gluc. (C) Quantification of β -glucuronidase activity in selected *tli* mutants. Activities were quantified as Miller units as described in Materials and Methods. Data for technical replicates from two independent experiments are shown with the average \pm standard deviation. (D and E) Tn5 insertions do not upregulate CdiB or CdiA production. Protein samples from wild-type ECL, the parental *tle*⁺ *tli*⁺ reporter strain, and *tli* mutants were subjected to immunoblot analysis using polyclonal antisera to CdiB (D) and CdiA (E). The *P*_{ara}-*cdi* sample is from an ECL strain that contains an arabinose-inducible promoter inserted upstream of the native *cdiBAI* gene cluster.

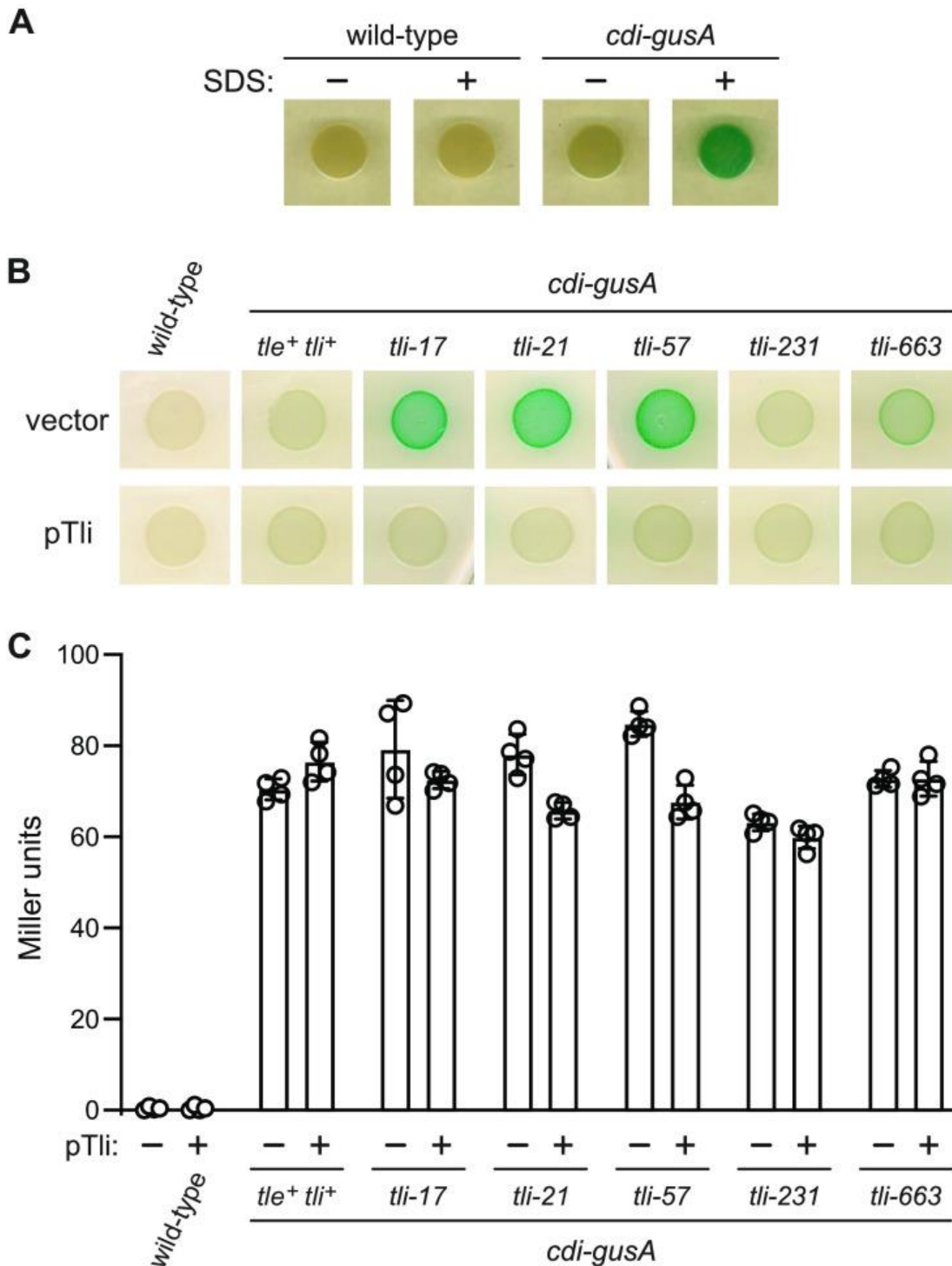


Figure 2 Disruption of *tli* increases cell permeability.

(A) ECL is impermeable to chromogenic X-Gluc substrate. Wild-type and *cdi-gusA* reporter cells were grown on LB agar supplemented with X-Gluc. Where

indicated, SDS solution (1% [wt/vol]) was applied to the edge of the colonies prior to imaging.

(B) The indicated ECL strains were complemented with plasmid-borne *tli* (pTli) or an empty vector and grown on LB agar supplemented with X-Gluc.

(C) Complementation with *tli* does not affect *cdi-gusA* reporter expression. β -Glucuronidase activities were quantified as Miller units as described in Materials and Methods. Data for technical replicates from two independent experiments are shown with the average \pm standard deviation.

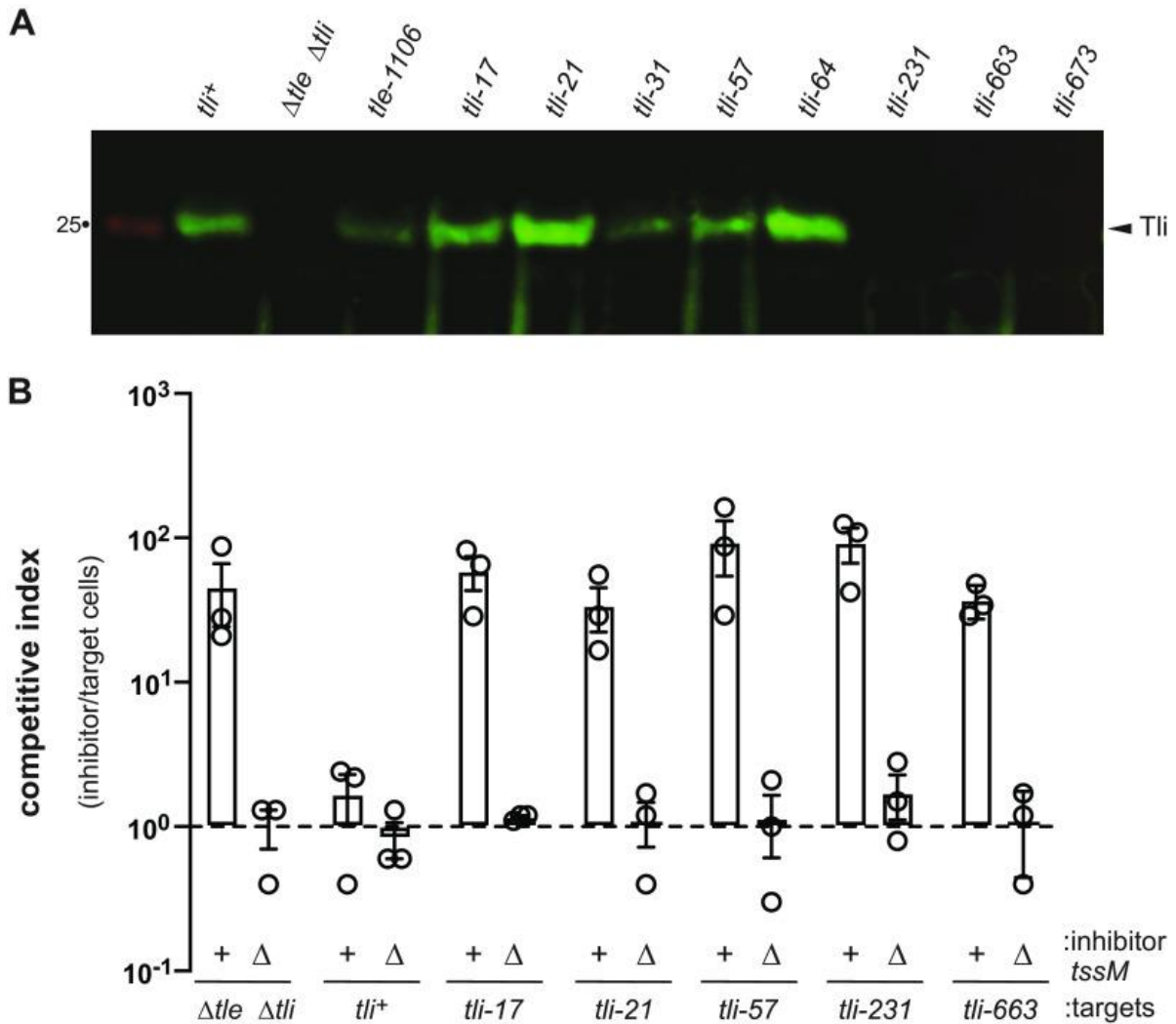


Figure 4 *tli* mutants produce Tli, but are not immune to Tle effector.

(A) *tli* mutants carrying Tn5 insertions in the lipoprotein signal sequence still produce immunity protein. Protein samples from the indicated ECL strains were subjected to immunoblot analysis using polyclonal antisera to Tli.

(B) Tn5 insertions ablate the immunity function of Tli. Wild-type ECL (*tssM*⁺) and mock ($\Delta tssM$) inhibitor strains were mixed with the indicated *tli* $\Delta tssM$ target cells and spotted onto LB agar. After 4 h of coculture, inhibitor and target cells were enumerated as CFU on selective media. The competitive index equals the final ratio of inhibitor to target cells divided by the initial ratio. Presented data are the average \pm standard error from three independent experiments.

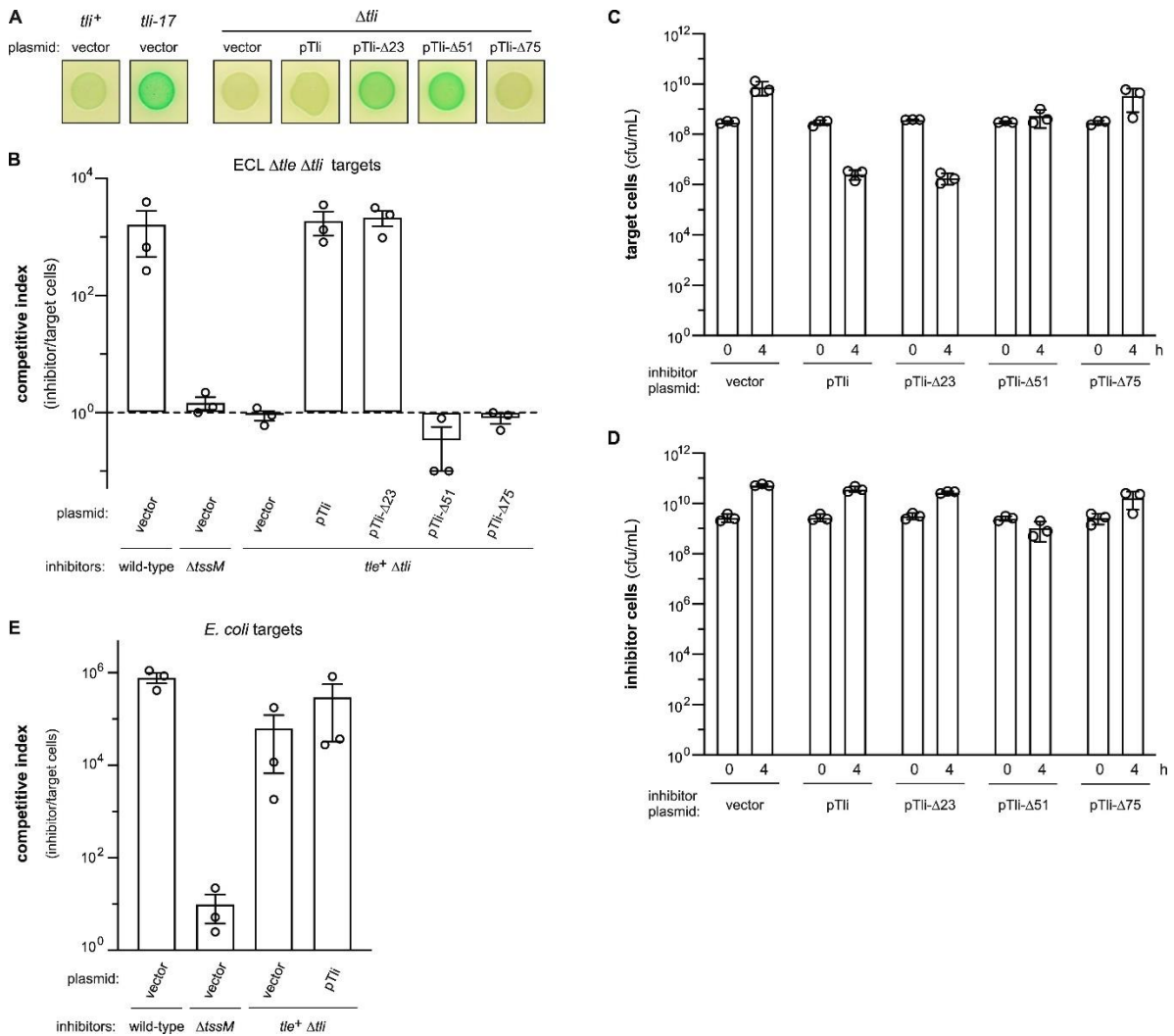


Figure 5 Δ *tli* mutants fail to deploy active Tle.

(A) ECL Δ *tli* mutants do not exhibit hyper-permeability. The indicated strains were grown on LB-agar supplemented with X-gluc. Where indicated, strains carried an empty vector or were complemented with plasmids that produce Tli variants.

(B) The indicated ECL inhibitor strains were mixed with ECL Δ *tle* Δ *tli* target cells and spotted onto LB-agar. After 4 h of co-culture, inhibitor and target cells were enumerated as colony forming units (cfu) on selective media. The competitive index equals the final ratio of inhibitor to target cells divided by the initial ratio. Presented data are the average \pm standard error from three independent experiments.

(C) Viable ECL Δ *tle* Δ *tli* target cell counts (cfu/mL) at 0 and 4 h for the cocultures shown in panel B.

(D) Viable inhibitor cell counts (cfu/mL) at 0 and 4 h for the cocultures shown in panel B. (E) ECL inhibitor strains were mixed with *E. coli* X90 target cells and spotted onto LB-agar. Co-culture conditions and cfu enumerations were the same as described for panel B.

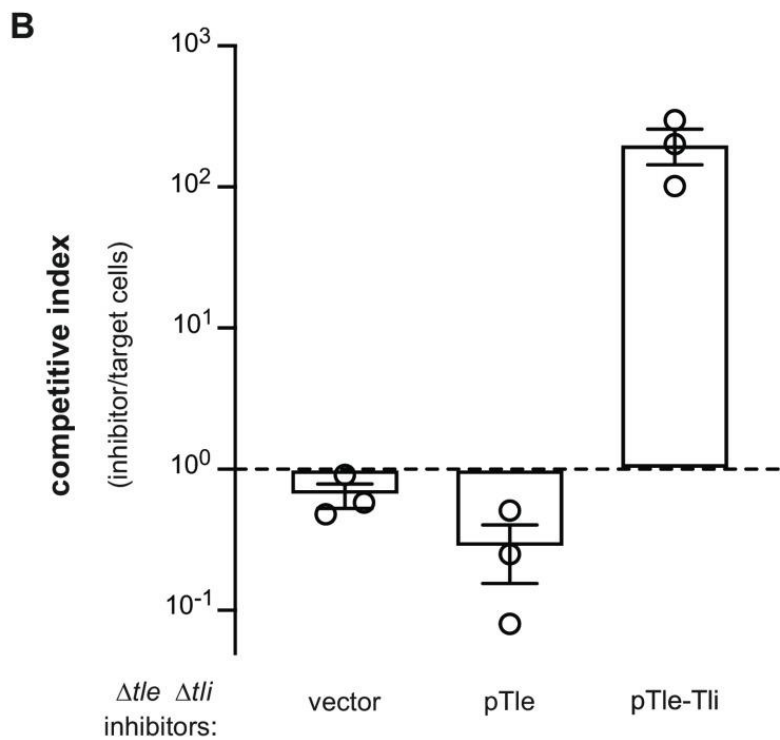
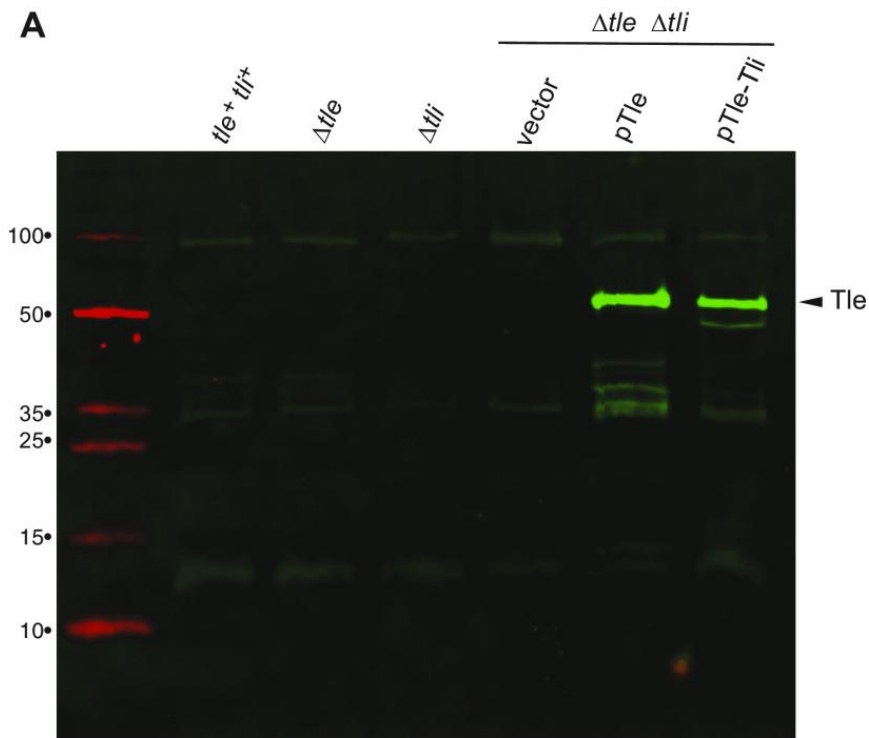


Figure 6 Tli is required for Tle-mediated growth inhibition.

(A) Cell extracts from the indicated ECL strains were subjected to immunoblot analysis using polyclonal antisera against the Tle lipase domain.

(B) The indicated ECL inhibitor strains were mixed with ECL $\Delta t/e$ $\Delta t/i$ target cells and spotted onto LB agar. After 4 h of coculture, inhibitor and target cells were enumerated as CFU on selective media. The competitive index equals the final ratio of inhibitor to target cells divided by the initial ratio. Presented data are the average \pm standard error from three independent experiments.

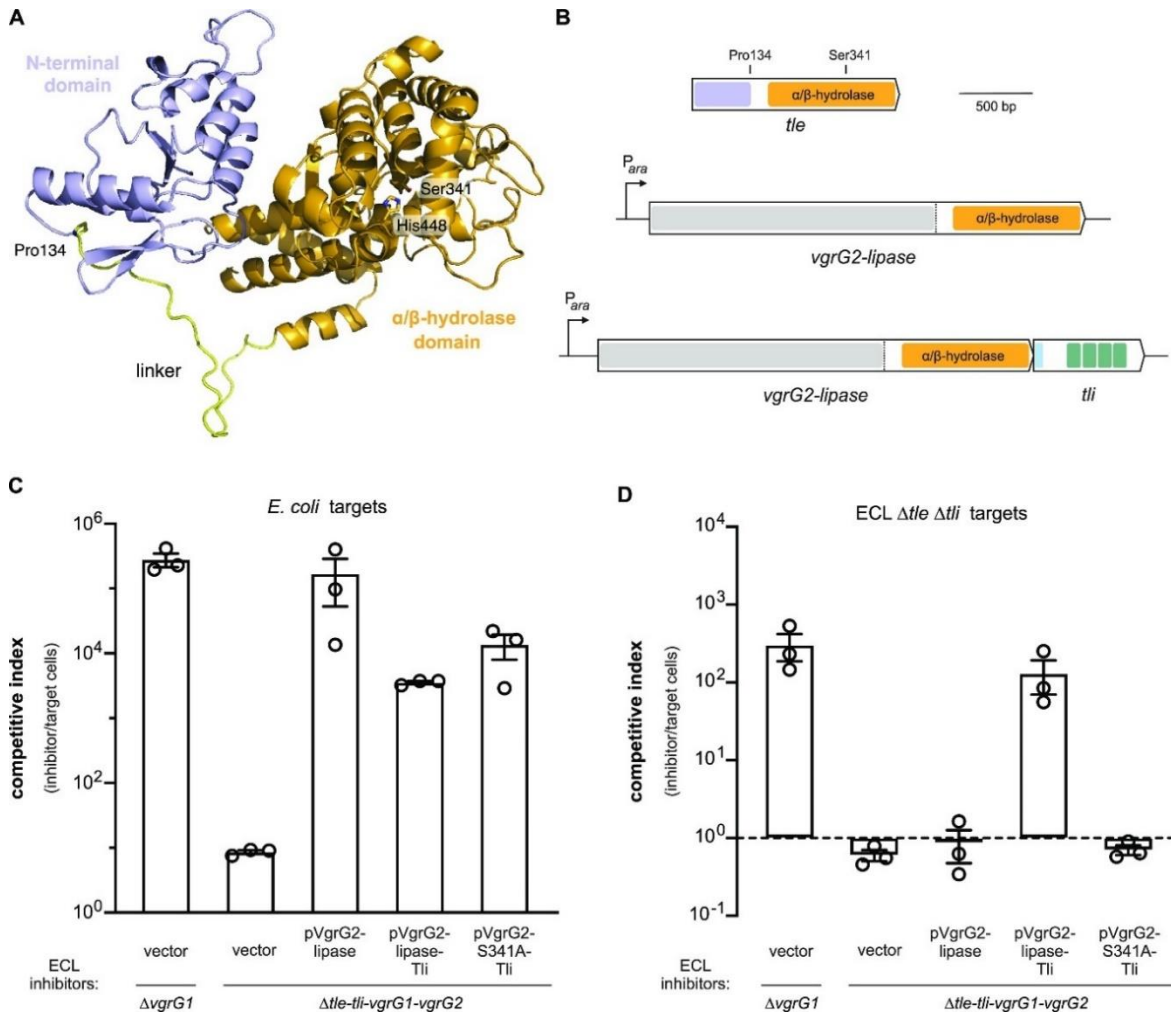


Figure 7 Tli is required to activate Tle prior to T6SS-mediated export.

(A) AlphaFold2 model of Tle. The C-terminal α/β -hydrolase domain is rendered in light orange and the linker region in yellow. The locations of predicted catalytic residues Ser341 and His448 are indicated. (B) VgrG2-lipase domain fusion schematic. Coding sequence for the Tle linker region (beginning at Pro134) and lipase domain was fused to *vgrG2* under the control of an arabinose-inducible promoter. A matched construct that also includes the wild-type *tli* gene was also generated. (C) The VgrG2-lipase fusion protein supports T6SS-1 activity. The indicated ECL inhibitor strains were mixed with *E. coli* X90 target cells and spotted onto LB agar supplemented with l-arabinose. After 4 h of coculture, inhibitor and target cells were enumerated as CFU on selective media. The competitive index equals the final ratio of inhibitor to target cells divided by the initial ratio. Presented data are the average \pm standard error from three independent experiments. (D) ECL inhibitor strains were mixed with ECL $\Delta tle \Delta tli$ target cells and spotted onto LB agar supplemented with l-arabinose. Coculture conditions and CFU enumerations were the same as described for panel C.

```

ECL_VgrG2      1 MLNR ITVQLFVEGLLFWKLSGREAMS ES FALTLTLLGTDAR IDRSK LLGQPVTVT IPTQNL LTPRY INGVTRVA 75
EH49162       1 MLNR ITVQLFVEGLLFWKLSGREAMS ES FALTLTLLGTDAR IDRSK LLGQPVTVT IPTQNL LTPRY INGVTRVA 75
NIC22         1 MLNR ITVQLFVEGLLFWKLSGREAMS ES FALTLTLLGTDAR IDRSK LLGQPVTVT IPTQNL LTPRY INGVTRVA 75
EH_e2355     1 MLNR ITVQLFVEGLLFWKLSGREAMS ES FALTLTLLGTDAR IDRSK LLGQPVTVT IPTQNL LTPRY INGVTRVA 75
EH_e1105     1 MLNR ITVQLFVEGLLFWKLSGREAMS ES FALTLTLLGTDAR IDRSK LLGQPVTVT IPTQNL LTPRY INGVTRVA 75
ECL_M-7-X3   1 MLNR ITVQLFAEGLLFWKLSGREAMS ES FALTLTLLGTDAR IDRSK LLGQPVTVT IPTHLL LTPRY INGVTRVA 75

ECL_VgrG2     76 VSAVELTGTRYAVYQLTVEPDLWPMKRDRNLRIFQGGTVVQIVKTL LLEGHQVNV EDKLTGSYR VWDYCVQYQESS 150
EH49162      76 VSAVELTGTRYAVYQLTVEPDLWPMKRDRNLRIFQGGTVVQIVKTL LLEGHQVNV EDKLTGSYR VWDYCVQYQESS 150
NIC22        76 VSAVELTGTRYAVYQLTVEPDLWPMKRDRNLRIFQGGTVVQIVKTL LLEGHQVNV EDKLTGSYR VWDYCVQYQESS 150
EH_e2355    76 VSAVELTGTRYAVYQLTVEPDLWPMKRDRNLRIFQGGTVVQIVKTL LLEGHQVNV EDKLTGSYR VWDYCVQYQESS 150
EH_e1105    76 VSAVELTGTRYAVYQLTVEPDLWPMKRDRNLRIFQGGTVVQIVKTL LLEGHQVNV EDKLTGSYR VWDYCVQYQESS 150
ECL_M-7-X3  76 VSAVELTGTRYAVYQLTVEPDLWPMKRDRNLRIFQGGTVVQIVKTL LLEGHQVNV EDKLTGSYR VWDYCVQYQESS 150

ECL_VgrG2    151 LDFISRLMELEGIAYYFSHEADKHTLVLTDAATQHQPFSGYEVIPIYHQTSGGGSTDEEGISQWAL EDSVTPGIYS 225
EH49162     151 LDFISRLMELEGIAYYFSHEADKHTLVLTDAATQHQPFSGYEVIPIYHQTSGGGSTDEEGISQWAL EDSVTPGIYS 225
NIC22       151 LDFISRLMELEGIAYYFSHEADKHTLVLTDAATQHQPFSGYEVIPIYHQTSGGGSTDEEGISQWAL EDSVTPGIYS 225
EH_e2355   151 LDFISRLMELEGIAYYFSHEADKHTLVLTDAATQHQPFSGYEVIPIYHQTSGGGSTDEEGISQWAL EDSVTPGIYS 225
EH_e1105   151 LDFISRLMELEGIAYYFSHEADKHTLVLTDAATQHQPFSGYEVIPIYHQTSGGGSTDEEGISQWAL EDSVTPGIYS 225
ECL_M-7-X3 151 LDFISRLMELEGIAYYFSHEADKHTLVLTDAATQHQPFSGYEVIPIYHQTSGGGSTDEEGISQWAL EDSVTPGIYS 225

ECL_VgrG2    226 LDDYDFRKPNAWLFQAQQNPASPKPGSIDVYDWPGRFVETGHA E FYARIRQERQVVEHQIQATATAAGIAPGHT 300
EH49162     226 LDDYDFRKPNAWLFQAQQNPASPKPGSIDVYDWPGRFVETGHA E FYARIRQERQVVEHQIQATATAAGIAPGHT 300
NIC22       226 LDDYDFRKPNAWLFQAQQNPASPKPGSIDVYDWPGRFVETGHA E FYARIRQERQVVEHQIQATATAAGIAPGHT 300
EH_e2355   226 LDDYDFRKPNAWLFQAQQNPASPKPGSIDVYDWPGRFVETGHA E FYARIRQERQVVEHQIQATATAAGIAPGHT 300
EH_e1105   226 LDDYDFRKPNAWLFQAQQNPASPKPGSIDVYDWPGRFVETGHA E FYARIRQERQVVEHQIQATATAAGIAPGHT 300
ECL_M-7-X3 226 LDDYDFRKPNAWLFQAQQNPASPKPGSIDVYDWPGRFVETGHA E FYARIRQERQVVEHQIQATATAAGIAPGHT 300

ECL_VgrG2    301 FTLTNAPFFSDNGEYLVTAAAGYHLEENRYASGEGETIHRIDFTVIPA SVSFRPAQSTAWPRTYGPQTA KVVGPQG 375
EH49162     301 FTLTNAPFFSDNGEYLVTAAAGYHLEENRYASGEGETIHRIDFTVIPA SVSFRPAQSTAWPRTYGPQTA KVVGPQG 375
NIC22       301 FTLTNAPFFSDNGEYLVTAAAGYHLEENRYASGEGETIHRIDFTVIPA SVSFRPAQSTAWPRTYGPQTA KVVGPQG 375
EH_e2355   301 FTLTNAPFFSDNGEYLVTAAAGYHLEENRYASGEGETIHRIDFTVIPA SVSFRPAQSTAWPRTYGPQTA KVVGPQG 375
EH_e1105   301 FTLTNAPFFSDNGEYLVTAAAGYHLEENRYASGEGETIHRIDFTVIPA SVSFRPAQSTAWPRTYGPQTA KVVGPQG 375
ECL_M-7-X3 301 FTLTNAPFFSDNGEYLVTAAAGYHLEENRYASGEGETIHRIDFTVIPA SVSFRPAQSTAWPRTYGPQTA KVVGPQG 375

ECL_VgrG2    376 ES IWTDKYGRVKVK FHWDR LAKGDDTSSCWVRVSSAWAGQGYGGVQIPRVGDEVVVD FINGDPRPIITGRVYND 450
EH49162     376 ES IWTDKYGRVKVK FHWDR LAKGDDTSSCWVRVSSAWAGQGYGGVQIPRVGDEVVVD FINGDPRPIITGRVYND 450
NIC22       376 ES IWTDKYGRVKVK FHWDR LAKGDDTSSCWVRVSSAWAGQGYGGVQIPRVGDEVVVD FINGDPRPIITGRVYND 450
EH_e2355   376 ES IWTDKYGRVKVK FHWDR LAKGDDTSSCWVRVSSAWAGQGYGGVQIPRVGDEVVVD FINGDPRPIITGRVYND 450
EH_e1105   376 ES IWTDKYGRVKVK FHWDR LAKGDDTSSCWVRVSSAWAGQGYGGVQIPRVGDEVVVD FINGDPRPIITGRVYND 450
ECL_M-7-X3 376 ES IWTDKYGRVKVK FHWDR LAKGDDTSSCWVRVSSAWAGQGYGGVQIPRVGDEVVVD FINGDPRPIITGRVYND 450

ECL_VgrG2    451 ASMP PWA LPA AATQMGFMSRTKDGSDVNANALRFEDKAGAEQVWIQAERNMDS IKNDETHSVGGERSHYVKKNE 525
EH49162     451 ASMP PWA LPA AATQMGFMSRTKDGSDVNANALRFEDKAGAEQVWIQAERNMDS IKNDETHSVGGERSHYVKKNE 525
NIC22       451 ASMP PWA LPA AATQMGFMSRTKDGSDVNANALRFEDKAGAEQVWIQAERNMDS IKNDETHSVGGERSHYVKKNE 525
EH_e2355   451 ASMP PWA LPA AATQMGFMSRTKDGSDVNANALRFEDKAGAEQVWIQAERNMDS IKNDETHSVGGERSHYVKKNE 525
EH_e1105   451 ASMP PWA LPA AATQMGFMSRTKDGSDVNANALRFEDKAGAEQVWIQAERNMDS IKNDETHSVGGERSHYVKKNE 525
ECL_M-7-X3 451 ASMP PWA LPA AATQMGFMSRTKDGSDVNANALRFEDKAGAEQVWIQAERNLDTSVKNDETHSVGGERSHYVKKNE 525

ECL_VgrG2    526 LHRVEANQIQAVKGGTEI LTGKGLDAAEQYV IASGTKRLVSGESA IELNANGK ILSLIGKEFN FVEGDGDI T 600
EH49162     526 LHRVEANQIQAVKGGTEI LTGKGLDAAEQYV IASGTKRLVSGESA IELNANGK ILSLIGKEFN FVEGDGDI T 600
NIC22       526 LHRVEANQIQAVKGGTEI LTGKGLDAAEQYV IASGTKRLVSGESA IELNANGK ILSLIGKEFN FVEGDGDI T 600
EH_e2355   526 LHRVEANQIQAVKGGTEI LTGKGLDAAEQYV IASGTKRLVSGESA IELNANGK ILSLIGKEFN FVEGDGDI T 600
EH_e1105   526 LHRVEANQIQAVKGGTEI LTGKGLDAAEQYV IASGTKRLVSGESA IELNANGK ILSLIGKEFN FVEGDGDI T 600
ECL_M-7-X3 526 LHRVEANQIQAVKGGTEI LTGKGLDAAEQYV IASGTKRLVSGESA IELNANGK ILSLIGKEFN FVEGDGDI T 600

ECL_VgrG2    601 TGKGLHLNLTSGAKPGTTAPGSHKGDIDAAVQAK FTTKGD----- 640
EH49162     601 TGKGLHLNLTSGTQPGTTAPGSHKGDIDAAVQEK FSPNKS AKNPAPAASAPAA--TRPKP---TTKFVSAPPLKG 670
NIC22       601 TGKGLHLNLTSGTQPGTTAPGSHKGDIDAAVQEK FSPGKESKAGAVA-SAPAD--T-PQA---ATPST----- 661
EH_e2355   601 TGKGLHLNLTSGTKPGTTAPGSHKGDIDAAVQEK FSPQRKKGAGAS-PVPS EATKPAPQATASNAT SAPP TQG 674
EH_e1105   601 TGKGLHLNLTSGTKPGTTAPGSHKGDIDAAVQEK FSPNKS AKNPAPAVSAPAA--SRPKP---TTKFAAPP LKG 670
ECL_M-7-X3 601 TGKGLHLNLTSGTKPGTTAPGSHKGDIDAAVQAY FSPDKAKKSAGAGAAGGAGKAA-PAQN--NSAASAGTDKTS 672

ECL_VgrG2    671 SYYYQNNSSYNSDVMPFS EDVVKIEINKSPTLQTQLKDLKDKGWA IQPGAAGGGSYAD----TNNK L-IVMDPE-H 738
EH49162     662 -----SNVPS SGGYKDVDSLVDK SPTMKND IATLKKRGWTFEEGEAGKGT FAN----RQTRV-ITVDKN-E 721
NIC22       675 EDKFSKIS-----P I I-----FQNEGGYVNDPNDSGGATNKG-----IAWK TWQYAK E-D 719
EH_e2355   671 SYYYQNNSSYNSDVMPFS EDVVKIEINKSPTLQTQLKDLKDKGWA IQPGAAGGGSYAD----TNNK L-IVMDPE-H 738
EH_e1105   671 SYYYQNNSSYNSDVMPFS EDVVKIEINKSPTLQTQLKDLKDKGWA IQPGAAGGGSYAD----TNNK L-IVMDPE-H 738
ECL_M-7-X3 673 EYDY-----S LQDMV DQK N L K A K P Q K W T R R G F V D A S E D D I - K Y A N P D N Y N T G D K Y Q F L D L S S 732

ECL_VgrG2    739 M---EDTATT VQT LAHEAGHATYPVAVDSSSKENFINSQ-----LMDEGGAT-----LNNIKIQRE 791
EH49162     722 L--GNPEVVQSLSHESGHALYEPNIDVSSREAYLNST-----LSDEGAAT-----LNNIRVRQE 774
NIC22       720 LGVEPTLDNLK NLTNEQAETIYRKYWEP S GFNNLNDPK-----LALMSYDWTITSGGAGKQIQKLLNNEFGQQ 788
EH_e2355   739 M---EDTATT VQT LAHEAGHATYPVAVDSSSKENFINSQ-----LMDEGGAT-----LNNIKIQRD 791
EH_e1105   733 SGVSE--TDMASFLK--GK-----GVLEGEQKTYLDAARKYVNS EVYLASHSALETGN GAS-E LAK-----G 789
ECL_M-7-X3

ECL_VgrG2    792 ILSNGGIDID IAGSAENLKAYNSAYDKMVNGELSRIDA-----AKAIGKVVYKGEI AS 844
EH49162     775 I IANKGGDIGIAGNPANQPQYNR IYDSL ERGAIKES EA-----RTQIGRIFGKGEQTS 827
NIC22       789 LIADGKIG-----PKTIEAMNSVSDSAKL-----TSR-----IADIRKEYYEN--LV 828
EH_e2355   792 PCKRRY-----797
EH_e1105   790-----V EV-----NGVKVY-----NMYG I GALDGNVAKTGSNYAYKMGWTSPEKAI EGGAKWIS EKYINNADYA 848
ECL_M-7-X3

ECL_VgrG2    845 GTNLNYNDYGGFYGK-----P----- 860
EH49162     828 TTQYQYEDYGGWYDKNY-----RCAQVAL----- 846
NIC22       829 VNSKNKAKFLTGLNLRVD----- 853
EH_e2355   849 QNN----LYKMRWNPA SPTGHQYATDVNVAWAQTS SMMKMFDFNFPAA NLSYDIPKFK 901
EH_e1105
ECL_M-7-X3

```

Figure S1. Evolved VgrG proteins from *Enterobacter* species.

VgrG2 from *Enterobacter cloacae* ATCC 13047 was aligned with homologs from *Enterobacter hormaechei* ATCC 49162 (NCBI Refseq: WP_006810934.1), *Enterobacter* sp. NIC22-4 (WP_221813114.1), *Enterobacter hormaechei* e2355 (WP_058700648.1), *Enterobacter hormaechei* e1105 (CZV11788.1), and

Enterobacter cloacae M-7-X3 (WP_165464354.1) using Clustal Omega and rendered with Jalview 2.11.2.6. Residues are colored according to sequence identity. The C-terminal extension domains from ATCC 49162, NIC22-4 and e1105 are predicted to fold into metallopeptidase domains by AlphaFold2. The effector domain from e2355 is homologous to *N*-acetylmuramidases (lysozyme), and the domain from M-7-X3 is a predicted LytD β -*N*-acetylglucosaminidase.

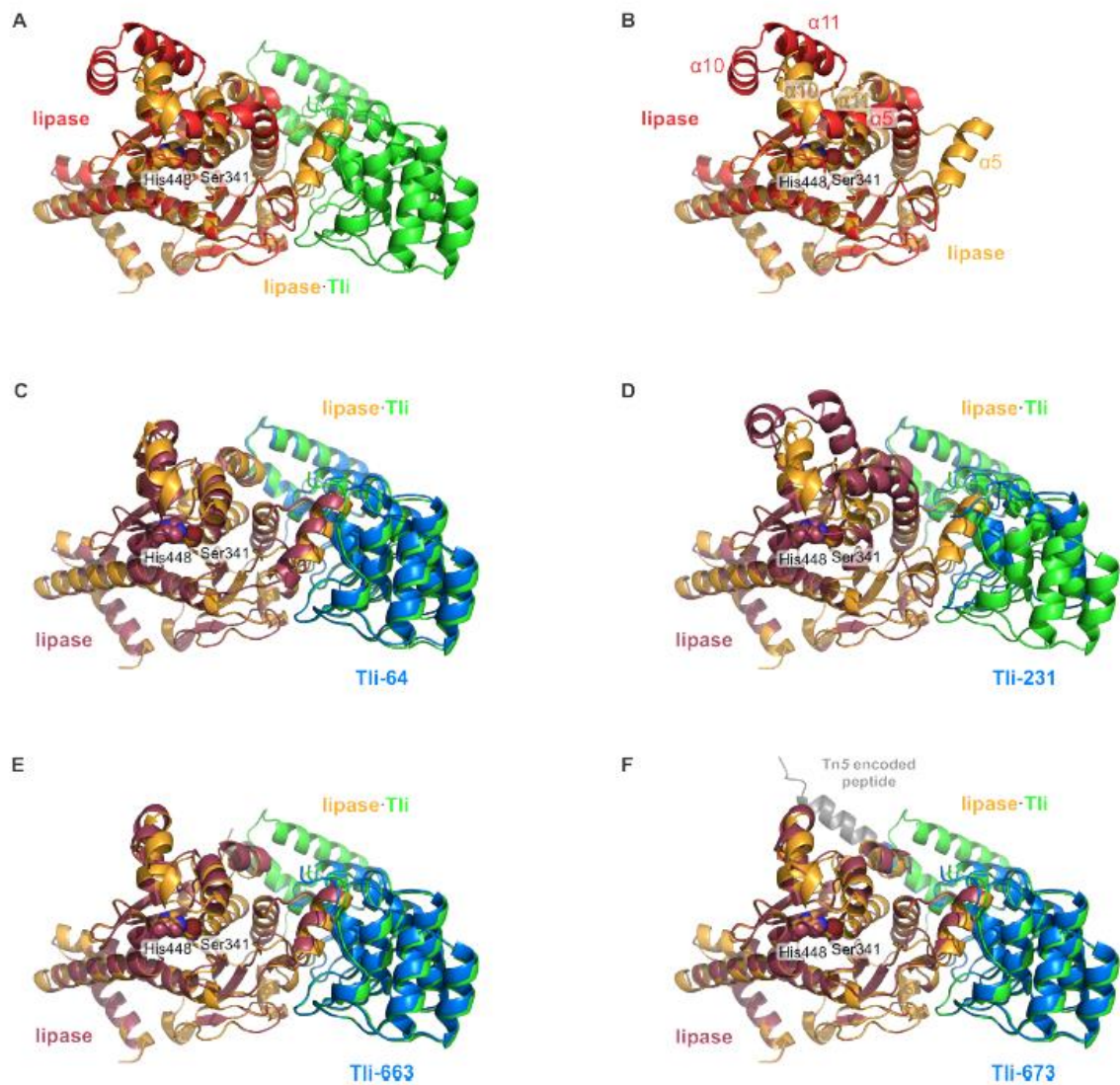


Figure S2. AlphaFold2 modeling of lipase-immunity protein complexes.

A) Superimposition of structural models for the isolated lipase domain (red) and the lipase (orange) • Tli (green) complex.

B) Predicted conformational changes in the lipase domains from panel A. The positions of helices $\alpha 5$, $\alpha 10$ and $\alpha 11$ are indicated for the isolated lipase (red) and Tli-bound domain (orange). Models of the lipase domain (raspberry) bound to Tli-64 (**C**), Tli-231 (**D**), Tli-663 (**E**) and Tli-673 (**F**) immunity proteins colored in marine. The latter complexes are superimposed onto the wild-type lipase•Tli complex from panel A for comparison. The Tn5 encoded extension at the C-terminus of Tli-673 is colored gray

(F). Catalytic Ser341 and His448 residues are rendered as spheres and indicated in each panel.

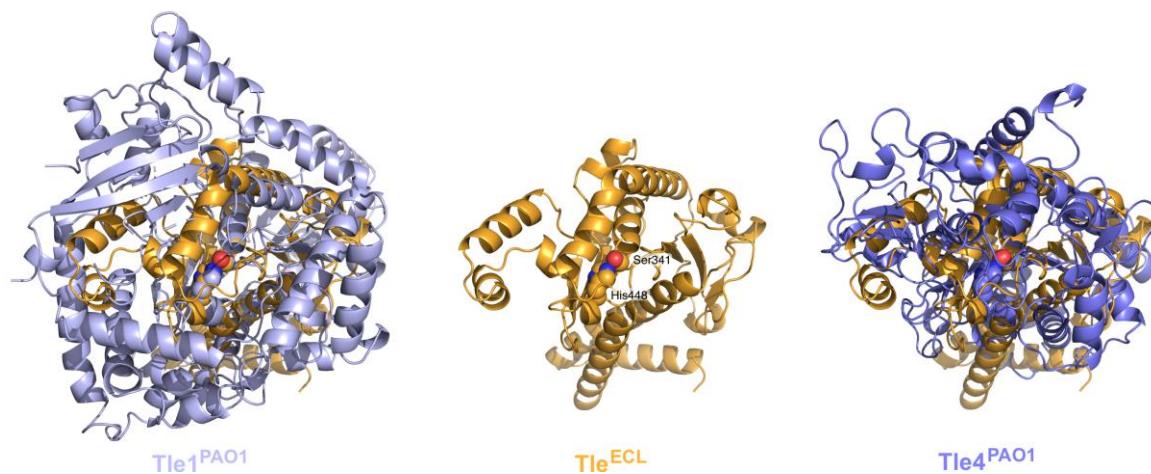


Figure S3. Superimposition of Tle1 and Tle4 with the structural model for the TleECL lipase domain.

The AlphaFold2 model of the TleECL lipase domain was superimposed onto the structures of Tle1 (PDB: 4O5P) and Tle4 (PDB: 4R1D) from *Pseudomonas aeruginosa* PAO1. The predicted active-site residues Ser341 and His448 are indicated in the Tle^{ECL} model, and corresponding Tle1 and Tle4 catalytic residues are rendered as spheres in the structure overlays.

Table 1 Bacterial strains used in this study

Strain	Description ^a	Reference or source
CH1360	ECL $\Delta tle-tli-vgrG1-vgrG2::kan$ Kan ^r	This study
CH2016	<i>E. coli</i> X90(DE3) $\Delta rna \Delta slyD::kan$ Kan ^r	(Garza-Sánchez et al., 2006a)
CH3469	ECL $\Delta tli glmS::cdi-gusA$ Gent ^r	This study
CH11196	ECL $\Delta tssM1::kan$ Kan ^r	(Beck et al., 2014)
CH11199	ECL $\Delta hcp1::spc$ Spec ^r	(Donato et al., 2020)
CH11248	ECL <i>araC</i> - $P_{BAD}::cdiB \Delta araBAD::kan$ Spec ^r Kan ^r	(Beck et al., 2014)
CH11396	ECL $\Delta tssM1$	(Donato et al., 2020)
CH11876	ECL $\Delta tle::kan$ Kan ^r	(Donato et al., 2020)
CH11895	ECL $\Delta tle \Delta tli::spc$ Spec ^r	(Donato et al., 2020)
CH12384	ECL $\Delta vgrG1::kan$ Kan ^r	(Whitney et al., 2014)
CH14384	ECL $\Delta tle \Delta tli::spc rif$ Spec ^r Rif ^r	This study
CH14587	ECL $\Delta tli::kan$ Kan ^r	This study
CH14588	ECL Δtli	This study
E2072	<i>E. coli</i> F ⁻ $\lambda^- mcrA \Delta(mrr-hsdRMS-mcrBC)$ $\phi 80dlacZ \Delta M15 \Delta lacX74 deoR recA1 endA1$ <i>galU galK rpsL nupG</i> $\Delta dapA::pir-lacI^q$ -Gent ^r - FRT8 <i>mob[recA::RP4-2 Tc::Mu-</i> Kan ^r] <i>leu</i> ⁺ Str ^r Gent ^r Kan ^r	(Zarzycki-Siek et al., 2013)
ECL	<i>Enterobacter cloacae</i> subsp. <i>cloacae</i> ATCC 13047	ATCC
MFD <i>pir</i>	<i>E. coli</i> MG1655 RP4-2-Tc::[$\Delta Mu1::aac(3)IV-$ $\Delta aphA-\Delta nic35-\Delta Mu2::zeo$] <i>dapA::(erm-pir)</i> $\Delta recA$ Apr ^r Zeo ^r Erm ^r	(Ferrières et al., 2010)
X90	<i>E. coli</i> F' <i>lacI</i> ^q <i>lac' pro' lara</i> $\Delta(lac-pro)$ <i>nal1</i> <i>argE</i> (Amb) <i>rif thi-1</i> Rif ^r	(Beckwith & Signer, 1966)
ZR71	ECL $glmS::cdi-gusA$ Gent ^r	This study
ZR135	ZR71 <i>tli-231</i> ; Tn5 insertion after <i>tli</i> nucleotide 231; Gent ^r Spec ^r	This study
ZR137	ZR71 <i>tli-21</i> ; Tn5 insertion after <i>tli</i> nucleotide 21; Gent ^r Spec ^r	This study
ZR138	ZR71 <i>tli-57</i> ; Tn5 insertion after <i>tli</i> nucleotide 57; Gent ^r Spec ^r	This study
ZR139	ZR71 <i>tli-663</i> ; Tn5 insertion after <i>tli</i> nucleotide 663; Gent ^r Spec ^r	This study
ZR140	ZR71 <i>tli-17</i> ; Tn5 insertion after <i>tli</i> nucleotide 17; Gent ^r Spec ^r	This study
ZR148	ZR71 <i>tli-231</i> $\Delta tssM::kan$ Gent ^r Spec ^r Kan ^r	This study
ZR149	ZR71 <i>tli-21</i> $\Delta tssM::kan$ Gent ^r Spec ^r Kan ^r	This study
ZR150	ZR71 <i>tli-57</i> $\Delta tssM::kan$ Gent ^r Spec ^r Kan ^r	This study
ZR151	ZR71 <i>tli-663</i> $\Delta tssM::kan$ Gent ^r Spec ^r Kan ^r	This study
ZR152	ZR71 <i>tli-17</i> $\Delta tssM::kan$ Gent ^r Spec ^r Kan ^r	This study

ZR161	ZR71 <i>tli-31</i> ; Tn5 insertion after <i>tli</i> nucleotide 31; Spec ^r Gent ^r	This study
ZR163	ZR71 <i>tIe-1106</i> ; Tn5 insertion after <i>tIe</i> nucleotide 1106; Spec ^r Gent ^r	This study
ZR165	ZR71 <i>tli-673</i> ; Tn5 insertion after <i>tli</i> nucleotide 673; Spec ^r Gent ^r	This study
ZR170	ZR71 <i>tli-64</i> ; Tn5 insertion after <i>tli</i> nucleotide 64; Spec ^r Gent ^r	This study
ZR200	ZR71 Δ <i>tssM::kan</i> Gent ^r Kan ^r	This study

TABLE 2 Plasmids used in this study

Plasmid	Description	Reference
pBR322	Cloning vector; Amp ^r Tet ^r	(Bolivar et al., 1977)
pCH70	pBluescript with FRT-flanked Kan ^r cassette ligated into SmaI restriction site; Amp ^r Kan ^r	(Hayes et al., 2002)
pCH371	pCATKAN- <i>pheS</i> (A294G); Cm ^r Kan ^r	This study
pCH377	pCAT- <i>pheS</i> (A294G); Cm ^r	This study
pCH417	pCH450:: <i>vgrG2</i> (ECL)- <i>CT/vgrI</i> (<i>Eh49162</i>); Tet ^r	This study
pCH450	pACYC184 derivative with <i>E. coli araC</i> and <i>araBAD</i> promoter for arabinose-inducible expression; Tet ^r	(Hayes & Sauer, 2003)
pCH494	pCH450K:: <i>tli</i> ; Tet ^r	(Donato et al., 2020)
pCH495	pCH450K:: <i>tli</i> ($\Delta 23$); Tet ^r	This study
pCH1359	pCATKAN- <i>pheS</i> (A294G)- $\Delta tle-tli-vgrG1-vgrG2$; Cm ^r Kan ^r	This study
pCH3128	pCH450:: <i>tle-tli</i> ; Tet ^r	This study
pCH3291	pET21:: <i>tli</i> ($\Delta 23$); Amp ^r	This study
pCH3468	pUC18T-mini-Tn7T-Gm with the ECL <i>cdi</i> promoter region fused to <i>E. coli gusA</i> within mini-Tn7; Amp ^r Gent ^r	This study
pCH3763	pCH450:: <i>vgrG2-lipase</i> (S341A)- <i>tli</i> ; Tet ^r	This study
pCH3884	pCATKAN- <i>pheS</i> (A294G)- Δtli ; Cm ^r Kan ^r	This study
pCH5036	pCH450K:: <i>tli</i> ($\Delta 51$); Tet ^r	This study
pCH5037	pCH450K:: <i>tli</i> ($\Delta 75$); Tet ^r	This study
pCH6118	pET21b:: <i>cdiB</i> (STEC3); Amp ^r	This study
pCH9062	pCH450:: <i>vgrG2-lipase-tli</i> ; Tet ^r	This study
pCH9063	pCH450:: <i>vgrG2-lipase</i> ; Tet ^r	This study
pCH9384	pBluescript with FRT-flanked Spec ^r cassette ligated into SmaI restriction site; Amp ^r Spec ^r	(Koskiniemi et al., 2013b)
pCH11050	pCH70 with regions upstream and downstream of ECL <i>tssM1</i> ; Amp ^r Kan ^r	(Beck et al., 2014)
pCH11198	pCH450:: <i>tssM</i> ; Tet ^r	This study
pCH14212	pCH450:: <i>tle</i> ; Tet ^r	This study
pCH15269	pSH21P:: <i>lipase</i> ; Amp ^r	This study
pCP20	Temp-sensitive replication origin, expresses FLP recombinase; Amp ^r Cm ^r	(Pérez et al., 2007)
pDAL912	pBR322:: <i>pheS</i> (A294G); Amp ^r	This study
pDAL6480	pRE118- <i>pheS</i> (A294G); Kan ^r	This study
pKOBEG	Temp-sensitive replication origin, expresses the Bet-Gam-Exo proteins from phage λ ; Cm ^r	(Cherepanov & Wackernagel, 1995)
pLG99	Tn5 transposase expression vector harboring a mini-Tn5 derivative with <i>P_{rhaB}</i> -out; Amp ^r Tmp ^r	(Gallagher et al., 2013)

pLG99- <i>spec</i>	pLG99 with <i>Spec^r</i> cassette cloned into Tn5; <i>Amp^r Spec^r</i>	This study
pRE118	Vector plasmid for <i>sacB</i> allelic exchange; <i>Kan^r</i>	(Edwards et al., 1998)
pSCBAD	pBBR1 derivative that carries <i>araC</i> and <i>P_{BAD}</i> promoter; <i>Tmp^r</i>	(Koskiniemi et al., 2015)
pTNS2	Expresses Tn7 transposase, <i>Amp^r</i>	(Choi et al., 2005)
pUC18T-mini-Tn7T-Gm	Tn7 transposase expression vector harboring mini-Tn7 with <i>Gent^r</i> cassette; <i>Amp^r Gent^r</i>	(Choi et al., 2008)
pZR42	pUC18T-mini-Tn7T-Gm with <i>E. coli gusA</i> ; <i>Amp^r Gent^r</i>	This study

Table S1. ECL Tle family phospholipases

Effector class	Bacterial strain	NCBI Refseq	length	predicted ankyrin-repeat immunity protein(s)
Tle	<i>Enterobacter cloacae</i> subsp. <i>cloacae</i> ATCC 13047	WP_013096193.1	472	WP_013096194.1
	<i>Enterobacter hormaechei</i> ATCC 49162	WP_006810941.1	488	WP_006810940.1
	<i>Pseudoscherichia vulneris</i> NCTC12130	WP_042387755.1	496	WP_042388579.1; WP_042387753.1; WP_115084734.1
	<i>Cronobacter sakazakii</i> ATCC BAA-894	WP_007853550.1	476	WP_007889010.1
	<i>Cronobacter condimenti</i> 1330	WP_007668262.1	488	WP_007668245.1
	<i>Kosakonia sacchari</i> SP1	WP_017456470.1	472	WP_017456469.1
	<i>Phytobacter massiliensis</i> JC163	WP_044180714.1	468	WP_237567481.1
	<i>Lelliottia nimpresuralis</i> 51	TFB20627.1	472	TFB20626.1
	<i>Citrobacter</i> sp. R56	WP_203360225.1	488	WP_203361220.1
	<i>Salmonella enterica</i> subsp. <i>enterica</i> serovar <i>Newport</i>	EBR8158188.1	488	EBR8158189.1
	<i>Franconibacter</i> sp. IITDAS19	WP_024557997.1	479	WP_247365411.1
	<i>Phytobacter</i> sp. SCO41	WP_108700663.1	474	WP_108700662.1
	<i>Serratia ureilytica</i> SER00108	WP_197777867.1	493	I5P71_RS11495 (pseudo); WP_197776957.1
	<i>Serratia marcescens</i> BWH-23	AVU29874.1	493	AVU29874.1; AVU29875.1
	<i>Serratia marcescens</i> MGH135	WP_033646675.1	493	WP_025302229.1
	<i>Serratia marcescens</i> Db11	WP_025302228.1	493	WP_025302229.1; WP_025302230.1
PAAR	<i>Lonsdalea quercina</i> NCCB 100489	WP_027063756.1	464	WP_026739306.1
	<i>Brenneria</i> sp. L3-3C-1	WP_199379546.1	456	WP_199379544.1; WP_199379560.1; WP_233356511.1
	<i>Pectobacterium carotovorum</i> subsp. <i>carotovorum</i> PC1	WP_015841393.1	456	WP_043881824.1
	<i>Dickeya dadantii</i> 3937	WP_013317122.1	456	WP_013317123.1; WP_237703452.1
	<i>Dickeya chrysanthemi</i> Ech1591	WP_012770502.1	456	WP_012770501.1; WP_012770500.1; WP_012770499.1
	<i>Vibrio nigrivulvatus</i> ATCC 27043	WP_004404991.1	513	WP_004404995.1
	<i>Vibrio parahaemolyticus</i> JW16-127	EHA1109881.1	513	EHA1109882.1
	<i>Vibrio mimicus</i> VM223	WP_001138502.1	505	WP_000199146.1; WP_000934380.1
	<i>Polyangium aurulentum</i> SDU3-1	WP_169508841.1	421	WP_136926720.1
DUF4150 (PAAR-like)	<i>Pantoea</i> sp. PSNIH2	AIX74951.1	422	AIX74950.1
	<i>Franconibacter pulveris</i> LMG 24059	WP_029591452.1	431	WP_029591453.1
	<i>Halopseudomonas salegens</i> CECT 8338	WP_092383249.1	434	WP_197675042.1
	<i>Tahibacter caeni</i> BUT-6	WP_257385295.1	424	WP_257385296.1
	<i>Xanthomonas translucens</i> pv. <i>cerealis</i>	WP_142742694.1	419	WP_221887383.1
	<i>Xanthomonas youngii</i> AmX2	WP_206232757.1	433	WP_206232758.1
	<i>Sorangium</i> sp. Soce836	AUX33661.1	396	AUX33660.1
	<i>Sorangium cellulosum</i> So0157-2	WP_020737320.1	409	WP_020737319.1
	<i>Thauera butanivorans</i> NBRC 103042	WP_068639422.1	433	WP_157659236.1; WP_068639420
	<i>Lamprospira aestuarii</i> YIM MLB12	WP_136407722.1	437	WP_136407723.1; WP_136407723.1
	<i>Burkholderia vietnamiensis</i> AU35216	WP_249181664.1	382	WP_150331737.1
	<i>Burkholderia thailandensis</i> B10013	WP_150331736.1	400	WP_150331737.1; WP_150331738.1
<i>Burkholderia pseudomallei</i> MSHR7500	WP_038799229.1	396	WP_038799227.1	
VgrG	<i>Aggregatibacter actinomycetemcomitans</i> SL7469	MBN6065491.1	1060	MBN6065490.1
	<i>Pasteurella testudinis</i> NCTC12150	WP_115306396.1	1018	WP_115306395.1
	<i>Burkholderia gladioli</i> BSR3	WP_013700226.1	996	WP_013700225.1
	<i>Burkholderia multivorans</i> AU16734	WP_105792066.1	1001	WP_059936093.1
	<i>Burkholderia cepacia</i> ATCC 25416	WP_027786768.1	999	WP_226153282.1
	<i>Desulfuromonas versatilis</i> NIT-T3	WP_221250508.1	1082	WP_221250509.1
	<i>Chondromyces crocatus</i> Cm c5	WP_063796395.1	1019	WP_050434209.1
	<i>Geobacter benzotilysiticus</i> Jerry-YX	WP_207164315.1	942	WP_207164316.1
	<i>Cystobacter fuscus</i> DSM 52655	WP_157758952.1	1050	WP_157758953.1
	Rhs	<i>Pseudomonas fluorescens</i> UM270	WP_042727971.1	4024
<i>Pseudomonas palleroniana</i> PS006		WP_060752379.1	3668	WP_158510675.1
<i>Vibrio vulnificus</i> NBRC 15645 = ATCC 27562		WP_017422738.1	1515	WP_017422739.1
<i>Vibrio cincinnatiensis</i> 19-VB00020		WP_238132309.1	1558	WP_238124837.1
CdiA	<i>Desulfovibrio subterraneus</i> ND17	WP_269890085.1	1965	WP_269890084.1
	<i>Cupidesulfovibrio liaohensis</i> XJ01	WP_167127856.1	1900	WP_167127853.1 (partial)
	<i>Desulfomicrobium</i> sp. ZS1	WP_254080456.1	2300	WP_254080455.1
	<i>Pseudodesulfovibrio piezophilus</i> C1TLV30	CCH47381.1	1774	CCH47382.1

Table S2. Oligonucleotides

Identifier	Description	Sequence	Reference
CH2020	ARB1	5' - GGC CAC GCG TCG ACT AGT ACN NNN NNN NNN GAT AT	This study
CH2021	ARB2	5' - GGC CAC GCG TCG ACT AGT AC	This study
CH2022	ARB6	5' - GGC CAC GCG TCG ACT AGT ACN NNN NNN NNN ACG CC	This study
CH3023	tssM-Nco-for	5' - TTT <u>CCA TGG</u> TGA CGA CTC TTC TTT C	This study
CH3024	tssM-Xho-rev	5' - TTT <u>CTC GAG</u> TTA TGG GCA TGA GAA ACG	This study
CH3025	gusA-Eco-for	5' - TTT <u>GAA TTC</u> TTAATG AGG AGT CCC TTA TCT TAC	This study
CH3026	gusA-Sac-rev	5' - TTT <u>GAG CTC</u> GAT TCA TTG TTT GCC TCC CTG	This study
CH3146	ECL-Pcdi-Kpn	5' - TTT <u>GGT ACC</u> GTT ACG GCG GTC AAT CAG ATC	This study
CH3147	ECL-PcdiB-Eco	5' - TTT <u>GAA TTC</u> ACT GCC ACT CCT TGC TAA AAG	This study
CH3197	vgrG2(KO)-Xho	5' - TTT <u>CTC GAG</u> GCT GGA GCG GTG CTT G	(Whitney et al., 2014)
CH3198	vgrG2(KO)-Kpn	5' - TTT <u>GGT ACC</u> CGA GTC CAG ACA ATC AGG	(Whitney et al., 2014)
CH3247	vgrG2-Xho-rev	5' - TTT <u>CTC GAG</u> GTT CCG CCT TTT ACC GC	This study
CH3373	tli(KO)-Sac	5' - CAA <u>GAG CTC</u> CGG GAT GGT TGC C	This study
CH3374	tli(KO)-Bam	5' - ATT <u>GGA TCC</u> GTC CTG TTA CCA GTC	This study
CH3377	tle(KO)-Xho	5' - CCA <u>ACT CGA</u> GTT AAA TAG GAA ACG	(Donato et al., 2020)
CH3378	tle(KO)-Kpn	5' - CCA <u>GGT ACC</u> AAA GTG CTG TGT GC	((Donato et al., 2020)
CH3418	tli-Kpn-for	5' - GAG <u>GGT ACC</u> ATG AAA TCG TTC TTA TCA GGC	(Donato et al., 2020)
CH3419	tli-Xho-rev	5' - ATA <u>CTC GAG</u> CTA TTT AAC CGG AGT TGG TG	(Donato et al., 2020)
CH3719	tli(M24)-Kpn-for	5' - AAA <u>GGT ACC</u> ATG GAT TTA AAA CCA G	This study
CH4154	tli-Xho(H6)-rev	5' - CGT <u>CTC GAG</u> TTT AAC CGG AGT TGG TG	This study

CH4452	vgrG-Eco-for	5' - ATA <u>GAA TTC</u> ATG CTC AAC CGA ATT ACC	This study
CH4762	tle-S341A-for	5' - CGA TAT TGC AGG CCA CGC TCT GGG TGG TGG G	This study
CH4763	tle-S341A-rev	5' - CCC ACC ACC CAG AGC GTG GCC TGC AAT ATC G	This study
CH5137	tli-l52-Kpn-for	5' - TTT <u>GGT ACC</u> ATG ATT AAA TTA GCG TCA GGG AC	This study
CH5138	tli-M76-Kpn-for	5' - TTT <u>GGT ACC</u> ATG AAT TCG ATC AAT AAT CAG AA	This study
CH5203	Eh-vgrG(G615)-Kpn-for	5' - CCG <u>GGT ACC</u> ACA GCA CCG GGA TC	This study
CH5204	Eh-vgrI-Pst-rev	5' - TTT <u>CTG CAG</u> CTC GAG CCC GTAAAG TTG CCT CGC	This study
CH5205	vgrG2(G615)-Kpn-rev	5' - CGT <u>GGT ACC</u> TGG CTT AGC G	This study
CH5269	cat-Xba-for	5' - TTT <u>TCT AGA</u> TGT TGA TAC CGG GAA GCC	This study
CH5270	cat-Nsi-rev	5' - TTT <u>ATG CAT</u> TTA CGC CCC GCC CT	This study
CH5770	Eh-vgrG-K639-Sac-rev	5' - TTA CTC GAG <u>GAG CTC</u> TTA TTC GGC GAA AAC TTC TCC TGC	This study
CH5772	tle-P134-Sac-for	5' - TTT <u>GAG CTC</u> TCC TGC GCC AAC GGT GCT G	This study
DL1667	RE118-down-rev	5' - GAG ATT TTG AGA CAC AAC GTG	This study
DL2194	pheS*-Sph-rev	5' - CAA CAA <u>GCA TGC</u> CCA TAG TGA TTT GAT TTG CCA GC	This study
DL2195	Ptet-for	5' - CTC ATG TTT GAC AGC TTA TCA TCG	This study
DL2196	pheS*-rev	5' - CCA TAG TGA TTT GAT TTG CCA GC	This study
DL2197	RE118-up-for	5' - GAA GAT CAG CAG TTC AAC CTG TTG	This study
DL2198	RE118-up-rev	5' - GCA TGA TAA GCT GTC AAA CAT GAG GGA TTT GCA GAC TAC GGG	This study
DL2199	RE118-down-for	5' - GCT GGC AAA TCA AAT CAC TAT GGG TCA AAG GGT GAC AGC AG	This study
DL2217	pheS*-EcoRV-for	5' - TTT <u>GAT ATC</u> TGA GAG GAA AAC CAT GTC	This study
	Tn5-right1	5' - GTG AGC ATC ACA TCA CCA CA	This study
	Tn5-right2	5' - TCA CGT TCA TCT TTC CCT GG	This study
	Tn5-right2	5' - CTG TAC AAG TAA GGC CTA GC	This study

	Tn5-left1	5' - ATG TTT GAA TCG CTT GAT TTG G	This study
	Tn5-left2	5' - ATT GCT CAT GAT TTC ACC TCG	This study
	Tn5-left3	5' - CAA TAA AGC TGA CCG TTA GCG	This study
ZR39	tli-KO-Sac	5' - TTT <u>GAG CTC</u> AAG GCA ACC TGA GTT TTT TCC	This study
ZR40	tli-KO-Bam	5' - TTT <u>GGA TCC</u> AAC GAT TTC ATG CAC GAC TCC	This study
ZR248	cdiB-Eco-for	5' - TTT <u>GAA TTC</u> GAC ATT ACA CAG GCC AGA ATA CG	This study
ZR443	cdiB-Xho-rev	5' - TTT <u>CTC GAG</u> GAT CCG TAA TAA TCC CTT AAA ACG CGA CG	This study
ZR444	tli-Xho-rev	5' - TTT <u>CTC GAG</u> CTG ATA AGA ACG ATT TCA TGC ACG	This study

Chapter III: Advanced Glycation End-product (AGE) Crosslinking Activates a Type 6 Secretion System Phospholipase Effector Protein

Note: This chapter is a reprint of a manuscript written by Christopher Hayes and is in preparation for publication. Bonnie Cuthbert and I made equal contributions to this study.

Introduction

All bacteria compete for limited resources in the environment, with many species deploying specialized secretion systems to deliver toxic effector proteins directly into neighboring cells (Ruhe et al., 2020). The type 6 secretion system (T6SS) is a common mechanism of effector delivery utilized by many Gram-negative bacteria. T6SSs are dynamic multi-protein machines that function like contractile bacteriophages (Allsopp et al., 2020; Basler et al., 2012; Hernandez et al., 2020). The T6SS duty cycle begins with the docking of a phage-like baseplate subassembly onto the membrane-embedded trans-envelope complex, which forms the export conduit across the inner and outer membranes of the bacterium (Brunet, Zoued, et al., 2015; Durand et al., 2015). The baseplate then serves as the origin for polymerization of an elongated contractile sheath that surrounds a central tube of Hcp hexamers (Zoued et al., 2016). The Hcp tube is capped with trimeric VgrG, which is structurally similar to phage tail-spike proteins (Leiman et al., 2009). Toxic effector proteins are packaged into the lumen of the Hcp tube and also carried by the VgrG spike (Hachani et al., 2014; Silverman et al., 2013; Whitney et al., 2014). Upon contraction of the sheath, the spike-tipped tube is ejected from the cell through the trans-envelope complex. Nearby bacteria are perforated by the projectile, allowing toxic effector proteins to be deposited directly into the target-cell periplasm.

Because antibacterial T6SS effectors are potentially auto-inhibitory, they are invariably encoded with cognate immunity proteins that protect the cell from self-intoxication (Hernandez et al., 2020; Ruhe et al., 2020) We recently reported that the T6SS lipase immunity (Tli) protein of *Enterobacter cloacae* is unusual in that it

performs two distinct functions (Jensen et al., 2023). The mature Tli lipoprotein is secreted to the periplasmic space, where it acts as a canonical immunity factor to neutralize incoming T6SS lipase effector (Tle) proteins (Jensen et al., 2023). *E. cloacae* cells also synthesize cytoplasmic Tli from alternative translation initiation sites downstream of the secretion signal sequence. This cytosolic pool of immunity protein is required for the secretion of active Tle (Jensen et al., 2023). Given that immunity proteins bind directly to their cognate effectors (Ruhe et al., 2020), Tle activation presumably depends on transient interactions with cytoplasmic Tli before the lipase is packaged into the T6SS apparatus for export. Thus, Tli immunity protein has the paradoxical ability to activate its cognate effector protein through an unknown mechanism. Here, we show that Tle activation entails covalent modification with endogenous methylglyoxal to form an intramolecular crosslink that stabilizes the lipase domain.

Results

Modification of the Tle phospholipase domain

To explore the biochemical basis of lipase activation, we used immunoblotting to monitor Tle produced in the absence and presence of Tli. When placed under the control of a plasmid-borne arabinose-inducible promoter, the isolated *tle* gene produces a single Tle protein species (**Fig. 1a**, lane 3). By contrast, expression of the *tle-tli* gene pair yields two Tle species, including an apparently processed form that migrates more rapidly during gel electrophoresis (**Fig. 1a**, lane 4). These same two species of Tle accumulate when the *tle-tli* construct is induced in *E. coli* cells (**Fig. 1a**, lanes 7 & 8), indicating that processing does not require factors encoded by

the T6SS locus of *E. cloacae*. Given that only about half of the Tle chains appear to be processed, we reasoned that the *tle-tli* construct may not produce enough cytoplasmic Tli to support complete effector conversion. Therefore, we deleted the secretion signal sequence from Tli (Δ ss-Tli) and placed the construct under the control of a strong isopropyl- β -D-thiogalactoside (IPTG) inducible promoter. We also generated a new arabinose-inducible construct that produces Tle with an N-terminal His₆ epitope to facilitate purification. Co-induction of these constructs produces fully converted His₆-Tle (**Supplementary Fig. 1a**, lane 3). Mass spectrometry of the purified His₆-Tle• Δ ss-Tli complex shows that the immunity protein has the expected mass (**Supplementary Fig. 1b**). However, His₆-Tle exhibits a +36 Da shift relative to the predicted mass (**Supplementary Fig. 1b**), indicating that the effector is not processed by proteases. We were unable to characterize unmodified His₆-Tle, because this form is insoluble (**Supplementary Fig. 1a**, lane 5) and does not ionize during electrospray mass spectrometry. We also examined the C-terminal lipase domain of Tle (corresponding to residues Thr172 - Ala472) and found that it is modified when produced with Δ ss-Tli (**Fig. 1b**, lane 1). The modified lipase domain can be isolated from the immunity protein by Ni²⁺-affinity chromatography under denaturing conditions for comparison with the unmodified form (**Fig. 1b**, lanes 2 & 3). The modified domain exhibits the same +36 Da mass shift observed with full-length Tle (**Fig. 1c**), but unfortunately the unmodified domain fails to ionize for mass spectrometry. *In vitro* enzyme assays show that the modified lipase catalyzes phospholipase A1 and A2 reactions, which entail hydrolysis of phospholipid *sn*-1 and *sn*-2 acyl chains, respectively (**Figs. 1d & 1e**). Both activities are neutralized when

the lipase domain is pre-incubated with purified Δ ss-Tli immunity protein (**Figs. 1d & 1e**). By contrast, unmodified lipase has no enzymatic activity *in vitro* (**Figs. 1d & 1e**). The modified form of full-length His₆-Tle also exhibits phospholipase A1 and A2 activities, albeit at lower levels than the lipase domain construct (**Supplementary Figs. 1c & 1d**). An inactive version (Ser341Ala) of the lipase domain is also modified when produced with Δ ss-Tli (**Fig. 1b**, lanes 4 & 5), which indicates that the lipase catalytic center is not required for modification. As expected, the Ser341Ala domain has no phospholipase activity regardless of modification status (**Figs. 1d & 1e**). Thus, the lipase domain of Tle is modified when synthesized with Tli, and this modification appears necessary for enzymatic activity.

Structure of the lipase•immunity protein complex

To identify the Tle modification, we solved the crystal structure of the His₆-lipase• Δ ss-Tli complex to 1.75 Å resolution using sulfur single-wavelength anomalous diffraction (**Table 1**). The lipase domain adopts an α/β -hydrolase fold with a central 7-strand β -sheet surrounded by 13 α -helices (**Fig. 2a**). Residues Ser341, Glu393 and His448 (numbered according to full-length Tle) comprise the lipase catalytic triad, with Ser341 projecting from a classical nucleophilic 'elbow' that connects β 4 to α 7 (**Fig. 2a**). A DALI server (Holm et al., 2023) search for structural homologs of the lipase domain recovered plant phospholipase A1 enzymes and several triacylglycerol lipases from fungi (**Supplementary Table 1**). Δ ss-Tli is entirely α -helical with six ankyrin repeats that form an open-solenoidal arc (**Figs. 2a & 2b**). The lipase-immunity protein interface is extensive ($\sim 3,900$ Å²), corresponding to 14.9% of lipase domain and 17.1% of Δ ss-Tli surface area. The inner helical layer

($\alpha 8$, $\alpha 10$ and $\alpha 12$) of the immunity protein solenoid accounts for most of the contacts with the lipase, though the long loop connecting the 2nd and 3rd ankyrin repeats also forms several hydrogen bonds (**Fig. 2b**). Overall, Δss -Tli resembles a hand cupped around the lipase, with the ankyrin repeats representing the palm and the connecting loops forming extended fingers. Strikingly, lipase helix $\alpha 6$ is pulled away from the main body of the domain through interactions with Δss -Tli (**Figs. 2a & 2b**). AlphaFold2 (Jumper et al., 2021a) modeling predicts that $\alpha 6$ covers the active site in the absence of Tli (**Fig. 2c**), suggesting that this helix corresponds to the "lid" found in other lipases (Khan et al., 2017). Conformational changes in the lid underlie the phenomenon of interfacial activation, in which lipases act only on phase-separated substrates. The mechanistic basis of interfacial activation is understood for the secreted lipase of *Rhizomucor miehei*, which is a structural homolog of the Tle lipase domain (**Fig. 2d, Supplementary Table 1**). In aqueous solution, the *R. miehei* lid helix occludes the lipase active site (**Fig. 2d**) (Brady et al., 1990). The active site becomes accessible once the lid is displaced by interfacial tension forces at the aqueous-lipid boundary (**Fig. 2d**) (Brzozowski et al., 1991). The everted helix exposes its hydrophobic face adjacent to the catalytic cleft (**Fig. 2e**), thereby facilitating penetration into lipid micelles. Surprisingly, Tle appears to adopt an activated conformation when bound to Tli, because the lipase catalytic triad is exposed to solvent in the crystal structure (**Figs. 2a, 2c, 2d & 2e**). However, the $\alpha 6$ lid helix of Tle is dislocated well beyond the open position observed in activated *R. miehei* lipase (**Fig. 2d**). Moreover, the hydrophobic face of $\alpha 6$ packs against the immunity protein (**Figs. 2b & 2d**), which should prevent its interaction with lipid

substrates. Thus, the immunity protein appears to block lipase activity by sequestering the amphipathic lid helix.

The crystal structure also reveals an unusual interaction between the positively charged sidechains of lipase residues Arg180 from helix $\alpha 1$ and Lys461 in helix $\alpha 13$ (**Fig. 2a**). $F_o - F_c$ difference maps show continuous electron density between these sidechains, suggesting that the residues are covalently linked (**Fig. 2f**). Arg-Lys crosslinks are known to form upon prolonged exposure to glyoxal or methylglyoxal (Sibbersen & Johannsen, 2020). These dicarbonyl compounds accumulate as toxic byproducts of metabolism, and they react non-enzymatically with proteins, lipids and nucleic acids to generate a diverse array of advanced glycation end-products (AGEs) (Galligan et al., 2018; Hipkiss, 2017). AGE protein damage is implicated in the pathology of several chronic degenerative diseases including Alzheimer's, atherosclerosis and diabetes mellitus (Chaudhuri et al., 2018; Goldin et al., 2006; Kold-Christensen & Johannsen, 2020; Perkins et al., 2020; Rabbani et al., 2016; Rabbani & Thornalley, 2014a). The +36 Da mass shift observed in the modified lipase domain is consistent with a methylglyoxal-derived imidazolium crosslink (MODIC) (**Fig. 1c**), and MODIC fits well into the electron density bridging Arg180 and Lys461 (**Fig. 2f**). MODIC density is also apparent in the crystal structure of chymotrypsin digested lipase $\bullet\Delta$ ss-Tli complex (**Supplementary Fig. 2**). In the latter structure, chymotrypsin has removed the entire catalytic core of the lipase domain (His340 - Leu445), yet helix $\alpha 13$ remains tethered to $\alpha 1$ via MODIC (**Supplementary Fig. 2**). Thus, AGE crosslinking joins the N- and C-termini of the lipase domain into a topological circle. This intramolecular crosslink explains

increased gel mobility because the lipase cannot be denatured into a fully extended polypeptide and therefore adopts a more compact hydrodynamic radius during electrophoresis.

AGE crosslinking is required for phospholipase activity

To confirm the crosslinking site, we generated Arg180Lys and Lys461Gln substitutions in the lipase domain and showed that these variants remain unmodified when produced with Δ ss-Tli (**Fig. 3a**, lanes 3 & 7). Mass spectrometry of purified lipase•immunity protein complexes also indicates that the Arg180Lys and Lys461Gln domains do not react with methylglyoxal *in vivo* (**Figs. 3b & 3c**). Because Glu458 forms a direct hydrogen bond with MODIC (**Fig. 2f**), we also examined a Glu458Gln substitution and observed significantly reduced crosslinking (**Fig. 3a**, lane 4). Substitutions of the adjacent Gln459 and Gln460 residues in helix α 13 have intermediate effects on MODIC formation (**Fig. 3a**, lanes 5 & 6). These results demonstrate that Arg180, Glu458 and Lys461 are critical for lipase modification. To determine whether crosslinking is required for enzyme function, we assayed the phospholipase A1 activities of each substituted variant. The Arg180Lys and Lys461Gln lipases have no enzymatic activity, whereas the activities of the other variants are commensurate with the degree of intramolecular crosslinking (**Figs. 3a & 3d**). This correlation suggests that MODIC is necessary for lipase function *in vitro*. We then introduced these mutations into the arabinose-inducible *tIe-tli* construct to examine how AGE crosslinking affects Tle-mediated growth inhibition activity. Wild-type *E. cloacae tIe⁺* cells inhibit the growth of *E. cloacae* Δ *tIe-tli* mutants during coculture, because the latter target cells lack immunity to Tle (**Fig. 3e**) (Donato et al.,

2020; Jensen et al., 2023). This competitive advantage is lost when the *E. cloacae* T6SS is inactivated through a deletion of *tssM* (**Fig. 3e**, $\Delta tssM$), which encodes an essential component of the trans-envelope assembly. Similarly, *E. cloacae* Δtle mutants – which cannot produce Tle effector – are also unable to inhibit $\Delta tle-tli$ target cells (**Fig. 3e**). However, *E. cloacae* Δtle cells regain the full competitive advantage when complemented with the wild-type *tle* gene (**Fig. 3e**). By contrast, plasmids that encode Tle Arg180Lys and Lys461Gln variants fail to restore inhibition activity (**Fig. 3e**). Immunoblot analysis showed that the Arg180Lys and Lys461Gln variants accumulate at levels comparable to wild-type Tle, but they exhibit no intramolecular crosslinking (**Fig. 3f**, lanes 4, 5 & 9). The Glu458Gln variant is also significantly attenuated for growth inhibition activity (**Fig. 3e**) with a corresponding defect in AGE crosslinking (**Fig. 3f**, lane 6). The Gln459Lys and Gln460Lys lipases retain robust growth inhibition activities (**Fig. 3e**), which correlate well with *in vivo* crosslinking efficiency (**Fig. 3f**, lanes 7 & 8). Collectively, these results indicate that AGE crosslinking is required for the *in vitro* and *in vivo* activities of Tle.

Aldehyde reductases suppress Tle crosslinking

Endogenous methylglyoxal is produced largely through the non-enzymatic decay of triose phosphates, though enterobacteria encode a methylglyoxal synthase (MgsA) enzyme that generates methylglyoxal during increased flux through the glycolytic pathway (Booth, 2005). However, MgsA activity does not contribute to crosslinking, because the lipase domain is still modified efficiently when produced in *E. coli* $\Delta mgsA$ cells (**Supplementary Fig. 3**, compare lanes 2 & 5). We also attempted to suppress endogenous methylglyoxal levels with aminoguanidine, which

reacts with the dicarbonyl to form non-toxic triazine compounds (Thornalley, 2003). Treatment with up to 50 mM aminoguanidine has no discernable effect on lipase domain crosslinking *in vivo* (**Supplementary Fig. 3**). We next tested whether methylglyoxal detoxification enzymes influence lipase crosslinking. The major detoxification pathway entails condensation with glutathione to form a hemithioacetal, which is subsequently converted into D-lactate by glyoxalase I and II enzymes (Lee & Park, 2017). In addition, *E. coli* encodes a glutathione-independent glyoxalase, HchA, and a number of NAD(P)H-dependent aldehyde reductases capable of methylglyoxal detoxification³⁰. We cloned various detoxification genes under the control of an arabinose-inducible promoter and asked whether their overexpression affects Tle crosslinking *in vivo*. Somewhat surprisingly, glyoxalase I (GloA) overexpression has little effect (**Fig. 4a**, lane 3), but HchA induction suppresses Tle crosslinking (**Fig. 4a**, lane 4). The YdjG and YqhD-YqhE aldehyde reductases also appear to decrease crosslinking efficiency in *E. coli* cells (**Fig. 4a**, lanes 5 & 6). We next introduced these plasmids into *E. cloacae* to test whether the detoxification enzymes decrease the level of activated Tle available for T6SS export. Each construct reduces the competitive fitness of wild-type *E. cloacae* against Δtle Δtli target bacteria, though the effects are modest (**Fig. 4b**). HchA has the greatest effect with a ~10-fold decrease in the competitive index (**Fig. 4b**). We note that these detoxification enzymes have Michaelis constants (K_m) for methylglyoxal in the low millimolar range (Di Luccio et al., 2006; Ko et al., 2005; Lee et al., 2010; Subedi et al., 2011), suggesting that the dicarbonyl is still present at micromolar concentrations in these cells.

In vitro activation of the Tle phospholipase domain

Given that AGE crosslinking is not enzyme-catalyzed, it should be possible to activate the lipase domain by methylglyoxal treatment *in vitro*. We mixed unmodified His₆-lipase with Δ ss-Tli and treated the purified complex with 1 mM methylglyoxal to monitor crosslink formation as a function of time. Intramolecular crosslinking is detectable after 1 h and increases up to the 24 h endpoint (**Supplementary Fig. 4**). We also examined different methylglyoxal concentrations and found that crosslinking is apparent at 100 μ M methylglyoxal and nears completion at 5 mM methylglyoxal (**Fig. 5a**). The lipase can also be crosslinked with glyoxal at lower efficiency (**Fig. 5b**). As predicted from the mutagenesis data presented above, the Arg180Lys and Lys461Gln lipase variants are not subject to methylglyoxal crosslinking *in vitro* (**Figs. 5c & 5d**). Moreover, lipase crosslinking is not observed in the absence of Δ ss-Tli (**Supplementary Fig. 5a**), indicating that the domain only reacts with methylglyoxal when bound to immunity protein. To determine whether the *in vitro* crosslinked lipases are active, we first isolated the His₆-lipase domains away from Δ ss-Tli by Ni²⁺-affinity chromatography under denaturing conditions. After refolding by dialysis, the activities of dicarbonyl treated lipases were determined. Remarkably, glyoxal and methylglyoxal crosslinking both promote phospholipase A1 activity, whereas the untreated lipase remains inert (**Fig. 5e**). Somewhat surprisingly, glyoxal treatment leads to greater enzymatic activity (**Fig. 5e**), despite more efficient crosslinking with methylglyoxal (**Figs. 5a & 5b**). However, we subsequently found that the glyoxal crosslink is thermolabile (**Supplementary Fig. 5b**, lanes 5 & 6), and therefore glyoxal crosslinking is underestimated in **Fig. 5b** because these samples were

heated to 95 °C prior to SDS-PAGE analysis. Importantly, the *in vitro* crosslinked lipases can be neutralized with purified Δ ss-Tli (**Fig. 5e**), indicating that the treated domains retain native interactions with the immunity protein.

Phospholipase activation with an engineered disulfide bond

AGE crosslinking presumably promotes lipase function by stabilizing tertiary structure. Thermodynamic stability is particularly important for lipases, which necessarily operate at the water-lipid interface. Interfacial tension at this phase boundary is known to disrupt protein structure and inactivate enzymes (Bergfreund et al., 2021; Zhai et al., 2013). Thus, the same interfacial forces that promote lipase activity through lid displacement also have the potential to inactivate the enzyme (Reis et al., 2009). We note that the lipase of *R. meiheii* contains a conserved Cys123-Cys362 disulfide bond that tethers the N- and C-termini (**Fig. 6a**). Given that disulfides protect proteins from denaturation at the water-lipid interface (Bergfreund et al., 2021), we reasoned that this bond may serve the same stabilizing function as MODIC in Tle. If this hypothesis is correct, then an engineered disulfide bond should be able to restore phospholipase activity to the Lys461Gln domain. Disulfide-by-design (Craig & Dombkowski, 2013) software predicts that Cys substitutions of Tle residues Lys186 and Ala472 should form a disulfide linking helices α 1 and α 13 (**Fig. 6b**). Indeed, the resulting lipase variant forms an intramolecular disulfide bond under oxidizing conditions when produced with Δ ss-Tli (**Fig. 6c**, lanes 5 & 6). In contrast to the Lys461Gln domain, the disulfide-linked variant has significant phospholipase A1 activity that is neutralizable with the Δ ss-Tli immunity protein (**Fig. 6d**). Moreover, phospholipase activity is diminished when the disulfide bond is reduced with

dithiothreitol (**Fig. 6d**). The residual activity in the latter experiment presumably reflects lipase that is resistant to reduction (**Supplementary Fig. 6a**, lanes 3 & 4). Importantly, dithiothreitol has no effect on the activity of MODIC modified wild-type lipase (**Fig. 6d**). Together, these data demonstrate that intramolecular crosslinking is necessary and sufficient for Tle phospholipase activity. Although the disulfide-linked lipase domain is active *in vitro*, the corresponding full-length Tle variant does not inhibit target bacteria in competition cocultures (**Fig. 3e**). Immunoblotting shows that the effector does not form an intramolecular disulfide *in vivo* (**Supplementary Fig. 6b**, lanes 3 & 4), consistent with the lack of growth inhibition activity in bacterial competitions.

Discussion

E. cloacae cells produce two forms of Tli immunity protein with distinct functions. Full-length Tli is secreted to the periplasm, where it is lipidated and embedded into membranes to protect against incoming Tle effectors (**Fig. 7**). Cytosolic Tli is synthesized from alternative translation start codons found downstream of the signal sequence (Jensen et al., 2023). The latter pool of immunity protein is required to activate Tle by promoting methylglyoxal crosslinking, suggesting that cytosolic Tli forms a transient complex with newly synthesized Tle prior to T6SS-mediated export (**Fig. 7**). MODIC formation must be efficient under physiological conditions, because T6SS effectors are deployed within minutes of synthesis (Basler et al., 2012). Moreover, endogenous methylglyoxal concentrations are estimated to be in the low micromolar range (Rabbani & Thornalley, 2014b), indicating that the Tle•Tli complex has high affinity for the dicarbonyl. The mechanism by which Tli promotes AGE

crosslinking is not clear. The immunity protein does not make contact with helix $\alpha 1$ or $\alpha 13$ of the lipase domain, and the MODIC residue is ~ 33 Å from Tli in the crystal structure. These observations suggest that Tli does not directly catalyze AGE crosslinking. Given that unmodified Tle is insoluble, perhaps Tli acts as a folding chaperone to guide the lipase into a conformation that is competent for crosslinking. This model implies an additional mechanism to dissociate Tli before the activated effector is loaded into the T6SS (**Fig. 7**). In principle, binding interactions between Tle and Hcp or VgrG could provide the free energy to remove Tli during packaging.

We propose that AGE crosslinking activates Tle by stabilizing its tertiary structure to resist denaturation at water-lipid phase boundaries. Structurally related triacylglycerol lipases from fungi use long-range disulfide bonds to address this biophysical problem (Bordes et al., 2010; Brady et al., 1990; M. Zhang et al., 2019). These neutral lipases are released into the environment to scavenge glycerol and fatty acids as nutrients. Before secretion, the newly synthesized lipases are first transferred into the endoplasmic reticulum lumen, where disulfide bond formation is orchestrated through the redox activities of Ero1p and Pdi1p (L. Wang & Wang, 2023). The lipases are then trafficked through the Golgi apparatus and ultimately secreted via exocytosis (Q. Wang et al., 2020). By contrast, T6SS effectors are transferred directly from the inhibitor-cell cytoplasm to the periplasm of target bacteria (**Fig. 7**). Because the bacterial cytosol is a reducing environment (Collet et al., 2020), T6SS effectors presumably cannot form disulfides prior to export, which may explain why the engineered disulfide approach fails to activate Tle in competition cocultures. Coulthurst and coworkers have shown that some T6SS

effectors can acquire disulfide bonds after delivery into the oxidizing environment of the target-cell periplasm (Mariano et al., 2018). However, like the MODIC residue, the engineered disulfide in Tle only forms when the effector is bound to immunity protein. These constraints presumably underly the evolutionary pressure for Tle to utilize an AGE crosslink in lieu of a disulfide bond.

Mougous and coworkers originally delineated five families of T6SS phospholipase effectors (Tle1-Tle5) (Russell et al., 2013). *E. cloacae* Tle does not belong to any of these families, though it is homologous to the Slp lipase effector from *Serratia marsescens* (Cianfanelli, Alcoforado Diniz, et al., 2016). We propose that this new phospholipase effector group be designated Tle6 in accordance with the nomenclature of Russel *et al* (Russell et al., 2013). Tle6 effectors are invariably encoded with ankyrin-repeat containing immunity proteins (Jensen et al., 2023), raising the possibility that these lipases are all subject to Tli-dependent AGE crosslinking. By contrast, representative Tle1, Tle2, Tle4 and Tle5 lipases are active *in vitro* when purified from heterologous expression systems (Flaughnatti et al., 2016; Jiang et al., 2016; Russell et al., 2013). Moreover, Tle1, Tle2 and Tle5 are readily deployed from mutant strains that lack the corresponding immunity genes (T. G. Dong et al., 2013; Flaughnatti et al., 2016; Russell et al., 2013). Given that other T6SS lipase effectors are intrinsically active, the advantage of AGE-mediated Tle6 activation is not clear. This phenomenon could represent a fail-safe mechanism that prevents auto-intoxication in Tle6 producing cells. The inner leaflet of the cytoplasmic membrane is composed of glycerophospholipid, and therefore cytosolic phospholipases could disrupt cell integrity. Activation in the context of the Tle6-Tli6

complex would ensure that the phospholipase remains neutralized until export (**Fig. 7**). Auto-intoxication is potentially a problem for other T6SS phospholipases as well, though these enzymes are generally not active when produced in the cytosol (Flaunatti et al., 2016; H. Hu et al., 2014; Jiang et al., 2016; Russell et al., 2013). In some instances, Tle effectors have been shown to be toxic only when directed to the periplasm with signal peptides (Berni et al., 2019; Flaunatti et al., 2016; Jiang et al., 2016; Russell et al., 2013). The mechanistic basis of this activation has not been explored, but the redox potential and increased Ca^{2+} ion content of the periplasm could conceivably modulate phospholipase activity.

In summary, decades of research have concluded that glycation adducts are invariably deleterious to protein function (Kold-Christensen & Johannsen, 2020; Schalkwijk & Stehouwer, 2020). However, our results show that methylglyoxal-mediated AGE crosslinking can be harnessed as a *bona fide* post-translational modification to promote protein function. Given that reactive dicarbonyl compounds accumulate in all cells – prokaryotic and eukaryotic – these findings raise the possibility that AGE crosslinking could be exploited to enhance the function of other proteins. This alternative strategy to fortify protein structure could be particularly advantageous in the cytoplasm, where the redox potential precludes disulfide bond formation.

Acknowledgments

We thank the Advanced Light Source at Berkeley National Laboratories and the Stanford Synchrotron Radiation Lightsource for help in data collection, and Julian

Whitelegge (University of California, Los Angeles) for discussions about mass spectrometry analyses.

Conceptualization: SJJ, CSH; Methodology: SJJ, BJC, FGS, RDM, CWG, CSH; Investigation: SJJ, BJC, FGS, CCH, CSH; Visualization: BJC, CWG, CSH; Funding acquisition: CWG, CSH; Project administration: CWG, CSH; Supervision: CWG, CSH; Writing – original draft: CSH; Writing – review & editing: SJJ, BJC, FGS, CWG, CSH. SJJ and BJC contributed equally to this work.

Materials and Methods

Bacterial strain and plasmid constructions.

Bacterial strains and plasmids are listed in **Supplementary Table 2**. The $\Delta mgsA::kan$ allele from the Keio strain collection⁵⁴ was transferred into strain CH6247 by phage P1 mediated transduction to generate strain CH5691. Oligonucleotide primers used for plasmid constructions are presented in **Supplementary Table 3**. All bacteria were grown at 37 °C in lysogeny broth (LB): 1% tryptone, 1% yeast extract, 0.5% NaCl. Media were supplemented with antibiotics at the following concentrations: ampicillin (Amp), 150 µg/mL; kanamycin (Kan), 50 µg/mL; rifampicin (Rif), 200 µg/mL; spectinomycin (Spc), 100 µg/mL; tetracycline (Tet), 15 µg/mL; and trimethoprim (Tp), 100 µg/mL, where indicated.

The Δss -Tli coding sequence was amplified with primers CH3719/CH3419 and ligated to pET21K and pCH450K using KpnI/XhoI restriction sites to generate plasmids pCH3291 and pCH495, respectively. The *tli* gene was also amplified with CH5751/CH3419 and ligated to pMCSG63 via KpnI/XhoI sites to generate plasmid

pCH7695, which appends a tobacco etch virus (TEV) protease cleavable His₆ epitope to the N-terminus of Δ ss-Tli. Full-length *tIe* was amplified with CH4703/ZR248 and the product ligated to pCH8259 (Garza-Sánchez et al., 2011) and pSH21 (Koskiniemi et al., 2014) using SpeI/XhoI to produce plasmids pCH7620 and pCH2199, respectively. Plasmid pCH5892 was generated by subcloning the *tIi* containing HindIII/XhoI fragment from pCH3128 into pCH2199. The coding sequence for the Tle lipase domain was amplified with CH5807/ZR248 and ligated to pCH8259 to generate plasmid pCH7088. Fragments containing *tIe* and *tIe-tIi* were subcloned from pCH14212 and pCH3128 (Jensen et al., 2023) into pSCBAD (Koskiniemi et al., 2015) using BamHI/XhoI restriction sites to generate plasmids pCH2826 and pCH4362, respectively. Missense mutations were introduced into *tIe* using forward primers CH5721 (Arg180Lys), CH5689 (Glu458Gln), CH5722 (Gln459Lys), CH5723 (Gln460Glu), CH5690 (Lys461Gln) in conjunction with CH3419. The resulting products were used as megaprimers in conjunction with CH4469 to amplify *tIe-tIi*, and the final products ligated to pCH4362 using KpnI/XhoI restriction sites to generate plasmids pCH5501 (Arg180Lys), pCH7600 (Glu458Gln), pCH5502 (Gln459Lys), pCH5503 (Gln460Glu) and pCH7601(Lys461Gln). The disulfide lipase variant containing Lys186Cys and Ala472Cys substitutions was generated by three rounds of overlap extension PCR using plasmid pCH4362 as a template. The endogenous Cys456 residue was first mutated to Ser in the *tIe(K461Q)* allele with primers CH943/CH5960 and CH5959/CH3419. The Ala472Cys (using primers CH943/CH6063 and CH6062/CH3419) and Lys186Cys (CH943/CH5908 and CH5907/CH3419) mutations were then introduced

sequentially. The final product was digested with BamHI/XhoI and ligated to pSCBAD to generate plasmid pCH3923.

His₆-tagged lipase domain constructs were amplified using primers CH5087/ZR248 and ligated to pCH8259 using SpeI/XhoI restriction sites to generate plasmids pCH8871 (Glu458Gln), pCH8717 (Gln459Lys), pCH8718 (Gln460Glu) and pCH8872 (Lys461Gln). The catalytically inactive *tle*(S321A) allele was amplified from pCH3763 (Jensen et al., 2023) with primers CH5087/ZR248 and ligated to pCH8259 using SpeI/XhoI site to generate plasmid pCH3936. The *tle*(R180K) allele was amplified with CH5688/ZR248 and ligated to pCH8259 using SpeI/XhoI sites to generate plasmid pCH7599. The *tle*(K186C,C456S,K461Q,A472C) allele was amplified with CH5087/CH5909 and ligated to pCH8259 using SpeI/XhoI sites to generate plasmid pCH1382.

Methylglyoxal detoxification genes were amplified from *E. coli* genomic DNA and placed under the control of an arabinose-inducible promoter on plasmid pSCBAD. *gloA* was amplified with primers CH5761/CH5762 and ligated using EcoRI/XhoI restriction sites. *hchA* was amplified with CH6310/CH6311 and the product digested with MfeI/SbfI for ligation to EcoRI/PstI-digested pSCBAD. *ydjG* was amplified with CH6312/CH6313 and ligated using EcoRI/PstI sites. The *yqhD-yqhE* gene pair was amplified with CH6314/CH6315 and ligated via EcoRI/PstI sites.

Tle-Tli coproduction.

E. coli X90 and *E. cloacae* ATCC 13047 cells were transformed with pCH2826 (*tle*) or pCH4362 (*tle-tli*), and cells were grown in Tp-supplemented LB media at 37 °C.

Once the cultures reached an optical density at 600 nm (OD₆₀₀) of ~ 0.4, they were split in two and one half was induced with 0.4% L-arabinose. After 1 h, cells were collected by centrifugation at 15,000 rpm in a microfuge and the cell pellets frozen at -80 °C. Frozen pellets were resuspended in urea lysis buffer [8 M urea, 20 mM Tris-HCl (pH 8.0), 100 mM NaCl] and subjected to another freeze-thaw cycle to break cells. Lysates were clarified by centrifugation at 15,000 rpm in a microfuge. Protein concentrations were estimated using Bradford reagent and equal amounts of lysate were analyzed by SDS-PAGE at 110 V using 7% polyacrylamide gels buffered with Tris-tricine. Gels were soaked for 10 min in 25 mM Tris, 192 mM glycine (pH 8.6), 20% methanol before transfer to polyvinylidene fluoride membranes at 17 V for 30 min using a semi-dry electroblotting apparatus. Membranes were blocked with 4% non-fat milk in 1X PBS for 45 min at ambient temperature, then incubated with a 1:5,000 dilution of rabbit anti-Tle polyclonal antisera (Jensen et al., 2023) in 1X PBS, 4% non-fat milk overnight. After three 10 min washes with 1X PBS, the membranes were incubated with IRDye 800CW-conjugated goat anti-rabbit IgG (LI-COR, 1:125,000 dilution) in 1X PBS for 45 min. Immunoblots were visualized using a LI-COR Odyssey infrared imager. The effect of methylglyoxal detoxification on AGE crosslinking was assessed in *E. coli* cells that overproduce His₆-Tle and Tli from an IPTG-inducible phage T7 promoter. *E. coli* CH2016 cells carrying plasmid pCH5892 (*his₆-tle/tli*) were transformed with pCH7694 (*gloA*), pCH5119 (*hchA*), pCH5120 (*ydjG*) or pCH5121 (*yqhDE*). The resulting strains were grown in LB media supplemented with Amp Tp to mid-log phase, and detoxifying enzyme expression was induced with 0.4% L-arabinose for 90 min. His₆-Tle/Tli production was then

induced with 1.5 mM IPTG for 30 min. Cells were collected by centrifugation, and His₆-Tle was purified by Ni²⁺-affinity chromatography under denaturing conditions as described above. Purified proteins were resolved by SDS-PAGE at 110 V on 7% polyacrylamide gels buffered with Tris-tricine.

His₆-lipase domain modification and purification.

To examine lipase domain modification, *E. coli* CH2016 cells (Garza-Sánchez et al., 2006) were co-transformed with pCH7088 (*his₆-lipase*) or pCH3936 (*his₆-lipase-S341A*) and pET21b or pCH3291 (Δ *ss-tli*). The resulting strains were grown to OD₆₀₀ ~ 1.0 in LB media supplemented with Amp Tet, and lipase domain production was induced with 0.4% L-arabinose for 1 h. Where indicated, aminoguanidine was added to cultures at the same time as L-arabinose. Δ *ss-Tli* expression was then induced with 1.5 mM IPTG for 90 min. Cell pellets were collected by centrifugation at 6,000 rpm for 10 min and frozen at -80 °C. To isolate His₆-lipase• Δ *ss-Tli* complexes, cells were resuspended in native lysis buffer [20 mM Tris-HCl (pH 7.5), 150 mM NaCl, 0.05% Triton X-100, 5 mM imidazole] and adjusted to 0.1 mg/mL lysozyme for 15 min prior to sonication. Sonicated cell lysates were clarified by centrifugation at 11,000 rpm for 10 min at 4 °C, and the supernatant incubated with Ni²⁺-nitrilotriacetic acid (Ni²⁺-NTA) agarose for 90 min at ambient temperature. Ni²⁺-NTA resins were washed five times with 10 volumes of native lysis buffer, and His₆-lipase• Δ *ss-Tli* complexes were eluted in native elution buffer [20 mM Tris-HCl (pH 7.5), 150 mM NaCl, 0.05% Triton X-100, 250 mM imidazole]. To isolate His₆-lipase domains, cell pellets were resuspended in guanidine lysis buffer [6 M guanidine-HCl, 20 mM Tris-HCl (pH 8.0), 1 mM imidazole] and sonicated. Lysates were clarified by

centrifugation at 11,000 rpm for 10 min at 4 °C, and the supernatants incubated with Ni²⁺-NTA agarose for 90 min at ambient temperature. Resins were washed four times with 10 volumes of 8 M urea, 1 mM imidazole, and His₆-lipase domains eluted with 8 M urea, 20 mM Tris-HCl (pH 8.0), 250 mM imidazole. Purified lipase domains were refolded by dialysis against 20 mM sodium phosphate (pH 7.0). His₆-lipase domain concentrations were quantified by absorbance at 280 nm (A_{280}) using an extinction coefficient of 35,410 M⁻¹ cm⁻¹. Modified full-length His₆-Tle was purified in the same manner under denaturing conditions and quantified using an extinction coefficient of 66,810 M⁻¹ cm⁻¹.

Δss-Tli purification.

E. coli CH2016 cells carrying plasmid pCH7695 were grown in Amp-supplemented LB medium at 37 °C. At OD₆₀₀ ~ 1.0, His₆-TEV-Δss-Tli production induced with 1.5 mM IPTG for 90 min. Cells were collected by centrifugation at 6,000 rpm for 10 min and frozen at -80 °C. Frozen cell pellets were resuspended in guanidine lysis buffer, and His₆-TEV-Δss-Tli was purified as described above for His₆-lipases. After dialysis into 20 mM sodium phosphate (pH 7.0), the N-terminal His₆ epitope was removed by digestion with tobacco etch virus (TEV) protease overnight at 37 °C in 20 mM sodium phosphate (pH 7.0) supplemented with 2 mM dithiothreitol (DTT). His₆-TEV protease and released His₆ epitopes were removed by incubation with Ni²⁺-NTA agarose for 90 min. Untagged Δss-Tli was quantified by A_{280} using an extinction coefficient of 27,960 M⁻¹ cm⁻¹.

Phospholipase activity assays.

Tle and lipase domain activities were measured by monitoring the hydrolysis of fluorogenic phospholipase substrates PED-A1 (PLA₁-specific) and PED6 (PLA₂-specific). PED-A1 and PED6 (1.5 μM) were incorporated into liposomes of dioleoylphosphatidylcholine (DOPC, 15 μM) and dioleoylphosphatidylglycerol (DOPG, 15 μM) according manufacturer's instructions (Invitrogen). His₆-Tle/His₆-lipase domains were assayed at 600 nM, and immunity blocking experiments were conducted by supplementing the reactions with 700 nM purified Δss-Tli. Assays were performed in 50 mM Tris-HCl (pH 7.5), 100 mM NaCl, 1 mM CaCl₂. Fluorescence was measured every 4 min for 1 h using a PerkinElmer Victor 3V Multilabel Plate Reader (**Figs. 1d, 1e, 3d, Supplementary Figs. 1c & 1d**), or every 4.5 min for 153 min using a Molecular Devices SpectraMax M5 fluorimeter (**Figs. 5e & 6d**). Fluorescence values were baseline corrected by subtracting the background fluorescence from mock control reactions containing only buffer and fluorogenic substrate. All assays were performed independently three times.

Mass spectrometry

Purified His₆-Tle•Δss-Tli and His₆-lipase•Δss-Tli complexes (5 μL at 0.02 mg/mL) were resolved on an Acquity UPLC Beh Phenyl VanGuard Pre-column (130 Å, 1.7 μm, 2.1 mm × 5 mm) using an ACQUITY UPLC H-class system (Waters). Molecular masses were determined using a Xevo G2-XS QToF quadrupole time-of-flight mass spectrometer (Waters) run in positive ion mode.

X-ray crystallography

E. coli CH2016 was transformed with pCH15269 and pCH495 (Jensen et al., 2023) to generate a strain that over-produces His₆-lipase and Δss-Tli. Cells were grown in LB supplemented with 50 µg/mL Amp and 15 µg/mL Tet at 37 °C to OD₆₀₀ ~ 0.6-0.7, and immunity protein expression was induced with 0.4% L-arabinose for 1 h. Lipase domain expression was then induced with 0.5 mM IPTG for 30 min. Cells were harvested by centrifugation for 30 min at 5,000 rpm and the pellets stored at -20 °C. Cells were broken by sonication in Buffer A (11.5 mM Na₂HPO₄, 8.5 mM NaH₂PO₄, 150 mM NaCl) with phenylmethylsulfonyl fluoride and lysozyme. Cell debris was removed by centrifugation at 14,000 rpm for 1 h, followed by filtration of the supernatant through a 0.45 µm filter. The complex was purified on a HisTrap column (GE healthcare) in Buffer A. The His₆-lipase•Tli complex was eluted with a linear gradient of 500 mM imidazole in Buffer A. Fractions containing the His₆-lipase•Tli complex were identified by SDS-PAGE, and concentrated for further purification on a S200/10/300 column (GE healthcare) in 20 mM Tris pH 7.5, 150 mM NaCl. Fractions with pure His₆-lipase•Tli complex were identified by SDS-PAGE analysis, concentrated to 80 mg/mL and screened for crystallization at room temperature and 4 °C. After 6 months, crystals were found in PACT 59 (0.2 M sodium citrate, 20% PEG 3350) at 4 °C. Crystallization was optimized and reproduced in 0.4 M sodium citrate, 22% PEG 3350. Crystals were collected after three weeks in mother liquor supplemented with 20% glycerol and cryo-cooled before data collection at SSRL beamline 12-2. Native (at 12398 eV) and sulfur single-wavelength anomalous diffraction (S-SAD) (at 7000 eV) datasets were

collected from a single crystal. The S-SAD data was processed by XDS (Kabsch, 2010) and scaled and truncated in Aimless to 2.1 Å resolution (Evans & Murshudov, 2013). The native dataset was handled identically and truncated to 1.75 Å (**Supplementary Table 1**). Phasing and initial model building were performed with the S-SAD datasets in Crank2 in ccp4i2 (Skubák et al., 2018). Subsequent model building and refinement were performed in phenix.refine and coot (Adams et al., 2010; Emsley & Cowtan, 2004). The S-SAD dataset was used to solve the native datasets by MR in Phaser (Adams et al., 2010), and refined as described above to a final R_{work} and R_{free} of 17.8 and 20.9%.

Chymotrypsin was used as an additive to facilitate crystallization through limited proteolysis during initial trials. Chymotrypsin was added to the His₆-lipase•Δss-Tli complex at a final concentration of 0.02 mg/mL. Proteolyzed His₆-lipase•Δss-Tli was crystallized in 0.25 M sodium citrate, 22% PEG-3350 and cryo-cooled in mother liquor supplemented with 20% glycerol. A dataset was collected at SSRL beamline 12-2 at 12659 eV. Phasing was initially determined in ARP-WARP (Chojnowski et al., 2020) with a search for Tli. Subsequently, the lipase domain structure was partially build in autobuild (Terwilliger et al., 2007). The remainder of the lipase domain was built and refined manually as described above to a final R_{work} and R_{free} of 16.4% and 18.8%.

Competition co-cultures. Inhibitor and target cells were grown overnight in LB media, then diluted 1:50 into fresh LB media and grown at 37 °C to mid-log phase. Cells were harvested by centrifugation at 3,400 $\times g$ for 2 min, resuspended to an OD₆₀₀ of 3.0 and mixed at a 10:1 ratio of inhibitor to target cells. Cell mixtures (10

μL) were spotted onto LB-agar supplemented with 0.4% L-arabinose and incubated at 37 °C. A portion of each cell mixture was serially diluted into 10⁶ M9 salts and plated onto antibiotic supplemented LB-agar to enumerate inhibitor and target cells as colony forming units (cfu) at *t* = 0 h. Inhibitor cells were scored by Tp^R (conferred by plasmid pSCBAD derivatives), and target cells were enumerated by Rif^R. After 4 h of co-culture, cells were harvested from the agar surface with polyester-tipped swabs and resuspended in 1.0 mL of 10⁶ M9 salts. To examine the effects of methylglyoxal detoxifying enzymes, wild-type *E. cloacae* inhibitor cells harboring plasmids pCH7694 (*gloA*), pCH5119 (*hchA*), pCH5120 (*ydjG*) or pCH5121(*yqhDE*) were co-cultured with *E. cloacae* Δ*tli* Δ*tli* target bacteria at a 1:1 ratio for 2 h on LB-agar supplemented with 0.4% L-arabinose. Cell suspensions were serially diluted in 1X M9 salts and plated as described above to quantify end-point cfu. Competitive indices were calculated as the final ratio of inhibitor to target cells divided by the initial ratio of inhibitor to target cells. All competitions were performed independently three times and data are presented as the mean ± standard error.

***In vitro* crosslinking.** Unmodified His₆-lipase domains (in 8 M urea) were mixed with purified Δ*ss*-Tli at 1.1:1 ratio, and the mixtures dialyzed against 20 mM sodium phosphate (pH 7.0) to allow complex formation. The resulting His₆-lipase•Δ*ss*-Tli complexes (17 μM) were treated with varying concentration of methylglyoxal or glyoxal at 37 °C for 3 h. Treated complexes were analyzed by SDS-PAGE. To isolate *in vitro* crosslinked lipases for activity assays, methylglyoxal (1 mM) and glyoxal (1 mM) treated complexes were bound to Ni²⁺-NTA agarose for 90 min, then Δ*ss*-Tli proteins were dissociated with three guanidine lysis buffer washes. His₆-lipase

domains were then eluted from the resins with 6 M guanidine-HCl, 20 mM Tris-HCl (pH 8.0), 250 mM imidazole. The proteins were then refolded by dialysis against 20 mM Tris-HCl (pH7.5), 100 mM NaCl, quantified and used in phospholipase A1 reactions.

Disulfide engineering, oxidation and analyses.

E. coli CH2016 cells carrying pCH3291 were transformed with pCH7088 (wild-type), pCH8872 (Lys461Gln) or pCH1382 (Lys461Gln + disulfide), and the resulting strains were grown and induced as described above. Cell pellets were resuspended in 20 mM Tris-HCl (pH 7.5), 150 mM NaCl, 0.05% Triton X-100, 5 mM imidazole, 10 μ M CuCl₂ and incubated with 0.1 mg/mL lysozyme for 15 min prior to sonication. Cell lysates were clarified by centrifugation at 11,000 rpm for 10 min at 4 °C, and the supernatants incubated with Ni²⁺-NTA agarose for 90 min at ambient temperature. Resins were washed 5 times with 8M urea for wild-type and Lys461Gln lipase domains, and 5 times with 3 M urea for the disulfide containing lipase. Samples were eluted in native elution buffer (20 mM Tris 7.5, 150 mM NaCl, 0.05% Triton X-100, 250 mM Imidazole). Purified His₆-lipase domains were dialyzed against 20 mM Tris-HCl (pH 7.5), 100 mM NaCl, quantified and assayed for phospholipase A1 activity.

Statistics and reproducibility.

Standard errors were calculated using either GraphPad Prism (version 9.4.0) or Microsoft Excel (version 16.63.1). All competition co-cultures, crosslinking experiments and phospholipase activity assays were performed independently at least three times with similar results.

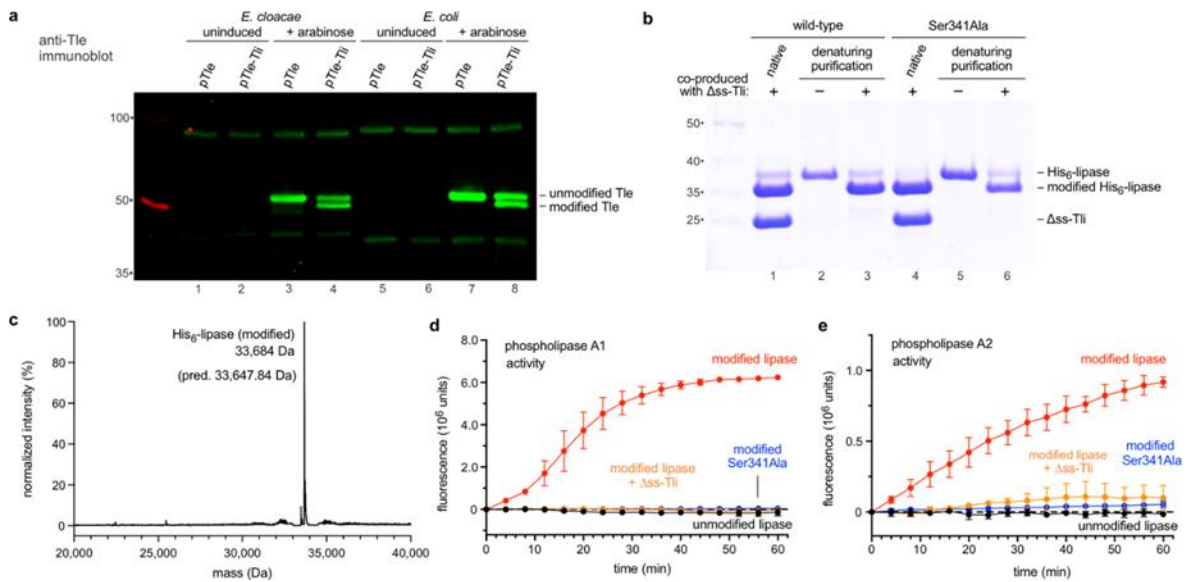


Fig. 1. Modification of the Tle phospholipase domain.

(a) Tle and Tle-Tli production was induced with arabinose in *E. cloacae* and *E. coli* cells. Urea-soluble total protein was extracted for immunoblot analysis using anti-Tle polyclonal antisera

(b) His₆-lipase domains were produced with (or without) Δ ss-Tli in *E. coli* cells, then purified by Ni²⁺-affinity chromatography under non-denaturing (native) or denaturing conditions for SDS-PAGE analysis.

(c) Deconvoluted mass spectrum of purified modified His₆-lipase domain.

(d) *In vitro* phospholipase A1 activities of purified lipase domains from panel b.

(e) *In vitro* phospholipase A2 activities of purified lipase domains from panel b.

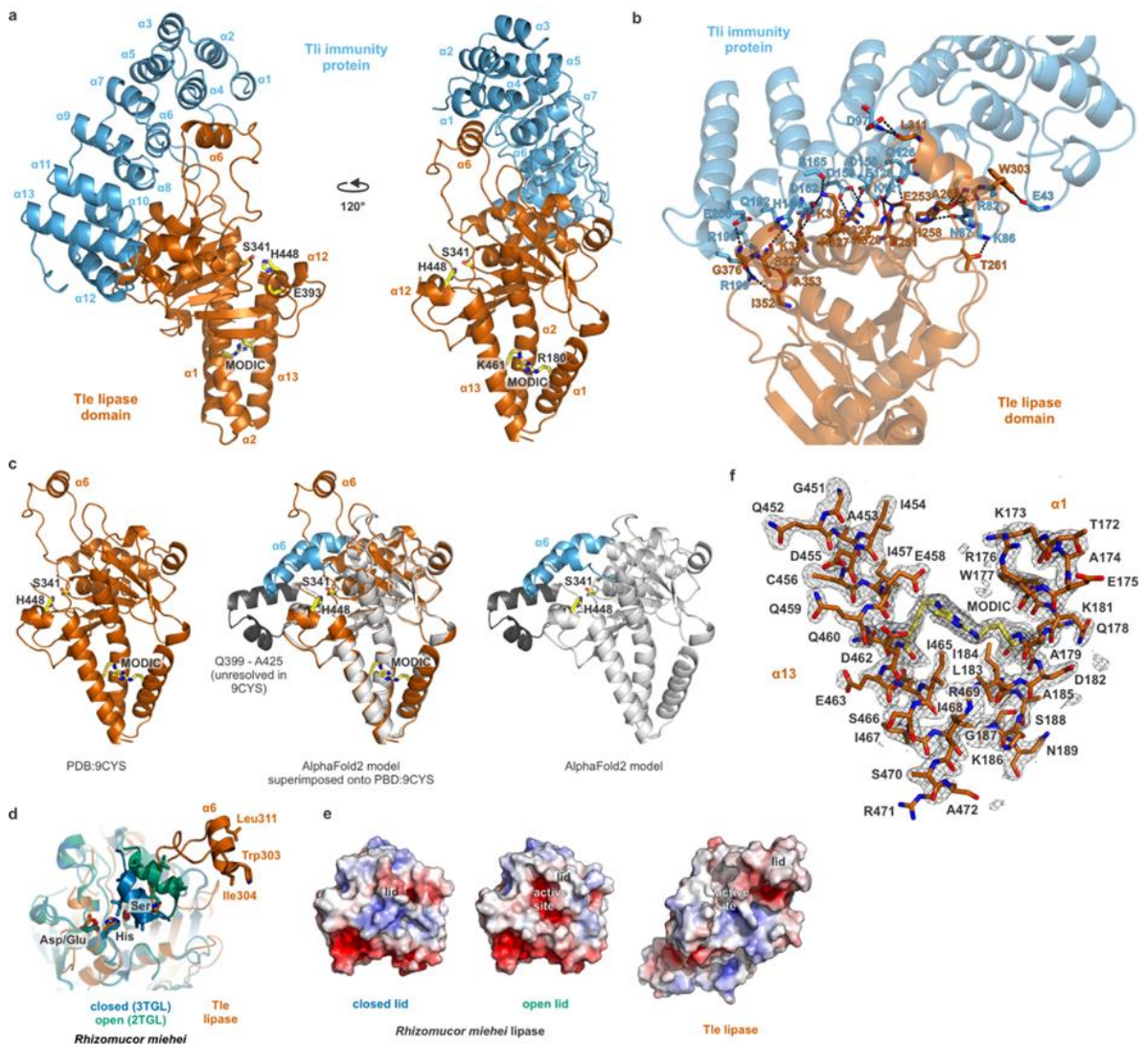


Fig. 2. Structure of the lipase•immunity protein complex.

(a) Structure of the lipase•immunity protein complex. Lipase active-site and MODIC residues are indicated in one-letter code. (b) Hydrogen-bond network of the lipase• Δ ss-Tli complex interface. (c) The AlphaFold2 model of Tle residues Thr172 - Ala472 superimposed onto the lipase domain structure (PDB: 9CYS). The AlphaFold2 modeled α 6 lid helix is shown in cyan, and the unresolved segment from the experimental model is rendered in charcoal. (d) Superimposition of the Tle lipase domain onto inactive (closed) and activated (open) forms of the *R. meiheii* triacylglycerol lipase. Residues are indicated using three-letter code. (e) Surface electrostatic potentials of lipase domains from panel d. Red surfaces are electronegative and blue surfaces are electropositive. (f) Omit map of lipase helices α 1 and α 13 to illustrate MODIC electron density.

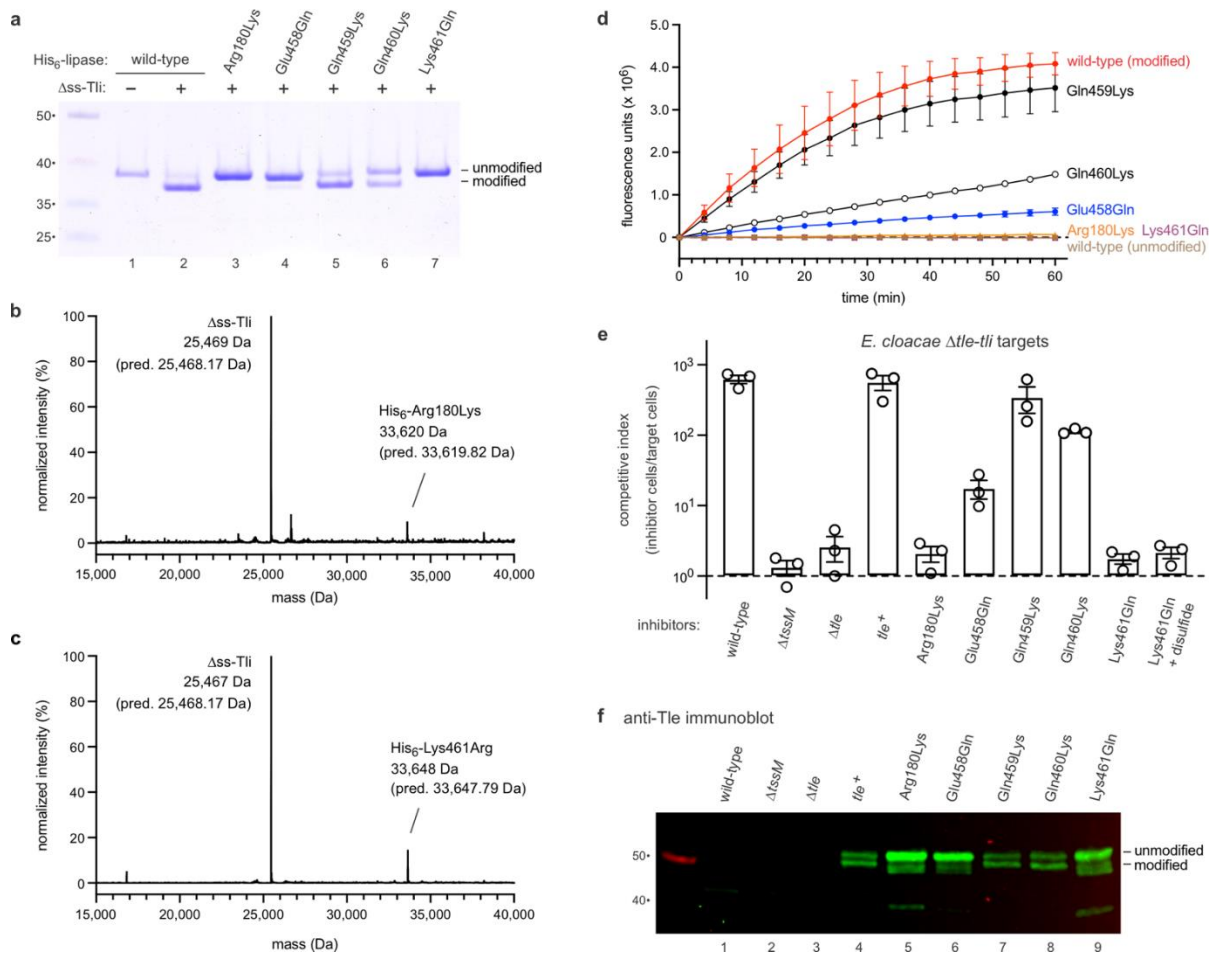


Fig. 3. AGE crosslinking is required for phospholipase activity. (a) The indicated His₆-lipase domain variants were produced with (or without) Δss-Tli, then purified by Ni²⁺-affinity chromatography under denaturing conditions for SDS-PAGE analysis. (b) Deconvoluted mass spectrum of the His₆-lipase(Arg180Lys)•Δss-Tli complex. (c) Deconvoluted mass spectrum of the His₆-lipase(Lys461Gln)•Δss-Tli complex. (d) *In vitro* phospholipase A1 activity assays of the purified domains from panel a. (e) Competition co-cultures. *E. cloacae* inhibitor strains were co-cultured with Δ*tle-tli* target bacteria and viable cells enumerated as described in Methods. Competitive indices are averages ± standard error for three independent experiments. (f) Urea-soluble cell lysates were prepared from the inhibitor strains in panel e and subjected to immunoblot analysis with polyclonal antibodies to Tle.

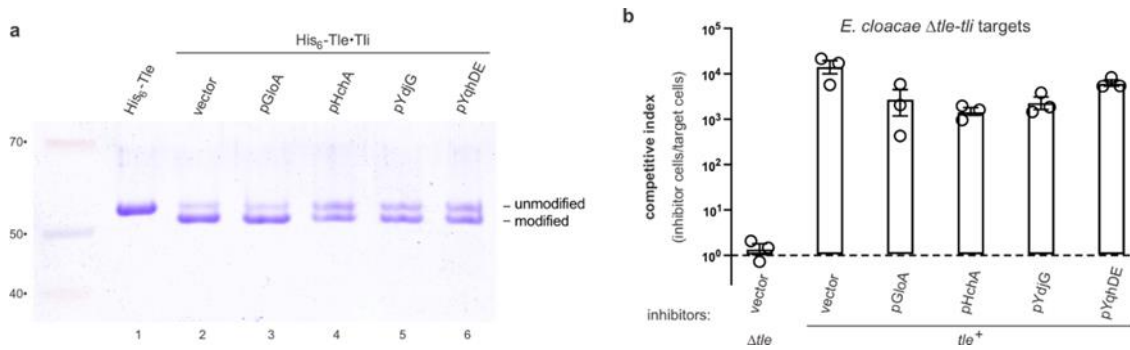


Fig. 4. Aldehyde reductases suppress Tle crosslinking.

(a) His₆-Tle was produced with Tli in *E. coli* cells that overexpress the indicated methylglyoxal detoxification enzymes. His₆-Tle was purified by Ni²⁺-affinity chromatography under denaturing conditions and analyzed by SDS-PAGE.

(b) Competition co-cultures. *E. cloacae* inhibitor strains that overexpress methylglyoxal detoxification enzymes were co-cultured with *E. cloacae* $\Delta tle-tli$ target bacteria and viable cells enumerated as described in Methods. Competitive indices are averages \pm standard error for three independent experiments.

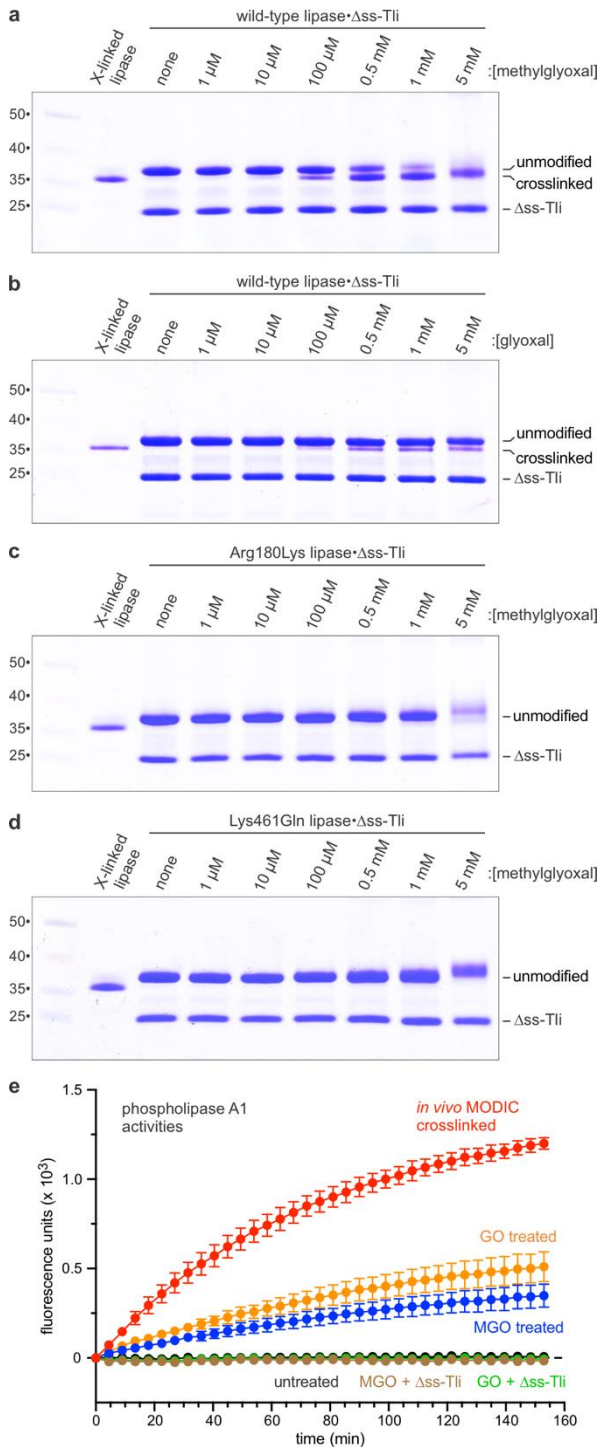


Fig. 5. *In vitro* activation of the phospholipase domain.

Unmodified lipase domain and Δ ss-Tli were mixed *in vitro* to form a complex, which was then treated with methylglyoxal (a) or glyoxal (b) at the indicated concentrations for 7 h at 37 °C. Treated complexes were analyzed by SDS-PAGE. Methylglyoxal

treatment of Arg180Lys (**c**) and Lys461Gln (**d**) lipase domains in complex with Δ ss-Tli. (**e**) *In vitro* crosslinked His₆-lipase domains were isolated from Δ ss-Tli by Ni²⁺-affinity chromatography under denaturing conditions, then refolded by dialysis for phospholipase A1 activity assays.

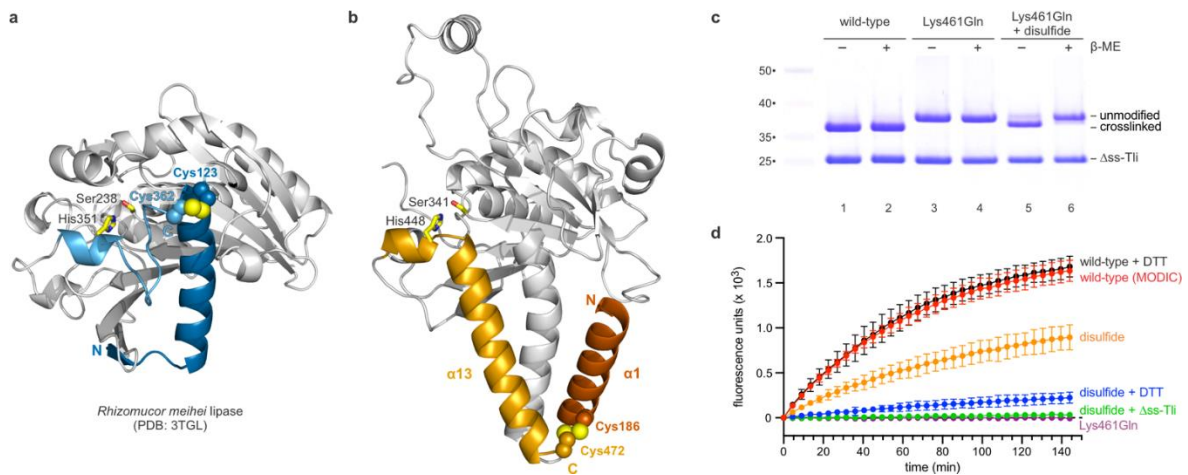


Fig. 6. Phospholipase activation with an engineered disulfide bond.

(a) Structure of *R. meihei* lipase illustrating the disulfide bond linking the N- and C-termini. (b) Predicted structure of Disulfide-by-design engineered Tle phospholipase domain (c) The indicated His₆-lipase variants were produced with Δ ss-Tli in *E. coli* cells, and the complexes purified by Ni²⁺-affinity chromatography under non-denaturing conditions. Complexes were analyzed by SDS-PAGE under oxidizing and reducing (β -mercaptoethanol, β -ME) conditions. (d) The indicated His₆-lipase domains were isolated from Δ ss-Tli by Ni²⁺-affinity chromatography under denaturing conditions, then refolded by dialysis for phospholipase A1 activity assays.

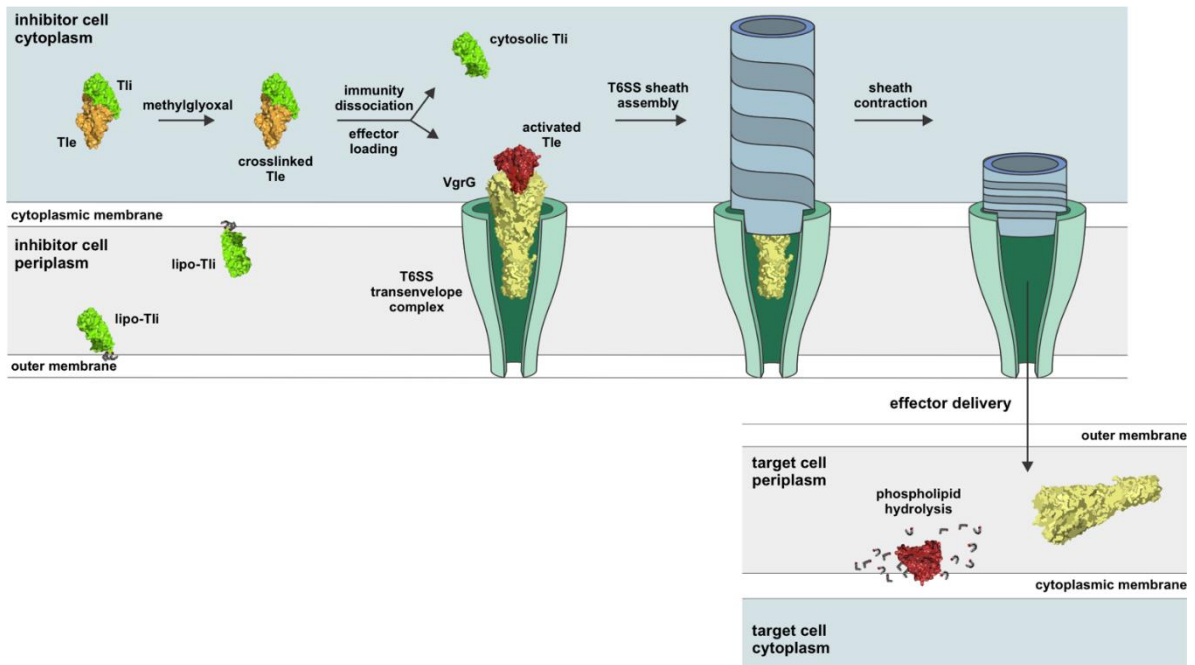
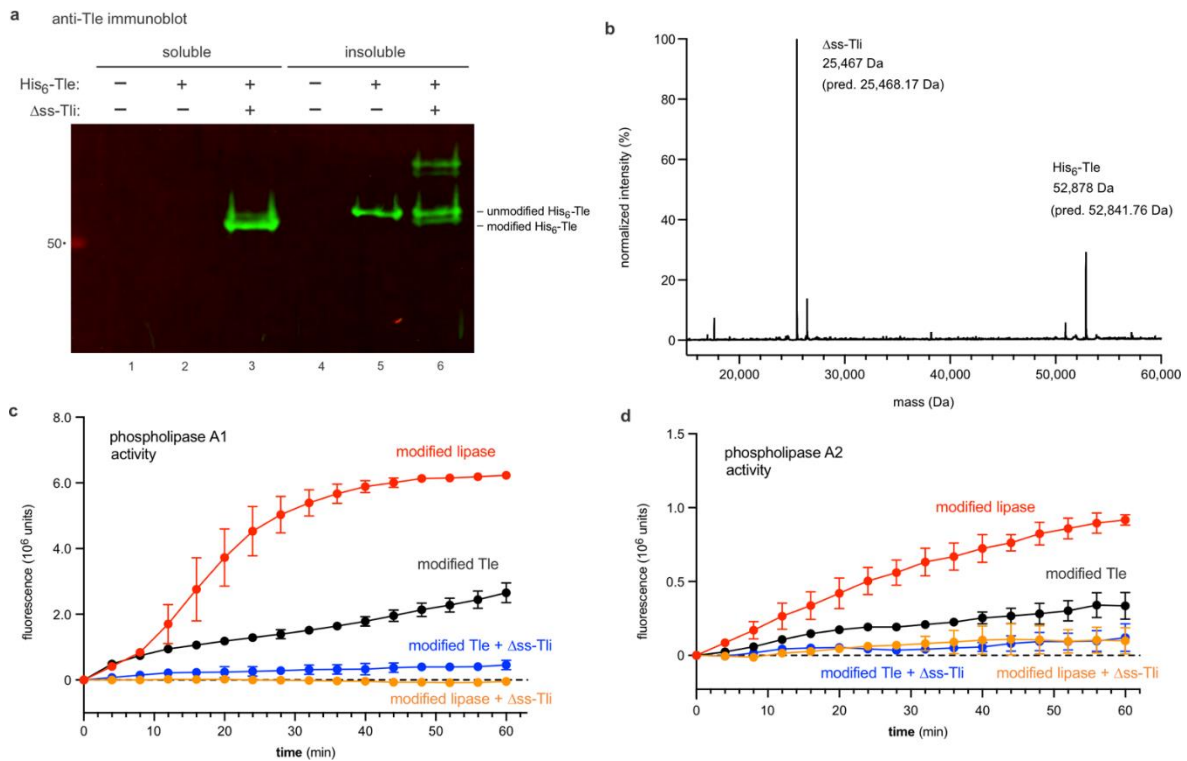


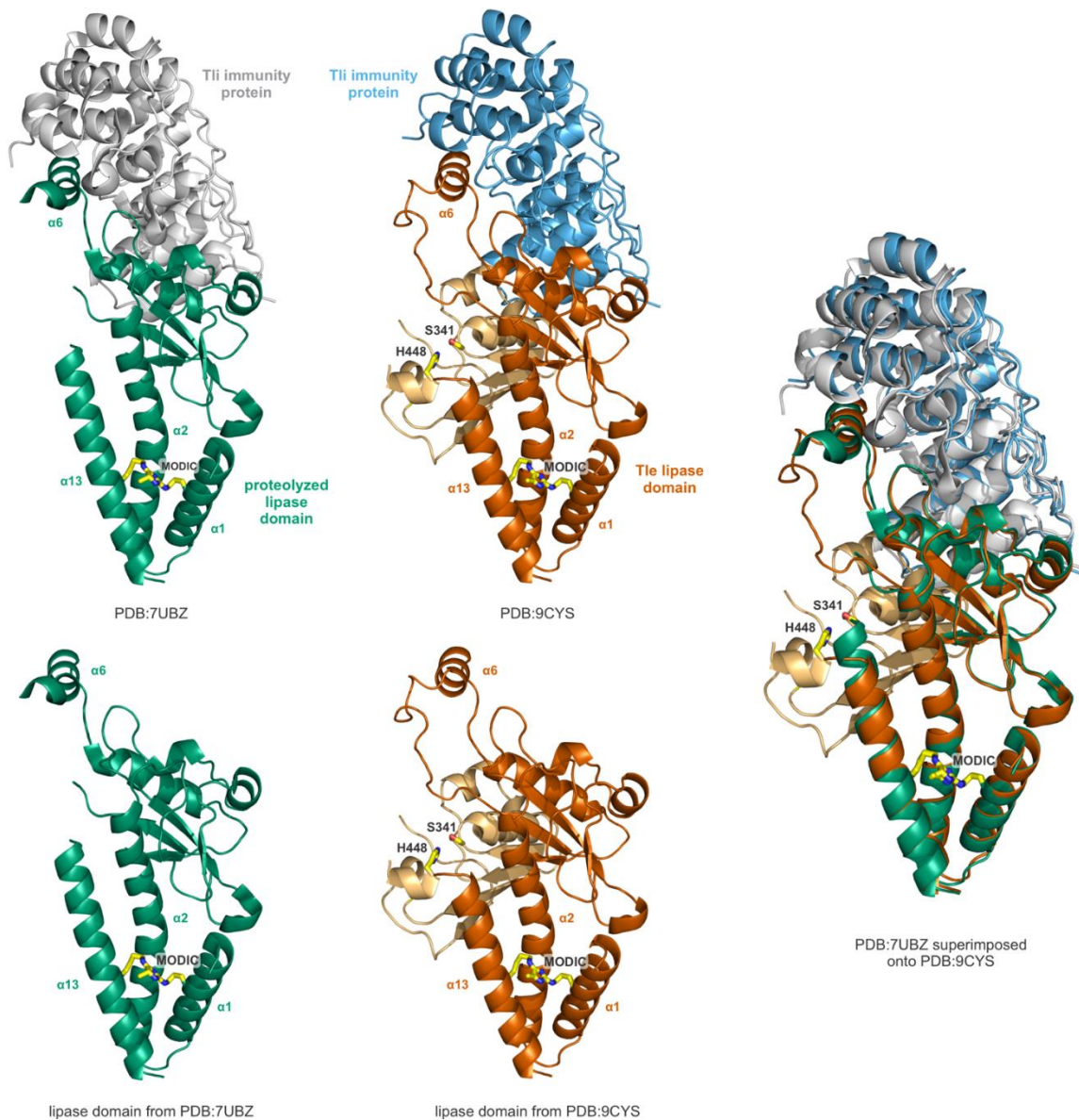
Fig. 7. Model for Tli-dependent Tle activation and T6SS mediated delivery.

Mature Tli (lipo-Tli) is secreted to the periplasm where it is lipidated and embedded in membranes to protect the cell from incoming Tle effectors. *E. cloacae* cells also produce cytosolic Tli, which presumably forms a transient complex with Tle to enable methylglyoxal crosslinking. The activated effector is then dissociated from the immunity protein and loaded into the T6SS apparatus for export. Upon delivery into the target-cell periplasm, activated Tle hydrolyzes membrane phospholipids.



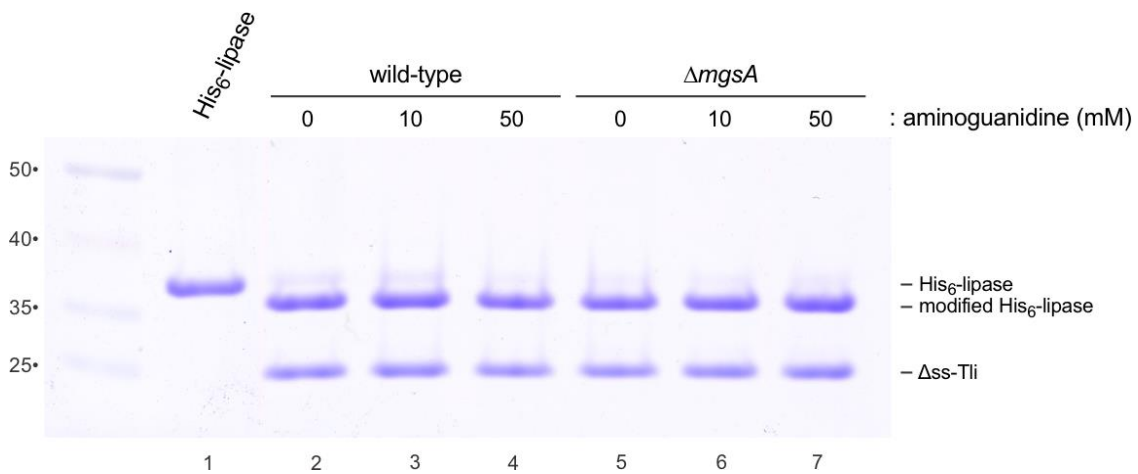
Supplementary Figure 1. Full-length Tle is modified.

(a) His₆-Tle was produced with (or without) Δss-Tli immunity protein in *E. coli* and the cells broken by French press for fractionation into soluble and insoluble fractions by centrifugation. Fractions were analyzed by immunoblotting with polyclonal antibodies to Tle. (b) Deconvoluted mass spectrum of purified the purified His₆-Tle•Δss-Tli complex. (c) Modified His₆-Tle was isolated from Δss-Tli using Ni²⁺-affinity chromatography under denaturing conditions, then refolded by dialysis for phospholipase A1 activity assays. (d) Phospholipase A2 activity assay of purified His₆-Tle.



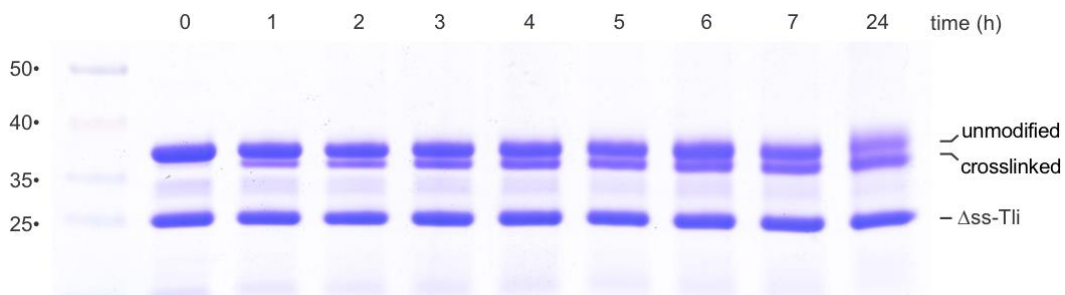
Supplementary Figure 2.

Crystal structure of chymotrypsin-treated lipase• Δ ss-Tli complex. The structure of the proteolyzed complex (PDB:7UBZ) is presented together with the native complex (PDB:9CYS). The digested lipase segment is depicted in gold in structure 9CYS. Images of the isolated lipase domains and a structure superimposition are shown for comparison

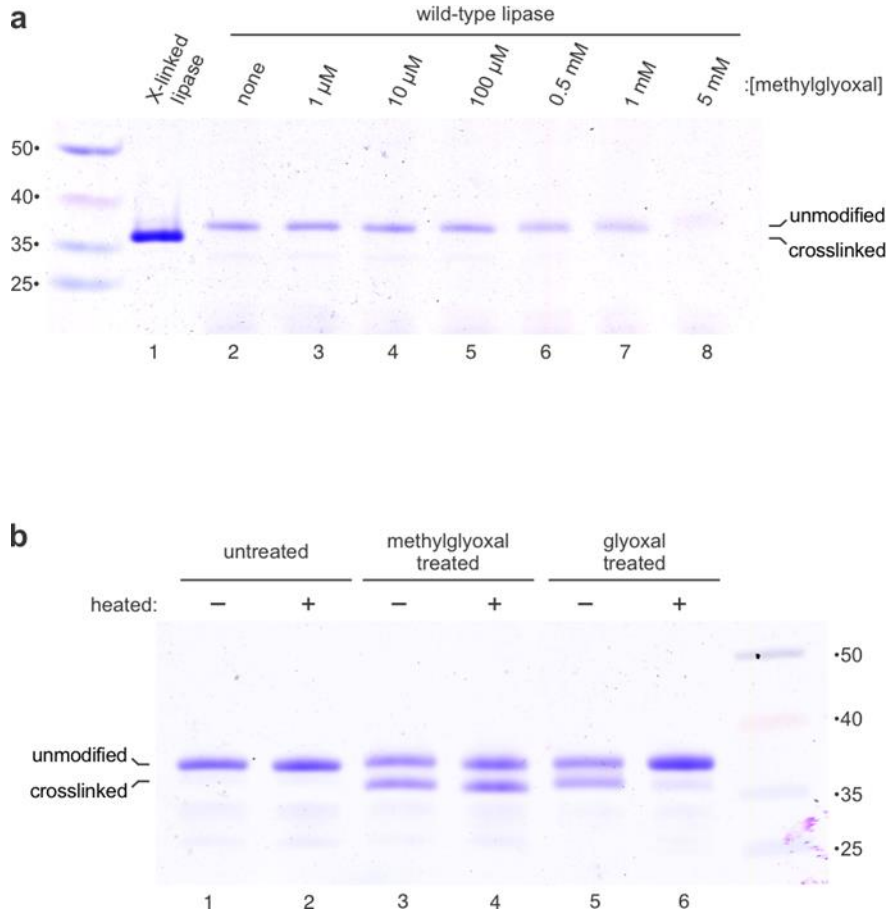


Supplementary Figure 3.

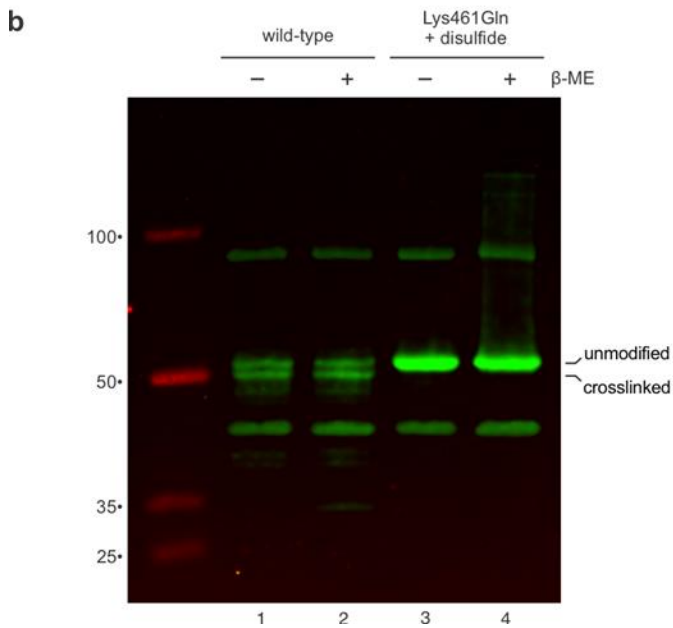
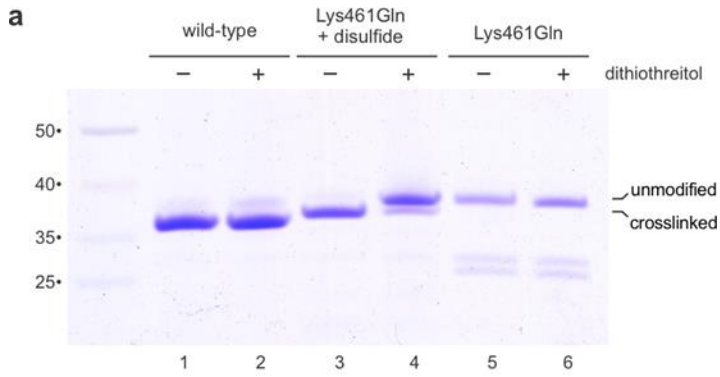
Aminoguanidine treatment and deletion of methylglyoxal synthase (*mgsA*) does not affect lipase domain crosslinking *in vivo*. His₆-lipase was produced with Δss-Tli in wild-type and Δ*mgsA* cells treated with aminoguanidine. The His₆-lipase•Δss-Tli complex was purified by Ni²⁺-affinity chromatography under non-denaturing conditions and analyzed by SDS-PAGE.



Supplementary Figure 4. *In vitro* methylglyoxal crosslinking time course. Unmodified His₆-lipase was purified and mixed with Δ ss-Tli *in vitro* to form a complex. The complex was incubated with 1 mM methylglyoxal at 37 °C for the indicated times and analyzed by SDS-PAGE.



Supplementary Figure 5. In vitro crosslinking of the Tle lipase domain. (a) Unmodified His6-lipase was incubated with methylglyoxal at the indicated concentrations for 7 h at 37 °C, then analyzed by SDS-PAGE. (b) The stability of methylglyoxal and glyoxal crosslinked His6-lipase was assessed by SDS-PAGE analysis of unheated and 95 °C heated samples.



Supplementary Figure 6. Analyses of disulfide containing lipase domain. (a) The indicated His6-lipase variants were produced with Δ ss-Tli in *E. coli* cells, then isolated by Ni²⁺-affinity chromatography under denaturing conditions. Purified His6-lipases were reduced with dithiothreitol for SDS-PAGE analysis and phospholipase A1 activity assays shown in Fig. 6d. (b) Tle-Tli and Tle(Lys461Gln-disulfide)-Tli production was induced with arabinose in *E. cloacae* cells. Urea-soluble total protein was extracted for immunoblot analysis using anti-Tle polyclonal antisera. Where indicated, samples were reduced with β -mercaptoethanol (β -ME).

Supplementary Table 1. Structural homologs of the Tle lipase domain.

Homolog	PDB identifier	Z-score	rmsd (Å) ^a	lali ^b	nres ^c	% identity ^d
<i>Capsicum annum</i> phospholipase A1	7X0D	13.3	3.8	194	386	15
<i>Arabidopsis thaliana</i> phospholipase A1	2YIJ	13.2	3.9	193	390	15
<i>Aspergillus niger</i> feruloyl esterase A	2IX9	12.7	3.4	186	386	15
<i>Rhizopus chinensis</i> triacylglycerol lipase	6A0W	12.7	3.7	173	287	16
<i>Thermomyces lanuginosus</i> lipase	4S0X	12.6	3.4	170	269	15
<i>Aspergillus oryzae</i> diacylglycerol lipase	5XK2	12.5	3.3	169	271	15
<i>Penicillium roqueforti</i> lipase	6L7N	12.3	3.2	170	270	12
<i>Rhizomucor miehei</i> triacylglycerol lipase	4TGL	12.3	3.3	172	265	20
<i>Rhizopus niveus</i> triacylglycerol lipase	1LGY	12.2	3.8	174	265	19
<i>Penicillium cyclopium</i> diacylglycerol lipase	5CH8	12.2	3.0	164	270	13
<i>Rasamsonia emersonii</i> lipase	6UNV	12.1	3.1	169	266	14
<i>Yarrowia lipolytica</i> triacylglycerol lipase	3O0D	12.0	3.6	171	296	15
^a root-mean-square deviation over aligned α -carbon atoms ^b number of residues in the structural alignment ^c number of total residues in the homologous protein ^d percent sequence identity between the aligned proteins						

Supplementary Table 2 Bacterial strains and plasmids.

Strain	Description	Reference
ECL	<i>Enterobacter cloacae</i> subsp. <i>cloacae</i> ATCC 13047	ATCC
X90	<i>E. coli</i> F' <i>lacI^q lac' pro' /ara Δ(lac-pro) nal1 argE(Am) rif^r thi-1, Rif^R</i>	
CH2016	<i>E. coli</i> X90 (DE3) Δ <i>rna ΔslyD::kan, Rif^R Kan^R</i>	(Garza-Sánchez et al., 2006)
CH5691	<i>E. coli</i> X90 (DE3) Δ <i>rna ΔslyD ΔmgsA::kan, Rif^R Kan^R</i>	this study
CH6247	<i>E. coli</i> X90 (DE3) Δ <i>rna ΔslyD, Rif^R</i>	
CH11396	<i>E. cloacae ΔtssM</i>	(Donato et al., 2020)
CH11895	<i>E. cloacae Δtle Δtli::spc, Spc^R</i>	(Donato et al., 2020)
CH14384	<i>E. cloacae Δtle Δtli::spc rif, Spc^R Rif^R</i>	(Jensen et al., 2023)
Plasmid		
pCH450	pACYC184 derivative with <i>E. coli araC</i> and <i>araBAD</i> promoter for arabinose-inducible expression, Tet ^R	(Garza-Sánchez et al., 2006)
pCH495	pCH450K::(Δ ss) <i>tli, Tet^R</i>	(Jensen et al., 2023)
pCH1382	pCH450:: <i>his₆-lipase(K186C,C456S,K461Q,A472C), Tet^R</i>	this study
pCH2199	pSH21:: <i>tle, Amp^R</i>	this study
pCH2826	pSCBAD:: <i>tle, Tp^R</i>	this study
pCH3128	pCH450:: <i>tle-tli, Tet^R</i>	(Jensen et al., 2023)
pCH3291	pET21P::(Δ ss) <i>tli, Amp^R</i>	this study
pCH3763	pCH450:: <i>vgrG2-lipase(S341A)-tli, Tet^R</i>	(Jensen et al., 2023)
pCH3923	pSCBAD:: <i>tle(K186C,C456S,K461Q,A472C)-tli, Tp^R</i>	this study
pCH3936	pCH450:: <i>his₆-lipase(S341A), Tet^R</i>	this study
pCH4362	pSCBAD:: <i>tle-tli, Tp^R</i>	this study
pCH5119	pSCBAD:: <i>hchA, Tp^R</i>	this study
pCH5120	pSCBAD:: <i>ydjG, Tp^R</i>	this study
pCH5121	pSCBAD:: <i>yqhDE, Tp^R</i>	this study
pCH5501	pSCBAD:: <i>tle(R180K)-tli, Tp^R</i>	this study
pCH5502	pSCBAD:: <i>tle(Q459K)-tli, Tp^R</i>	this study
pCH5503	pSCBAD:: <i>tle(Q460E)-tli, Tp^R</i>	this study
pCH5892	pSH21:: <i>tle-tli, Amp^R</i>	this study
pCH7088	pCH450:: <i>his₆-lipase, Tet^R</i>	this study
pCH7599	pCH450:: <i>his₆-lipase(R180K), Tet^R</i>	this study

pCH7600	pSCBAD:: <i>tle(E458Q)-tli</i> , Tp ^R	this study
pCH7601	pSCBAD:: <i>tle(K461Q)-tli</i> , Tp ^R	this study
pCH7620	pCH450:: <i>his₆-tle</i> , Tet ^R	this study
pCH7694	pSCBAD:: <i>gloA</i> , Tp ^R	this study
pCH7695	pMCSG63:: <i>TEV-(Δss)tli</i> , Amp ^R	this study
pCH8259	pCH450:: <i>his₆-arfA</i> , Tet ^R	(Garza-Sánchez et al., 2011)
pCH8717	pCH450:: <i>his₆-lipase(Q459K)</i> , Tet ^R	this study
pCH8718	pCH450:: <i>his₆-lipase(Q460E)</i> , Tet ^R	this study
pCH8871	pCH450:: <i>his₆-lipase(E458Q)</i> , Tet ^R	this study
pCH8872	pCH450:: <i>his₆-lipase(K461Q)</i> , Tet ^R	this study
pCH8904	pSH21:: <i>lipase(K186C,C456S,K461Q,A472C)</i> , Amp ^R	this study
pCH14212	pCH450:: <i>tle</i> , Tet ^R	(Jensen et al., 2023)
pCH15269	pSH21:: <i>lipase</i> , Amp ^R	(Jensen et al., 2023)
pSCBAD	pBBR1 derivative that carries <i>araC</i> and P _{BAD} promoter, Tp ^R	(Koskiniemi et al., 2015)
Abbreviations: Amp ^R , ampicillin resistant; Kan ^R , kanamycin resistant; Rif ^R , rifampicin resistant; Spc ^R , spectinomycin resistant; Tet ^R , tetracycline resistant; Tp ^R , trimethoprim resistant		

Supplementary Table 3. Oligonucleotides.

Identifier	Description	Sequence
CH943	ara-for	5' - GAT TAG CGG ATC CTA CCT GAC GCT TTT TAT CGC
CH3719	tli-M24-Kpn-for	5' - AAA GGT ACC ATG GAT TTA AAA CCA G
CH3419	tli-Xho-rev	5' - ATA CTC GAG CTA TTT AAC CGG AGT TGG TG
CH4469	tle-Eco-for	5' - AGG GAA TTC CGA ATG TAC AAC ATA AAA TTT GTC
CH4703	tle-Spe-for	5' - TTT ACT AGT ATG TAC AAC ATA AAA TTT GTC TAT CTT TTC AG
CH4762	tle-S341A-for	5' - CGA TAT TGC AGG CCA CGC TCT GGG TGG TGG G
CH4763	tle-S341A-rev	5' - CCC ACC ACC CAG AGC GTG GCC TGC AAT ATC G
CH5087	tle-T172-Spe-for	5' - TTT ACT AGT ACC AAA GCT GAA CGC TGG C
CH5539	tle-H448A-for	5' - GTC CAT TGG ACC GCG CTG GCA TTG GTC AGG
CH5675	tle-K461Q-Xho-rev	5' - TTC TCG AGT TAT GCA CGA CTC CTA ATA ATT GAA ATG TCT TCA TCC TGT TGC TGT TCT ATG
CH5688	tle-R180K-Spe-for	5' - CAC ACT AGT ACC AAA GCT GAA CGC TGG CAG GCG AAG AAG GAT CTG ATT GC
CH5689	tle-E458Q-for	5' - GGC AAT AGA TTG CAT ACA ACA GCA AAA GGA TGA
CH5690	tle-461Q-for	5' - GAT TGC ATA GAA CAG CAA CAG GAT GAA GAC ATT TCAA
CH5721	tle-R180K-for	5' - CGC AAT CAG ATC CTT CTT CGC CTG CCA GCG TT
CH5722	tle-Q459K-for	5' - GCA ATA GAT TGC ATA GAA AAG CAA AAG GAT GAA GAC
CH5723	tle-Q460E-for	5' - ATA GAT TGC ATA GAA CAG GAA AAG GAT GAA GAC ATT TC
CH5751	ECL-tli-TEV-D25-Kpn-for	5' - TTT GGT ACC GAG AAC CTG TAC TTC CAA TCC GAT TTA AAA CCA GAT AAT TAC TTT AGC GGA
CH5761	gloA-Eco-for	5' - TTT GAA TTC ATG CGT CTT CTT CAT ACC ATG
CH5762	gloA-Xho-rev	5' - TTT CTC GAG TTA GTT GCC CAG ACC G
CH5879	tle-E393A-for	5' - CGT GTT GAA GGT GCA TTG CTG ACA AAA ATC C
CH5907	tle-K186C-for	5' - AAG GAT CTG ATT GCG TGT GGG AGT AAT AGC CTC

CH5908	tle-K186C-rev	5' - GAG GCT ATT ACT CCC ACA CGC AAT CAG ATC CTT
CH5909	tle-A472C-Xho-rev	5' - AAG CTC GAG TTC AAC AAC GAC TCC TAA TAA TTG AAA TGT C
CH5959	tle-C456S-for	5' - GGT CAG GCA ATA GAT TCC ATA GAA CAG CAA
CH5960	tle-C456S-rev	5' - TTG CTG TTC TAT GGAATC TAT TGC CTG ACC
CH6062	tle-A472C-tli-for	5' - ATT TCA ATT ATT AGG AGT CGT TGT TGA TGA AAT CGT TCT TAT CAG GCT GG
CH6063	tle-A472C-tli-rev	5' - CCA GCC TGA TAA GAA CGA TTT CAT CAA CAA CGA CTC CTA ATA ATT GAA AT
CH6310	hchA-Mfe-for	5' - AAG CAA TTG ACT ATG ACT GTT CAA ACA AGT AAA AAT CC
CH6311	hchA-Sbf-rev	5' - AAC CCT GCA GGG ATT AAC CCG CGT AAG CTG CC
CH6312	ydjG-Eco-for	5' - TAA GAA TTC CAA ATG AAA AAG ATA CCT TTA GGC
CH6313	ydjG-Pst-rev	5' - CGT CTG CAG TAT TTA ACG CTC CAG G
CH6314	yqhD-Eco-for	5' - AGG GAA TTC GTA ATG AAC AAC TTT AAT CTG
CH6315	yqhE-Pst-rev	5' - GAA TCT GCA GGT TAG CCG CCG AAC TG
ZR248	tle-Xho-rev	5' - TTT CTC GAG CTG ATA AGA ACG ATT TCA TGC ACG

Chapter IV: Characterization of ECL Tle-Tli homologs

Introduction

The modular nature of the type VI secretion system (T6SS) makes it well suited for delivering a diversity of effector proteins. A wide variety of anti-prokaryotic and anti-eukaryotic activities have been observed from T6SS effectors as bacteria have adapted the system for antagonization of different targets (Singh & Kumari, 2023). But there is also diversity seen within effectors that share a similar function. For example, type VI amidase effectors (Tae), which target the Gram-negative cell wall, have been categorized into four families based on primary sequence identities and peptidoglycan cleavage sites (Russell et al., 2012). There are several hypotheses on the evolutionary drive behind differentiation of effectors with similar functions. Concurrent secretion of similar effectors may yield a more thorough degradation of the target substrate, or different effector families may be better suited for certain target species and/or environmental conditions (Whitney et al., 2013). Lastly, speciation and the accumulation of orphan immunity genes may also be driving effector differentiation as a strategy for restricting effector neutralization to a small subset of kin (Russell et al., 2012).

In Russell *et al.*'s study on type VI lipase effectors (Tle), predicted Tle genes separated into 5 families based on sequence and phylogeny, Tle1-Tle5 (Russell et al., 2013). Members of Tle1-4 all had a similar GX SXG active site motif, while those in Tle5 had a unique HXKXXXD active site. This active site difference was reflective of the phospholipase cleavage site, as the Tle1 and Tle2 effectors used in the study had phospholipase A activity while the selected Tle5 protein was shown to have

phospholipase D activity. More specifically, the Tle1 and Tle2 effectors had phospholipase A₁ (PLA₁) and A₂ (PLA₂) activities, respectively. However, Flaugnatti *et al.* later demonstrated that a Tle1 homolog from entero-aggregative *Escherichia coli* had both PLA₁ and PLA₂ activity (Flaugnatti *et al.*, 2016). Thus, functional differences amongst effectors in the Tle1-4 families remains unclear.

Studies from Chapters II and III have revealed that the Tle encoded by *Enterobacter cloacae* displays certain characteristics that distinguish itself from previously characterized Tle proteins. Tle^{ECL} requires co-expression of its cognate Tli protein to display phospholipase activity, but activity assays in previous Tle studies were carried out with purified lipases expressed in isolation of their immunity proteins (Flaugnatti *et al.*, 2016; Russell *et al.*, 2013). Furthermore, the reported structures of Tle1 and Tle4 from *Pseudomonas aeruginosa* show no evidence of having intramolecular cross-links like the methylglyoxal-derived imidazolium crosslink (MODIC) structure required for Tle^{ECL} activity (H. Hu *et al.*, 2014; Lu *et al.*, 2014). This seemed to indicate that Tle^{ECL} was representative of a sixth, previously uncharacterized family of Tle proteins. A sequence alignment search revealed the presence of multiple Tle^{ECL} homologs. Furthermore, two of these Tle^{ECL} homologs from *Serratia marcescens* and *Dickeya dadantii* were examined to see if the mechanism of activation was conserved across these species

Results

MODIC site conservation and ankyrin Tli are hallmarks of Tle^{ECL} homologs

The primary sequence of Tle^{ECL} was used as a BLAST search query to identify homologous effectors across Gram negative bacteria (**Table 1**). Alignments were also attempted between Tle^{ECL} and examples from the Tle1-5 families established by Russell *et al.* (Russell et al., 2013) Uncharacterized homologs with >50% sequence identities were found in various Enterobacteriales genera including *Serratia* and *Cronobacter*, while less conserved examples were found in *Burkholderia* and *Dickeya* species. Meanwhile, none of the attempted alignments with members of the Tle1-5 families yielded sequence identity values above 10%. An alignment of the lipase domain of Tle^{ECL} with its predicted homologs shows much of the shared sequence identity is between residues that comprise or are near the catalytic triad: Ser341, Glu393, His448 (**Fig. 1A**). There is also sequence conservation at the N- and C-terminus of the domain, which was noted as the MODIC-linked residues, Arg180 and Lys461, are located in these regions (**Fig.1B**). These residues are highly conserved across the selection of homologs analyzed, although both residues are absent in the Tle homolog from *Burkholderia cenocepacia*. There are other residues in these helices that are conserved with the MODIC sites, such as Arg176, Glu458, and Asp464. It has been thought that protein glycation site selectivity can be influenced by nearby charged residues, so the conservation of these residues near the MODIC site suggests that they are important for the unusually specific nature of Tle^{ECL} glycation (Ahmed et al., 2005).

Because Tli has an essential role in Tle^{ECL} modification, I also examined the sequence conservation of the predicted immunity proteins for this selection of Tle homologs (**Table 1**). As expected, the percent identities with Tli^{ECL} were similar to that of their cognate effectors. Several of these immunities are present in their chromosomes in adjacent pairs of near-duplicate genes. Notably, all the identified Tle^{ECL} homologs were paired with Tli containing predicted ankyrin repeat domains. Ankyrin repeats have not been seen in previously studied Tli proteins and were not present in the Tle1-5-associated immunity proteins we analyzed. Conservation of the ankyrin-repeat domain across Tle^{ECL} homologs may imply this is a necessary feature that permits these immunity proteins to participate in a shared lipase activation process.

The conserved MODIC site is essential for phospholipase activity in Tle^{SMA}

Primary sequence analysis suggested Tli-dependent MODIC activation was shared amongst Tle^{ECL} homologs, so I investigated the *in vitro* activity of one such homolog to see if it displayed functional similarities to Tle^{ECL}. I chose to characterize the predicted Tle from *Serratia marcescens* Db11 (Tle^{SMA}) which has moderate homology with Tle^{ECL}. From Db11's parental strain *Serratia marcescens* Db10, the lipase domain (Thr177-Ile494) of Tle^{SMA} was cloned into a plasmid with an N-terminal His6 tag, while the Tli directly downstream from Tle^{SMA} was cloned into a separate plasmid without its lipoprotein signal sequence (Δ ssTli^{SMA}) for cytoplasmic overexpression. Tle^{SMA} was overexpressed in *E. coli* cells in the absence or presence of Δ ssTli^{SMA}, then purified under native conditions to pull down any Tle-associated Tli. Pull-downs were analyzed via SDS-PAGE to check for a Tli-

dependent mobility shift in Tle^{SMA}, as this mobility shift was a trait associated with crosslink-activated Tle^{ECL}. When co-expressed with Δ ssTli^{SMA}, Tle^{SMA} runs as a doublet with a majority of the sample in the higher mobility band (**Fig.2A**). However, direct comparison with the sample not co-expressed with Tli was not possible, as Tle^{SMA} was unable to be purified from cells expressing the effector alone. Attempts of a denaturing purification of Tle^{SMA} alone were also unsuccessful. Thus, Arg185Lys and Lys482Gln point mutations were introduced into Tle^{SMA} as an alternative approach to disrupt potential crosslinking via substitution of the residues predicted to participate in MODIC. When co-expressed with immunity both point mutation lipases run as a single band on an SDS-PAGE gel, with a mobility that matches that of the lower mobility band of the wild-type doublet. Enzymatic activity of the lipases was measured via phospholipase activity assays alongside Tle^{ECL} (**Fig. 2B**). Wild-type Tle^{SMA} displays clear phospholipase activity while both the Arg185Lys and Lys482Gln point mutations completely remove activity. Thus the presence of a modified lipase species with higher SDS-PAGE mobility is correlated with enzymatic activity in Tle^{SMA} just as it is in Tle^{ECL}. This, combined with the observation that the conserved Arg-Lys pair in the N- and C-terminal helices is essential for its mobility shift has led to the conclusion that Tle^{SMA} is activated via AGE-crosslinking similarly to Tle^{ECL}.

Tle^{DDA} is activated by Tli1 and does not interact with Tli2

Due to the difficulty of purifying Tle^{SMA} in the absence of its cognate immunity protein, the Tli-dependent nature of Tle modification was further investigated by focusing on a Tle homolog from a different species, *Dickeya dadantii* 3937 (Tle^{DDA}).

His6-tagged Tle^{DDA} was overexpressed with or without its two downstream immunity Tli proteins, Tli1 and Tli2 (**Fig. 3A**). Unlike Tle^{SMA}, Tle^{DDA} was successfully overexpressed and purified in the absence of its immunity proteins (**Fig. 3B**). However, Tle^{DDA} does not display a visible mobility shift on SDS-PAGE gels when co-expressed with Tli. Tli co-expression did not alter Tle^{DDA} solubility either, as full-length Tle^{DDA} appears to be more soluble than Tle^{ECL} even in the absence of immunity. Despite the lack of these features associated with Tli-activation, *in vitro* activity assays show that Tle^{DDA} requires immunity co-expression to display phospholipase activity (**Fig. 3C**). The activity of Tle^{DDA} that was overexpressed alone shows similar activity to that of the Tli-neutralized sample.

Next, I sought to individually examine Tli1 and Tli2 regarding their capabilities of Tle^{DDA} neutralization and activation. H6-Tle^{DDA} was co-expressed with either Tli1 or Tli2, then purified to assess *in vivo* activity. Tween esterase assays show that Tli1 co-expression is sufficient to activate Tle^{DDA}, while Tli2 co-expression does not yield enzymatic activity (**Fig.4A**). To assess effector neutralization, purified Tli1 and Tli2 were added to esterase reactions. A similar trend was observed in which active Tle^{DDA} was neutralized by Tli1 but not Tli2. Seeing that only Tli1 was capable of Tle^{DDA} activation and neutralization, a pull-down experiment was performed to determine if Tli2 maintains significant non-covalent interactions with the effector. His6-TEV-tagged Tli1, Tli2 and Tli^{ECL} were purified then treated with TEV protease to yield untagged Tli isolates. Purified Tli samples were then incubated with purified His6-Tle^{DDA} under non-denaturing conditions to enable formation of Tle-Tli complexes. Affinity purifications of His6-Tle^{DDA} were performed and analyzed via

SDS-PAGE to determine which Tli proteins were co-purified with the effector. Results of the pull-down reveal that only Tli1 forms a stable complex with Tle^{DDA} (**Fig. 4B**). This is surprising due to the overall sequence similarity between Tli1 and Tli2. However, there is a region corresponding to Ile196-Leu233 of Tli1, in which the sequences of these proteins appear more divergent (**Fig. 3A**). AlphaFold2 modeling suggests that this region of sequence divergence corresponds to the C-terminal pair of α -helices of these proteins (**Fig. 5A**) (Jumper et al., 2021). In the crystalized Tle-Tli complex from *E. cloacae*, the C-terminal α -helices of Tli appear to contact the surface of Tle (**Fig. 5B**). It is feasible that the sequence divergence in this region is responsible for the lack of interaction between Tli2 and Tle^{DDA}. Interestingly, Tli2 is nearly identical to a predicted Tli sequence from another species, *Dickeya fangzhongdai* (**Fig. 3A**). Having shown that Tli2 has no apparent effect on the function Tle^{DDA}, Tli2 may instead be a remnant from an ancestral effector that provides cross-species immunity.

Discussion

Tle deployed by *E. cloacae* is notable for two characteristics that have not been observed in previously described type VI effectors: its activity is reliant on simultaneous expression with its cognate Tli, and an essential AGE crosslink forms within the effector prior to its secretion. My investigation of uncharacterized Tle^{ECL} homologues from *D. dadantii* and *S. marcescens* suggests that both characteristics are common to a family of related Tle that can be found in at least 5 genera of bacteria. The effectors in this family also have similar immunity proteins, as the downstream Tli are all predicted to have ankyrin repeats. Ankyrin repeats are well-

known to act as interfaces for protein-protein interactions, so their utilization for effector-immunity interactions seems natural (Mosavi et al., 2004). However, ankyrin repeats have not been previously seen in other Tli or any type VI immunity proteins in general. Instead, ankyrin repeats have been observed in virulence factors delivered by the type IV secretion system and are thought to allow association with the endoplasmic reticulum (Lehman et al., 2018; Pan et al., 2008). The reduced presence of ankyrin proteins in bacterial genomes compared to those from eukaryotes has led some to hypothesize that bacterial ankyrin proteins are the result of horizontal gene transfer (Bork, 1993). The shared identity between Tle^{ECL} and fungal lipases, noted in Chapter III, may further suggest a eukaryotic origin of this lineage of Tle and Tli.

Sequence alignments show that the MODIC-linked residues of Tle^{ECL} are well-conserved in its homologues, pointing towards a shared cross-linking activation process across this protein family. Disruption of the predicted crosslinked residues in Tle from *S. marcescens*, Arg185 and Lys482, abrogated effector modification and enzymatic activity. Additional charged residues near the crosslink sites are also conserved, resulting in Rxxx**R** and Exx**K**xxD motifs for the N- and C-terminal cross-link sites, respectively. The conservation of the glutamate in the C-terminal helix coincides with our finding from Chapter III that mutation of Glu458 in ECL^{Tle} significantly reduces Tle modification and activity. Conservation of residues near the crosslink site may therefore imply a role in the efficient and/or site-specific nature of Tle glycation. Peptide mapping of glycated serum albumin by Ahmed *et al.* found hot spots of methylglyoxal modification at surface-exposed arginine residues

positioned near Asp, Ile, and Lys residues (Ahmed et al., 2005). A proteome-wide analysis in *Arabidopsis* by Bilova *et al.* not only found that glycation hotspots frequently occurred near Lys, Arg, Glu, Asp and Leu residues, but also saw that the residues were often spaced in patterns indicative of α -helical structure (Bilova et al., 2017). Thus, the observed crosslink motifs of Tle are in accordance with previous observations on glycation site determinants. The rapid and specific nature of Tle glycation may make its motifs a suitable model to use for predicting spontaneous glycation targets or identifying other potential examples of AGE-activated proteins.

Despite the overall similarities amongst the examined lipases, some differences amongst these proteins were also noted. First, expression of the lipase domain of Tle^{SMA} in the absence of its cognate Tli could not be achieved in this study. Tli^{ECL} had notably reduced solubility in absence of its Tli, but it seems the stability of Tle^{SMA} is even worse when its unmodified and not bound to its immunity protein. The immunity-dependent nature of Tle glycation seems apparent in this case: unmodified Tle^{SMA} is tentatively stabilized when bound to Tli^{SMA}. This allows glycation to occur, after which modified Tle^{SMA} can persist without the aid of Tli^{SMA}. Although the unmodified forms of Tle^{ECL} and Tle^{DDA} appear to be more stable without their respective Tli, these findings hint that their structures may be instable to a degree that prevents proper glycation from occurring. Another deviation from Tle^{ECL} was seen in Tle^{DDA} after co-expression with Tli1 and Tli2. Tle^{DDA} similarly required Tli co-expression to be enzymatically active, yet samples of the activated effector did not display increased mobility on an SDS-PAGE gel. This mobility shift is associated with Tle^{ECL} activity and crosslinking and could even be observed in the full-length effector.

Yet it appears that crosslinked Tle^{DDA} might not have a similar change in its hydrodynamic character, perhaps obfuscated by its N-terminal PAAR domain. Although the presence of a mobility shift can be a straightforward method to assess the presence of an AGE crosslink, it is now apparent that such shifts may not always accompany these modifications.

Finally, the interactions between Tle^{DDA} and its immunity proteins, Tli1 and Tli2, were studied as an example of a *tle^{ECL}* homologue with two downstream immunity genes. I found that Tli1 is capable of both activating and neutralizing Tle^{DDA} while Tli2 is capable of neither function. Furthermore, Tli2 appears to have no specific affinity for Tle^{DDA} and its sequence is nearly identical to a Tli from *D. fangzongdai* (Tle^{DDF}). It seems likely that Tli2 has no interaction with Tle^{DDA} and is instead the cognate immunity of Tle^{DDF}. A major region of sequence divergence in Tli2 occurs at its C-terminus and corresponds to its final pair of α -helices. Ankyrin repeat domains are known to be modular, as changes in protein interaction partners are often determined by the addition, exchange or deletion of repeats (Al-Khodor et al., 2010). It seems likely that one such repeat swap has caused the sequence and Tle-specificity divergence of Tli1 and Tli2. This leads to the question of why *D. dadantii* has the non-cognate *tli2* genetically adjacent to its cognate *tli1*. The duplication of an ancestral *tli* resembling *tli^{DDF}* could have been caused by their ankyrin domains, as their repetitive nature can lead to more frequent duplication events (Lynch & Conery, 2000). After this supposed duplication, an ankyrin repeat swap in *tli1* may have allowed the emergence of a divergent *tle* in *D. dadantii*. Regardless of its origin,

retention of *tli2* likely allows *D. dadantii* to neutralize Tle from *D. fangzongdai* inhibitors.

Materials and Methods

Bacterial strains, growth conditions, and plasmid constructs

The bacterial strains, plasmids, and oligonucleotides used in this study are listed in **Table 2**, **Table 3**, and **Table 4**. All bacteria were grown in shaking lysogeny broth (LB) or LB-agar at 37°C. Media were supplemented with antibiotics at the following concentrations: 15 µg/mL tetracycline (Tet) and 150 µg/mL ampicillin (Amp). To construct the His6-tagged lipase domain of *S. marcescens* Db10 Tle, oligos CH6147/CH6148 were used to amplify SMDB11_0927, and the resulting product was ligated into pCH7620 via SpeI/XhoI restriction sites to generate plasmid pCH4025. Arg185Lys and Lys482Gln mutations were introduced via amplification with oligo pairs CH6153/CH6148 and CH6147/CH6154, respectively, then ligated as described above to generate plasmids pCH4249 and pCH4250. ss-Tli^{SMA} was cloned by amplifying SMDB11_0928 with oligos CH6149/CH6150 and ligating the product into pET21P using NcoI/XhoI restriction sites to yield pCH4026. His6-tagged Tle from *D. dadantii* 3937 was constructed by amplifying Dda3937_00831 with oligos CH5115/CH5116 and ligating the product into pCH15269 via SpeI/XhoI restriction sites to yield pCH5603. To clone His6-tagged Tle^{DDA} with Tli1 and Tli2, oligos CH5115/5117 were used to generate an amplicon with Dda3937_00831, 00830, and 00829, which was then ligated into pCH15269 via SpeI/XhoI restriction sites to generate pCH5604. Thioredoxin-TEV-His6-tagged ss-Tli1 and ss-Tli2 were

generated by first amplifying Dda3937_00830 and 00829 with oligo pairs CH5346/CH5631 and CH5348/5117, respectively, then ligated via KpnI/XhoI restriction sites into pCH9764 to yield pCH7024 and pCH7027.

Tle overexpression and purification

Wild-type, Arg185Lys and Lys482Gln lipase domains of Tle^{SMA} were overexpressed from *E. coli* CH2016 cells transformed with pCH4025, pCH4249 and pCH4250, respectively. Cells were co-transformed with pCH4026 for ss-Tli^{SMA} co-expression. The resulting strains were grown in shaking LB cultures until reaching an OD600 of 1.0, after which Tle expression was induced by adding 0.4% L-arabinose to the media. After 60 minutes of L-arabinose induction, Tli expression was induced by adding 1.5 mM IPTG, after which cultures were incubated for another 90 minutes. Cells were pelleted via centrifugation at 6000 RPM for 10 minutes. To purify His6-Tle^{SMA}-Tli^{SMA} complexes, cell pellets were first resuspended in a Tris native lysis buffer (20 mM Tris-HCl pH7.5, 150 mM NaCl, 0.05% Triton X-100, 15 mM imidazole) and incubated with 0.1 mg/mL lysozyme for 15 minutes on ice. Cells were lysed via sonication, after which lysates were clarified via centrifugation at 11000 RPM for 10 minutes at 4°C. The resulting supernatants were incubated with Ni²⁺-NTA resin at 4°C for 90 minutes. The Ni-NTA resin was washed with 5 volumes of native lysis buffer, then samples were eluted in native lysis buffer supplemented with 250 mM imidazole. To isolate His6-Tle^{SMA} by itself, cell pellets were resuspended in denaturing lysis buffer (6M guanidine-HCl, 20 mM Tris-HCl pH 8.0, 15 mM imidazole). Lysates were clarified via centrifugation at 11000 RPM for 10 minutes. The resulting supernatants were incubated with Ni²⁺-NTA resin for 90

minutes. The Ni-NTA resin was washed with 5 volumes of urea lysis buffer (8M urea, 10 mM Tris-HCl pH 8.0), then samples were eluted in urea lysis buffer supplemented with 250 mM imidazole. Tle from *Dickeya dadantii* was overexpressed by itself or with Tli1-Tli2 co-expression from *E. coli* CH2016 cells transformed with pCH5603 or pCH5604, respectively. These strains were grown in shaking LB cultures until reaching an OD600 of 1.0, after which overexpression was induced by adding 1.5 mM IPTG. Cells were harvested after 90 minutes of induction via centrifugation at 11000 RPM for 10 minutes. Tle^{DDA} was purified under denaturing conditions as described above with Tle^{SMA}. Denatured Tle^{SMA} and Tle^{DDA} isolates were refolded by dialysis into a native buffer (20 mM Tris-HCL pH 7.5, 150 mM NaCl).

Tle activity assays

Tle^{SMA} and Tle^{DDA} phospholipase activity was assessed through the hydrolysis of a PEDA1 fluorogenic phospholipid incorporated in liposomes. To prepare liposomes, 1.5 μ M PEDA1 was stirred with 15 μ M dioleoylphosphatidylglycerol (DOPG) and 15 μ M dioleoylphosphatidylcholine in lipase buffer (50 mM Tris-HCl pH7.5, 100 mM NaCl, 1mM CaCl₂) in accordance with the manufacturer's protocol (Invitrogen). Activity assays were performed at room temperature with 600 nM Tle. 750 nM of Tli^{DDA} were used to neutralize Tle^{DDA} reactions. Fluorescence was measured every 4 minutes with 485/535 nm excitation/emission wavelengths using a Molecular Devices SpectraMax M5 plate reader for Tle^{SMA} assays and a PerkinElmer Victor 3V Multilabel Plate Reader for Tle^{DDA} assays. Tween activity assays with Tle^{DDA} were carried out at a Tle concentration of 600 nM in tween esterase buffer (2% tween 80, 20 mM Tris-HCl pH 7.5, 100 mM NaCl, 3 mM CaCl₂); immunity

neutralization reactions were done with the addition of 750 mM Tli. Reactions were incubated at room temperature with constant rotation for 24 hours, after which OD600 values were recorded to measure the accumulation of calcium oleate hydrolysis product.

Tle^{DDA} pull-down assay

Pull-down assays were done with purified His6-Tle^{DDA} and un-tagged Tli isolates. To prepare un-tagged Tli isolates, His6-thioredoxin-TEV-Tli fusion proteins were purified under native conditions (see Overexpression and purification section). TEV protease cleavage was done at a 3:1 substrate-to-protease ratio at 37°C for 4 hours in TEV digestion buffer (20 mM Tris-HCl pH7.5, 150 mM NaCl, 25 mM β -mercaptoethanol). After digestion, samples were mixed with Ni-NTA resin and 15 mM imidazole and incubated for 1 hour at room temperature. Samples were centrifuged to pellet the Ni-NTA resin, and the unbound supernatant was dialyzed in native sodium phosphate buffer (20 mM Sodium phosphate pH7.5, 150 mM NaCl). Purified Tle and Tli samples were mixed at a 1:1 ratio and incubated at 4°C for 15 minutes, after which Ni-NTA and 15 mM imidazole were added to samples and incubation continued for an additional 60 minutes. Ni-NTA resin was washed with 5 volumes of sodium phosphate buffer supplemented with 20 mM imidazole. Washed samples were eluted with urea elution buffer (8M urea, 10 mM Tris-HCl pH 8.0, 250 mM imidazole).

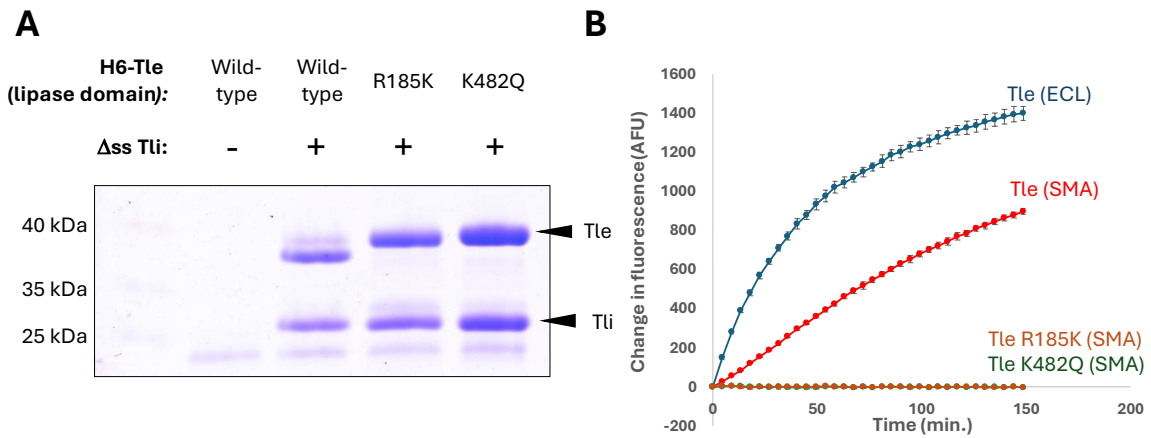


Figure 2 *S. marcescens* Tle requires conserved crosslink residues for activity

A) SDS-PAGE of natively purified His6-tagged lipase domain of Tle from *Serratia marcescens* in absence or presence of cognate Tli co-expression

B) *In vitro* phospholipase A1 assays of indicated *Serratia marcescens* and *Enterobacter cloacae* Tle lipase domain constructs.

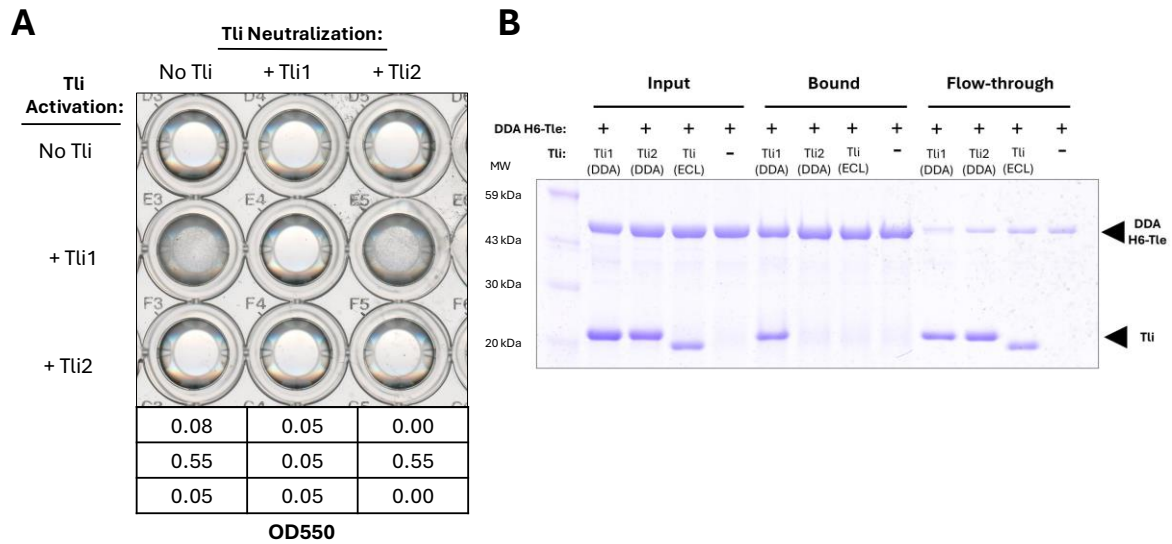


Figure 4 Interaction of Tle^{DDA} with Tli1/Tli2

- A) Tween esterase activity assays with Tle^{DDA} shown in well plate. Row labels indicate Tli co-expression prior to Tle purification, while column labels indicate Tli added to the reaction for activity neutralization. OD550 values of the samples in each well are listed in the table below.
- B) Pull-down assays using His6-Tle^{DDA} bait with various Tli prey. Shown are the input samples taken prior to Ni-NTA binding, bound samples eluted after 5 wash cycles, and flow-through collected from the first wash cycle.

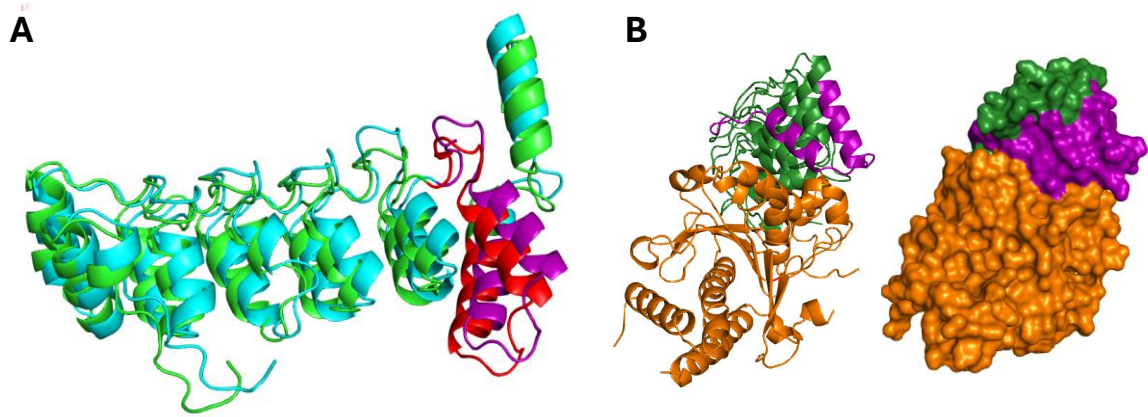


Figure 5 The variable region of *D. dadantii* Tli1/2 maps to the C-terminal pair of α -helices

- A) AlphaFold2 predictions of Tli1 (green) and Tli2 (turquoise) structures. The region of non-conserved residues is labeled in red for Tli1 (Ile196-Leu233) and purple for Tli2 (Val202-Gln239).
- B) Structure of the Tle-Tli complex from *E. cloacae* in cartoon (left) and surface (right) displays. The C-terminal pair of α -helices is labeled in purple.

Table 1 Similarity between Tle^{ECL} and other Tle proteins

Tle Family *	Strain	Tle/Tli Genes	% Identity Tle (ECL)	% Identity Tli (ECL)	Ankyrin domains in Tli?
N/A	<i>Enterobacter hormaechei</i> 34983	LI64_12530 /12525	72.5%	63.6%	Yes
N/A	<i>Cronobacter sakazakii</i> ES15	ES15_3828 /3827	76.0%	72.3%	Yes
N/A	<i>Serratia marcescens</i> Db11	SMDB11_0927 /0928 / 0929	60.4%	56.9% /40.0%	Yes
N/A	<i>Dickeya dadantii</i> 3937	Dda3937_0083 1/00830/00829	32.5%	25.7% /25.3%	Yes
N/A	<i>Geomonas oryzae</i> RG10	KP004_12225/ 12220	27.2%	22.9%	Yes
N/A	<i>Burkholderia cenocepacia</i> J2315	BACL1296 / 1297	44.0%	28.8%	Yes
N/A	<i>Burkholderia glumae</i> BGR1	bglu_2g02560 / 02570	38.8%	30.4%	Yes
t1e1	<i>Burkholderia thailandensis</i> E264	BTH_12698 / 12699 / 126700	0.0%	0.0% /0.0%	No
t1e2	<i>Vibrio cholerae</i> ATCC 39315	VC_1418 / 1419	3.6%	0.00%	No
t1e3	<i>Klebsiella aerogenes</i> KCTC 2190	EAE_15950 / 15955 / 15960	0.0%	3.1% /0.0%	No
t1e4	<i>Photobacterium asymbiotica</i> ATCC43949	PAU_02319 / 02318	7.8%	0.0%	No
t1e5	<i>Pseudomonas aeruginosa</i> PAO1	PA3487/3488	0.00%	7.90%	No

Predicted Tle and Tli proteins from other strains listed with their amino acid sequence percent identity to Tle and Tli from *Enterobacter cloacae* ATCC 13047 (ECL). Strains with two Tli proteins have both percent identity values listed. The presence of predicted ankyrin domains in the Tli protein(s) is indicated. Tle proteins sorted into families by Russell et al. have their Tle family listed *.

Table 2 Bacterial strains

Strain	Description	Reference
X90	<i>E. coli</i> F' <i>lacI^q lac' pro' ara</i> (<i>lac-pro</i>) <i>nal1</i> <i>argE(amb) rif thi-1</i> Rif ^R	
<i>Serratia marcescens</i> Db10 (SMA)	Parental strain of <i>Serratia marcescens</i> Db11	(Flyg et al., 1980)
<i>Dickeya dadantii</i> 3937 (DD)		(Kotoujansky et al., 1985)
CH2016	<i>E. coli</i> X90 (DE3) <i>rna slyD::kan</i> (Kan ^R)	

Table 3 Plasmids

Number	Description	Reference
	pET21P, Amp ^R	Novagen
pCH7620	pCH450:: <i>his6-tle</i> (ECL), Tet ^R	Chapter III
pCH4025	pCH450:: <i>his6-tle</i> (177-) (SMA), Tet ^R	This study
pCH4249	pCH450:: <i>his6-tle</i> (177-) (R185K) (SMA), Tet ^R	This study
pCH4250	pCH450:: <i>his6-tle</i> (177-) (K482Q) (SMA), Tet ^R	This study
pCH4026	pET21p::(<i>sstli</i> (SMA), Amp ^R	This study
pCH15269	pSH21p:: <i>tle</i> (172-472), Amp ^R	Chapter II
pCH5603	pET21p:: <i>His6-tle</i> (DDA), Amp ^R	This study
pCH5604	pET21p:: <i>His6-tle-tli1-tli2</i> (DDA), Amp ^R	This study
pCH9764	pET21p:: <i>his6-trxA-TEV-cysE</i> , Amp ^R	Fernando Garza
pCH7024	pET21p:: <i>his6-trxA-TEV-(ss)tli1</i> (DDA), Amp ^R	This study
pCH7027	pET21p:: <i>his6-trxA-TEV-(ss)tli2</i> (DDA), Amp ^R	This study
pCH7695	pMCSG63:: <i>TEV-(ss)tli</i> (ECL), Tet ^R	Chapter III

Table 4 Oligonucleotides

Number	Description	Sequence	Reference
CH6147	Db11-tle(T177)-Spe-for	5' - TTT <u>ACT AGT ACC</u> AAG GCA GAA CGC TGG CAA GAA C -3'	This study
CH6148	Db11-tle-Xho-rev	5' - TTT <u>CTC GAG</u> TTA TAT TCT TCC CTT GAT TGT GGC AAT GTC ATC GTC -3'	This study
CH6153	Db11-tle(R185K)-Spe-for	5' - TTT <u>ACT AGT ACC</u> AAG GCA GAA CGC TGG CAA GAA AAG CAG TAC CTG ATA G -3'	This study
CH6154	Db11-tle(K482Q)-Xho-rev	5' - TTT <u>CTC GAG</u> TTA TAT TCT TCC CTT GAT TGT GGC AAT GTC ATC GTC ATC GTC TTG TTC ATT TTC AAT -3'	This study
CH6149	Db11-tli1(M24)-Kpn/Nco-for	5' - CGA <u>AGG TAC CAT</u> GGA TTT ACA ACC GCA GG -3'	This study
CH6150	Db11-tli1-Xho-rev	5' - GAG <u>CTC GAG</u> CTA TTG ACT GAC AGG AGC AGG CG -3'	This study
CH5115	3937-tle-Spe-for	5' - TTT <u>ACT AGT</u> ATG CCA GGA GCT GC -3'	This study
CH5116	3937-tle-Xho-rev	5' - TTT <u>CTC GAG</u> TTA TGC CCC CTT AAG CG -3'	This study
CH5117	3937-tli2-Xho-rev	5' - TTT <u>CTC GAG</u> TTA AAG GGA TTC ACC CC -3'	This study
CH5346	3937-tli1-del(ss)-Kpn-for	5'- TTT <u>GGT ACC</u> ATG GCA GGA GGG CAC AG -3'	This study
CH5631	3937-tli1-Xho-rev	5'- TTT <u>CTC GAG</u> TCA AAG CGG CTC TCC -3'	This study
CH5348	3937-tli2-del(ss)-Kpn-for	5'- TTT <u>GGT ACC</u> ATG GTA GGG GGA AGC AGC -3'	This study

Chapter V: Concluding Remarks

Many Gram-negative pathogens and constituents of the human microbiome utilize the type VI secretion system (T6SS) to enhance host colonization or inhibit the growth of competitor species in their environment. In Chapter I, I presented an overview of the research that has built our current understanding of the T6SS. My goal was to contribute to this body of knowledge with the study presented in Chapter II. In this chapter, I investigated the relation between Tle and Tli in *Enterobacter cloacae* and conclude it as a novel instance in which a T6SS effector protein is activated by its cognate immunity protein. When considering the pre-delivery interactions between T6SS effectors and immunities in inhibitor cells, it is uncertain how immunity proteins are reliably excluded from the secreted T6SS payload. The necessary interaction between Tle and Tli prior to secretion implies the existence of a mechanism to separate this, and perhaps other, effector immunity pairs prior to delivery.

Further investigation of Tle, detailed in Chapter III, revealed the nature of its Tli-dependent activation was a reaction with the dicarbonyl compound methylglyoxal that yielded a specific advanced glycation end-product (AGE) crosslink. The current research on AGEs focuses on their deleterious effects on protein structure and determining their link to various degenerative diseases. However, the crosslink activation of Tle goes against the notion that AGEs are solely a form of protein damage and instead demonstrates that they can act as something more akin to post translation modifications. The utilization of an AGE in this manner is likely enabled

by the notably rapid and site-specific nature of Tle glycation compared to the typical formation of AGE adducts. It is not clear how Tle and methylglyoxal react with such speed and precision, as the *in vitro* recreations of this modification required longer durations to achieve lower protein conversion compared to *in vivo* Tle crosslinking. However, further investigations that look at Tle in different glycation environments and compare it with other AGE targets may reveal key factors that permit its unique reactivity methylglyoxal.

In Chapter IV, I showed evidence that Tle homologs from *S. marcescens* and *D. dadantii* also undergo activation via AGE crosslinking. Sequence comparison reveals the conservation of the crosslinked arginine and lysine, along with other nearby charged residues. These conserved residues may not just represent a central motif for the specific AGE formation in Tle, but could also be a motif for targeted AGE formation found in entirely different proteins. This, along with the noted similarities and differences amongst Tle homologs, may help direct bioinformatic and proteomic inquiries into the existence of other AGE-activated proteins.

In conclusion, this investigation of the bacterial phospholipase effector Tle and its cognate immunity protein Tli has yielded new findings that are not just relevant to study of the T6SS, but also bring exciting new ideas to the current perception of advanced glycation end-products.

References

- Adams, P. D., Afonine, P. V, Bunkóczi, G., Chen, V. B., Davis, I. W., Echols, N., Headd, J. J., Hung, L.-W., Kapral, G. J., Grosse-Kunstleve, R. W., McCoy, A. J., Moriarty, N. W., Oeffner, R., Read, R. J., Richardson, D. C., Richardson, J. S., Terwilliger, T. C., & Zwart, P. H. (2010). PHENIX: a comprehensive Python-based system for macromolecular structure solution. *Acta Crystallographica. Section D, Biological Crystallography*, 66(Pt 2), 213–221. <https://doi.org/10.1107/S0907444909052925>
- Ahmed, N., Dobler, D., Dean, M., & Thornalley, P. J. (2005). Peptide mapping identifies hotspot site of modification in human serum albumin by methylglyoxal involved in ligand binding and esterase activity. *The Journal of Biological Chemistry*, 280(7), 5724–5732. <https://doi.org/10.1074/jbc.M410973200>
- Alcoforado Diniz, J., & Coulthurst, S. J. (2015). Intraspecies Competition in *Serratia marcescens* Is Mediated by Type VI-Secreted Rhs Effectors and a Conserved Effector-Associated Accessory Protein. *Journal of Bacteriology*, 197(14), 2350–2360. <https://doi.org/10.1128/JB.00199-15>
- Al-Khodor, S., Price, C. T., Kalia, A., & Abu Kwaik, Y. (2010). Functional diversity of ankyrin repeats in microbial proteins. *Trends in Microbiology*, 18(3), 132–139. <https://doi.org/10.1016/j.tim.2009.11.004>
- Allsopp, L. P., Bernal, P., Nolan, L. M., & Filloux, A. (2020). Causalities of war: The connection between type VI secretion system and microbiota. *Cellular Microbiology*, 22(3), e13153–e13153. <https://doi.org/10.1111/cmi.13153>
- Alteri, C. J., Himpsl, S. D., Pickens, S. R., Lindner, J. R., Zora, J. S., Miller, J. E., Arno, P. D., Straight, S. W., & Mobley, H. L. T. (2013). Multicellular bacteria deploy the type VI secretion system to preemptively strike neighboring cells. *PLoS Pathogens*, 9(9), e1003608–e1003608. <https://doi.org/10.1371/journal.ppat.1003608>
- Alteri, C. J., Himpsl, S. D., Zhu, K., Hershey, H. L., Musili, N., Miller, J. E., & Mobley, H. L. T. (2017). Subtle variation within conserved effector operon gene products contributes to T6SS-mediated killing and immunity. *PLoS Pathogens*, 13(11), e1006729–e1006729. <https://doi.org/10.1371/journal.ppat.1006729>
- Amouroux, C., Lazzaroni, J.-C., & Portalier, R. (1991). Isolation and characterization of extragenic suppressor mutants of the *tolA-876* periplasmic-leaky allele in *Escherichia coli* K-12. *FEMS Microbiology Letters*, 78(2–3), 305–314. <https://doi.org/10.1111/j.1574-6968.1991.tb04461.x>
- Aoki, S. K., Diner, E. J., de Roodenbeke, C. T., Burgess, B. R., Poole, S. J., Braaten, B. A., Jones, A. M., Webb, J. S., Hayes, C. S., Cotter, P. A., & Low, D. A. (2010). A widespread family of polymorphic contact-dependent toxin delivery systems in bacteria. *Nature*, 468(7322), 439–442. <https://doi.org/10.1038/nature09490>

- Aoki, S. K., Pamma, R., Hernday, A. D., Bickham, J. E., Braaten, B. A., & Low, D. A. (2005). Contact-Dependent Inhibition of Growth in *Escherichia coli*. *Science*, *309*(5738), 1245–1248. <https://doi.org/10.1126/science.1115109>
- Aubert, D. F., Xu, H., Yang, J., Shi, X., Gao, W., Li, L., Bisaro, F., Chen, S., Valvano, M. A., & Shao, F. (2016). A Burkholderia Type VI Effector Deamidates Rho GTPases to Activate the Pyrin Inflammasome and Trigger Inflammation. *Cell Host & Microbe*, *19*(5), 664–674. <https://doi.org/10.1016/j.chom.2016.04.004>
- Basler, M. (2015). Type VI secretion system: secretion by a contractile nanomachine. *Philosophical Transactions of the Royal Society of London. Series B, Biological Sciences*, *370*(1679). <https://doi.org/10.1098/rstb.2015.0021>
- Basler, M., Ho, B. T., & Mekalanos, J. J. (2013). Tit-for-tat: type VI secretion system counterattack during bacterial cell-cell interactions. *Cell*, *152*(4), 884–894. <https://doi.org/10.1016/j.cell.2013.01.042>
- Basler, M., Pilhofer, M., Henderson, G. P., Jensen, G. J., & Mekalanos, J. J. (2012). Type VI secretion requires a dynamic contractile phage tail-like structure. *Nature*, *483*(7388), 182–186. <https://doi.org/10.1038/nature10846>
- Beck, C. M., Morse, R. P., Cunningham, D. A., Iniguez, A., Low, D. A., Goulding, C. W., & Hayes, C. S. (2014). CdiA from *Enterobacter cloacae* delivers a toxic ribosomal RNase into target bacteria. *Structure (London, England : 1993)*, *22*(5), 707–718. <https://doi.org/10.1016/j.str.2014.02.012>
- Beckwith, J. R., & Signer, E. R. (1966). Transposition of the lac region of *Escherichia coli*. *Journal of Molecular Biology*, *19*(2), 254–265. [https://doi.org/10.1016/s0022-2836\(66\)80003-7](https://doi.org/10.1016/s0022-2836(66)80003-7)
- Benson, S. A., & Decloux, A. (1985). Isolation and characterization of outer membrane permeability mutants in *Escherichia coli* K-12. *Journal of Bacteriology*, *161*(1), 361–367. <https://doi.org/10.1128/jb.161.1.361-367.1985>
- Benson, S. A., Occi, J. L. L., & Sampson, B. A. (1988). Mutations that alter the pore function of the ompF porin of *Escherichia coli* K12. *Journal of Molecular Biology*, *203*(4), 961–970. [https://doi.org/10.1016/0022-2836\(88\)90121-0](https://doi.org/10.1016/0022-2836(88)90121-0)
- Benz, J., Sendlmeier, C., Barends, T. R. M., & Meinhart, A. (2012). Structural insights into the effector-immunity system Tse1/Tsi1 from *Pseudomonas aeruginosa*. *PloS One*, *7*(7), e40453. <https://doi.org/10.1371/journal.pone.0040453>
- Bergfreund, J., Diener, M., Geue, T., Nussbaum, N., Kummer, N., Bertsch, P., Nyström, G., & Fischer, P. (2021). Globular protein assembly and network formation at fluid interfaces: effect of oil. *Soft Matter*, *17*(6), 1692–1700. <https://doi.org/10.1039/d0sm01870h>
- Bernard, C. S., Brunet, Y. R., Gavioli, M., Llobès, R., & Cascales, E. (2011). Regulation of type VI secretion gene clusters by sigma54 and cognate enhancer binding proteins. *Journal of Bacteriology*, *193*(9), 2158–2167. <https://doi.org/10.1128/JB.00029-11>

- Bernard, C. S., Brunet, Y. R., Gueguen, E., & Cascales, E. (2010). Nooks and crannies in type VI secretion regulation. *Journal of Bacteriology*, *192*(15), 3850–3860. <https://doi.org/10.1128/JB.00370-10>
- Berni, B., Soscia, C., Djermoun, S., Ize, B., & Bleves, S. (2019). A Type VI Secretion System Trans-Kingdom Effector Is Required for the Delivery of a Novel Antibacterial Toxin in *Pseudomonas aeruginosa*. *Frontiers in Microbiology*, *10*, 1218. <https://doi.org/10.3389/fmicb.2019.01218>
- Bilova, T., Paudel, G., Shilyaev, N., Schmidt, R., Brauch, D., Tarakhovskaya, E., Milrud, S., Smolikova, G., Tissier, A., Vogt, T., Sinz, A., Brandt, W., Birkemeyer, C., Wessjohann, L. A., & Frolov, A. (2017). Global proteomic analysis of advanced glycation end products in the Arabidopsis proteome provides evidence for age-related glycation hot spots. *The Journal of Biological Chemistry*, *292*(38), 15758–15776. <https://doi.org/10.1074/jbc.M117.794537>
- Bleves, S., Sana, T. G., & Voulhoux, R. (2014). The target cell genus does not matter. *Trends in Microbiology*, *22*(6), 304–306. <https://doi.org/10.1016/j.tim.2014.04.011>
- Bolivar, F., Rodriguez, R. L., Greene, P. J., Betlach, M. C., Heyneker, H. L., Boyer, H. W., Crosa, J. H., & Falkow, S. (1977). Construction and characterization of new cloning vehicle. II. A multipurpose cloning system. *Gene*, *2*(2), 95–113. [https://doi.org/10.1016/0378-1119\(77\)90000-2](https://doi.org/10.1016/0378-1119(77)90000-2)
- Bönemann, G., Pietrosiuk, A., Diemand, A., Zentgraf, H., & Mogk, A. (2009). Remodelling of VipA/VipB tubules by ClpV-mediated threading is crucial for type VI protein secretion. *The EMBO Journal*, *28*(4), 315–325. <https://doi.org/10.1038/emboj.2008.269>
- Booth, I. R. (2005). Glycerol and Methylglyoxal Metabolism. *EcoSal Plus*, *1*(2). <https://doi.org/10.1128/ecosalplus.3.4.3>
- Bordes, F., Barbe, S., Escalier, P., Mourey, L., André, I., Marty, A., & Tranier, S. (2010). Exploring the conformational states and rearrangements of *Yarrowia lipolytica* Lipase. *Biophysical Journal*, *99*(7), 2225–2234. <https://doi.org/10.1016/j.bpj.2010.07.040>
- Bork, P. (1993). Hundreds of ankyrin-like repeats in functionally diverse proteins: mobile modules that cross phyla horizontally? *Proteins*, *17*(4), 363–374. <https://doi.org/10.1002/prot.340170405>
- Bosch, D. E., Abbasian, R., Parajuli, B., Peterson, S. B., & Mougous, J. D. (2023). Structural disruption of Ntox15 nuclease effector domains by immunity proteins protects against type VI secretion system intoxication in Bacteroidales. *MBio*, *14*(4), e0103923. <https://doi.org/10.1128/mbio.01039-23>
- Boyer, F., Fichant, G., Berthod, J., Vandenbrouck, Y., & Attree, I. (2009). Dissecting the bacterial type VI secretion system by a genome wide in silico analysis: what can be learned from available microbial genomic resources? *BMC Genomics*, *10*, 104. <https://doi.org/10.1186/1471-2164-10-104>

- Brackmann, M., Nazarov, S., Wang, J., & Basler, M. (2017). Using Force to Punch Holes: Mechanics of Contractile Nanomachines. *Trends in Cell Biology*, 27(9), 623–632. <https://doi.org/10.1016/j.tcb.2017.05.003>
- Brady, L., Brzozowski, A. M., Derewenda, Z. S., Dodson, E., Dodson, G., Tolley, S., Turkenburg, J. P., Christiansen, L., Høge-Jensen, B., Nørskov, L., Thim, L., & Menge, U. (1990). A serine protease triad forms the catalytic centre of a triacylglycerol lipase. *Nature*, 343(6260), 767–770. <https://doi.org/10.1038/343767a0>
- Brocca, S., Secundo, F., Ossola, M., Alberghina, L., Carrea, G., & Lotti, M. (2003). Sequence of the lid affects activity and specificity of *Candida rugosa* lipase isoenzymes. *Protein Science*, 12(10), 2312–2319. <https://doi.org/10.1110/ps.0304003>
- Brooks, T. M., Unterweger, D., Bachmann, V., Kostiuik, B., & Pukatzki, S. (2013). Lytic activity of the *Vibrio cholerae* type VI secretion toxin VgrG-3 is inhibited by the antitoxin TsaB. *The Journal of Biological Chemistry*, 288(11), 7618–7625. <https://doi.org/10.1074/jbc.M112.436725>
- Brunet, Y. R., Khodr, A., Logger, L., Aussel, L., Mignot, T., Rimsky, S., & Cascales, E. (2015). H-NS Silencing of the *Salmonella* Pathogenicity Island 6-Encoded Type VI Secretion System Limits *Salmonella enterica* Serovar Typhimurium Interbacterial Killing. *Infection and Immunity*, 83(7), 2738–2750. <https://doi.org/10.1128/IAI.00198-15>
- Brunet, Y. R., Zoued, A., Boyer, F., Douzi, B., & Cascales, E. (2015). The Type VI Secretion TssEFGK-VgrG Phage-Like Baseplate Is Recruited to the TssJLM Membrane Complex via Multiple Contacts and Serves As Assembly Platform for Tail Tube/Sheath Polymerization. *PLoS Genetics*, 11(10), e1005545. <https://doi.org/10.1371/journal.pgen.1005545>
- Brzozowski, A. M., Derewenda, U., Derewenda, Z. S., Dodson, G. G., Lawson, D. M., Turkenburg, J. P., Bjorkling, F., Høge-Jensen, B., Patkar, S. A., & Thim, L. (1991). A model for interfacial activation in lipases from the structure of a fungal lipase-inhibitor complex. *Nature*, 351(6326), 491–494. <https://doi.org/10.1038/351491a0>
- Cambillau, C. (1996). Acyl glycerol hydrolases: inhibitors, interface and catalysis. *Current Opinion in Structural Biology*, 6(4), 449–455. [https://doi.org/10.1016/S0959-440X\(96\)80108-4](https://doi.org/10.1016/S0959-440X(96)80108-4)
- Caro, F., Caro, J. A., Place, N. M., & Mekalanos, J. J. (2020). Transcriptional Silencing by TsrA in the Evolution of Pathogenic *Vibrio cholerae* Biotypes. *MBio*, 11(6), e02901-20. <https://doi.org/10.1128/mBio.02901-20>
- Casabona, M. G., Silverman, J. M., Sall, K. M., Boyer, F., Couté, Y., Poirel, J., Grunwald, D., Mougous, J. D., Elsen, S., & Attree, I. (2013). An ABC transporter and an outer membrane lipoprotein participate in posttranslational activation of type VI secretion in *Pseudomonas aeruginosa*. *Environmental Microbiology*, 15(2), 471–486. <https://doi.org/10.1111/j.1462-2920.2012.02816.x>
- Chaudhuri, J., Bains, Y., Guha, S., Kahn, A., Hall, D., Bose, N., Gugliucci, A., & Kapahi, P. (2018). The Role of Advanced Glycation End Products in Aging and Metabolic Diseases: Bridging

Association and Causality. *Cell Metabolism*, 28(3), 337–352.
<https://doi.org/10.1016/j.cmet.2018.08.014>

- Cherepanov, P. P., & Wackernagel, W. (1995). Gene disruption in *Escherichia coli*: TcR and KmR cassettes with the option of Flp-catalyzed excision of the antibiotic-resistance determinant. *Gene*, 158(1), 9–14. [https://doi.org/10.1016/0378-1119\(95\)00193-a](https://doi.org/10.1016/0378-1119(95)00193-a)
- Cherrak, Y., Flaugnatti, N., Durand, E., Journet, L., & Cascales, E. (2019). Structure and Activity of the Type VI Secretion System. *Microbiology Spectrum*, 7(4).
<https://doi.org/10.1128/microbiolspec.psib-0031-2019>
- Cherrak, Y., Rapisarda, C., Pellarin, R., Bouvier, G., Bardiaux, B., Allain, F., Malosse, C., Rey, M., Chamot-Rooke, J., Cascales, E., Fronzes, R., & Durand, E. (2018). Biogenesis and structure of a type VI secretion baseplate. *Nature Microbiology*, 3(12), 1404–1416.
<https://doi.org/10.1038/s41564-018-0260-1>
- Choi, K.-H., Gaynor, J. B., White, K. G., Lopez, C., Bosio, C. M., Karkhoff-Schweizer, R. R., & Schweizer, H. P. (2005). A Tn7-based broad-range bacterial cloning and expression system. *Nature Methods*, 2(6), 443–448. <https://doi.org/10.1038/nmeth765>
- Choi, K.-H., Mima, T., Casart, Y., Rholl, D., Kumar, A., Beacham, I. R., & Schweizer, H. P. (2008). Genetic tools for select-agent-compliant manipulation of *Burkholderia pseudomallei*. *Applied and Environmental Microbiology*, 74(4), 1064–1075.
<https://doi.org/10.1128/AEM.02430-07>
- Chojnowski, G., Choudhury, K., Heuser, P., Sobolev, E., Pereira, J., Oezugurel, U., & Lamzin, V. S. (2020). The use of local structural similarity of distant homologues for crystallographic model building from a molecular-replacement solution. *Acta Crystallographica. Section D, Structural Biology*, 76(Pt 3), 248–260. <https://doi.org/10.1107/S2059798320000455>
- Cianfanelli, F. R., Alcoforado Diniz, J., Guo, M., De Cesare, V., Trost, M., & Coulthurst, S. J. (2016). VgrG and PAAR Proteins Define Distinct Versions of a Functional Type VI Secretion System. *PLoS Pathogens*, 12(6), e1005735–e1005735.
<https://doi.org/10.1371/journal.ppat.1005735>
- Cianfanelli, F. R., Monlezun, L., & Coulthurst, S. J. (2016). Aim, Load, Fire: The Type VI Secretion System, a Bacterial Nanoweapon. In *Trends in Microbiology* (Vol. 24, Issue 1, pp. 51–62). Elsevier Ltd. <https://doi.org/10.1016/j.tim.2015.10.005>
- Collet, J.-F., Cho, S.-H., Iorga, B. I., & Goemans, C. V. (2020). How the assembly and protection of the bacterial cell envelope depend on cysteine residues. *The Journal of Biological Chemistry*, 295(34), 11984–11994. <https://doi.org/10.1074/jbc.REV120.011201>
- Coulthurst, S. (2019). The Type VI secretion system: A versatile bacterial weapon. *Microbiology (United Kingdom)*, 165(5), 503–515. <https://doi.org/10.1099/mic.0.000789>
- Craig, D. B., & Dombkowski, A. A. (2013). Disulfide by Design 2.0: a web-based tool for disulfide engineering in proteins. *BMC Bioinformatics*, 14, 346. <https://doi.org/10.1186/1471-2105-14-346>

- Derewenda, Z. S., & Sharp, A. M. (1993). News from the interface: the molecular structures of triacylglyceride lipases. *Trends in Biochemical Sciences*, 18(1), 20–25. [https://doi.org/10.1016/0968-0004\(93\)90082-X](https://doi.org/10.1016/0968-0004(93)90082-X)
- Di Luccio, E., Elling, R. A., & Wilson, D. K. (2006). Identification of a novel NADH-specific aldo-keto reductase using sequence and structural homologies. *The Biochemical Journal*, 400(1), 105–114. <https://doi.org/10.1042/BJ20060660>
- Diner, E. J., Beck, C. M., Webb, J. S., Low, D. A., & Hayes, C. S. (2012). Identification of a target cell permissive factor required for contact-dependent growth inhibition (CDI). *Genes & Development*, 26(5), 515–525. <https://doi.org/10.1101/gad.182345.111>
- Donato, S. L., Beck, C. M., Garza-Sánchez, F., Jensen, S. J., Ruhe, Z. C., Cunningham, D. A., Singleton, I., Low, D. A., & Hayes, C. S. (2020). The β -encapsulation cage of rearrangement hotspot (Rhs) effectors is required for type VI secretion. *Proceedings of the National Academy of Sciences of the United States of America*, 117(52), 33540–33548. <https://doi.org/10.1073/pnas.1919350117>
- Dong, H., Xiang, Q., Gu, Y., Wang, Z., Paterson, N. G., Stansfeld, P. J., He, C., Zhang, Y., Wang, W., & Dong, C. (2014). Structural basis for outer membrane lipopolysaccharide insertion. *Nature*, 511(7507), 52–56. <https://doi.org/10.1038/nature13464>
- Dong, T. G., Ho, B. T., Yoder-Himes, D. R., & Mekalanos, J. J. (2013). Identification of T6SS-dependent effector and immunity proteins by Tn-seq in *Vibrio cholerae*. *Proceedings of the National Academy of Sciences*, 110(7), 2623–2628. <https://doi.org/10.1073/pnas.1222783110>
- Douzi, B., Brunet, Y. R., Spinelli, S., Lensi, V., Legrand, P., Blangy, S., Kumar, A., Journet, L., Cascales, E., & Cambillau, C. (2016). Structure and specificity of the Type VI secretion system ClpV-TssC interaction in enteroaggregative Escherichia coli. *Scientific Reports*, 6, 34405. <https://doi.org/10.1038/srep34405>
- Douzi, B., Spinelli, S., Blangy, S., Roussel, A., Durand, E., Brunet, Y. R., Cascales, E., & Cambillau, C. (2014). Crystal structure and self-interaction of the type VI secretion tail-tube protein from enteroaggregative Escherichia coli. *PloS One*, 9(2), e86918. <https://doi.org/10.1371/journal.pone.0086918>
- Durand, E., Cambillau, C., Cascales, E., & Journet, L. (2014). VgrG, Tae, Tle, and beyond: the versatile arsenal of Type VI secretion effectors. *Trends in Microbiology*, 22(9), 498–507. <https://doi.org/10.1016/j.tim.2014.06.004>
- Durand, E., Nguyen, V. S., Zoued, A., Logger, L., Péhau-Arnaudet, G., Aschtgen, M.-S., Spinelli, S., Desmyter, A., Bardiaux, B., Dujeancourt, A., Roussel, A., Cambillau, C., Cascales, E., & Fronzes, R. (2015). Biogenesis and structure of a type VI secretion membrane core complex. *Nature*, 523(7562), 555–560. <https://doi.org/10.1038/nature14667>
- Edwards, R. A., Keller, L. H., & Schifferli, D. M. (1998). Improved allelic exchange vectors and their use to analyze 987P fimbria gene expression. *Gene*, 207(2), 149–157. [https://doi.org/10.1016/s0378-1119\(97\)00619-7](https://doi.org/10.1016/s0378-1119(97)00619-7)

- Emsley, P., & Cowtan, K. (2004). Coot: model-building tools for molecular graphics. *Acta Crystallographica Section D Biological Crystallography*, 60(12), 2126–2132. <https://doi.org/10.1107/s0907444904019158>
- Evans, P. R., & Murshudov, G. N. (2013). How good are my data and what is the resolution? *Acta Crystallographica. Section D, Biological Crystallography*, 69(Pt 7), 1204–1214. <https://doi.org/10.1107/S0907444913000061>
- Eydoux, C., Spinelli, S., Davis, T. L., Walker, J. R., Seitova, A., Dhe-Paganon, S., De Caro, A., Cambillau, C., & Carrière, F. (2008). Structure of human pancreatic lipase-related protein 2 with the lid in an open conformation. *Biochemistry*, 47(36), 9553–9564. <https://doi.org/10.1021/bi8005576>
- Ferrières, L., Hémerly, G., Nham, T., Guérout, A.-M., Mazel, D., Beloin, C., & Ghigo, J.-M. (2010). Silent mischief: bacteriophage Mu insertions contaminate products of Escherichia coli random mutagenesis performed using suicidal transposon delivery plasmids mobilized by broad-host-range RP4 conjugative machinery. *Journal of Bacteriology*, 192(24), 6418–6427. <https://doi.org/10.1128/JB.00621-10>
- Flaugnatti, N., Le, T. T. H., Canaan, S., Aschtgen, M., Nguyen, V. S., Blangy, S., Kellenberger, C., Roussel, A., Cambillau, C., Cascales, E., & Journet, L. (2016). A phospholipase A₁ antibacterial Type VI secretion effector interacts directly with the C-terminal domain of the VgrG spike protein for delivery. *Molecular Microbiology*, 99(6), 1099–1118. <https://doi.org/10.1111/mmi.13292>
- Flaugnatti, N., Rapisarda, C., Rey, M., Beauvois, S. G., Nguyen, V. A., Canaan, S., Durand, E., Chamot-Rooke, J., Cascales, E., Fronzes, R., & Journet, L. (2020). Structural basis for loading and inhibition of a bacterial T6 <scp>SS</scp> phospholipase effector by the VgrG spike. *The EMBO Journal*, 39(11). <https://doi.org/10.15252/embj.2019104129>
- Flyg, C., Kenne, K., & Boman, H. G. (1980). Insect pathogenic properties of Serratia marcescens: phage-resistant mutants with a decreased resistance to Cecropia immunity and a decreased virulence to Drosophila. *Journal of General Microbiology*, 120(1), 173–181. <https://doi.org/10.1099/00221287-120-1-173>
- Gallagher, L. A., Ramage, E., Patrapuvich, R., Weiss, E., Brittnacher, M., & Manoil, C. (2013). Sequence-defined transposon mutant library of Burkholderia thailandensis. *MBio*, 4(6), e00604–e613. <https://doi.org/10.1128/mBio.00604-13>
- Galligan, J. J., Wepy, J. A., Streeter, M. D., Kingsley, P. J., Mitchener, M. M., Wauchope, O. R., Beavers, W. N., Rose, K. L., Wang, T., Spiegel, D. A., & Marnett, L. J. (2018). Methylglyoxal-derived posttranslational arginine modifications are abundant histone marks. *Proceedings of the National Academy of Sciences of the United States of America*, 115(37), 9228–9233. <https://doi.org/10.1073/pnas.1802901115>
- Garza-Sánchez, F., Janssen, B. D., & Hayes, C. S. (2006). Prolyl-tRNA(Pro) in the A-site of SecM-arrested ribosomes inhibits the recruitment of transfer-messenger RNA. *The Journal of Biological Chemistry*, 281(45), 34258–34268. <https://doi.org/10.1074/jbc.M608052200>

- Garza-Sánchez, F., Schaub, R. E., Janssen, B. D., & Hayes, C. S. (2011). tmRNA regulates synthesis of the ArfA ribosome rescue factor. *Molecular Microbiology*, *80*(5), 1204–1219. <https://doi.org/10.1111/j.1365-2958.2011.07638.x>
- Ge, P., Scholl, D., Leiman, P. G., Yu, X., Miller, J. F., & Zhou, Z. H. (2015). Atomic structures of a bactericidal contractile nanotube in its pre- and postcontraction states. *Nature Structural & Molecular Biology*, *22*(5), 377–382. <https://doi.org/10.1038/nsmb.2995>
- Gerc, A. J., Diepold, A., Trunk, K., Porter, M., Rickman, C., Armitage, J. P., Stanley-Wall, N. R., & Coulthurst, S. J. (2015). Visualization of the Serratia Type VI Secretion System Reveals Unprovoked Attacks and Dynamic Assembly. *Cell Reports*, *12*(12), 2131–2142. <https://doi.org/10.1016/j.celrep.2015.08.053>
- Goldin, A., Beckman, J. A., Schmidt, A. M., & Creager, M. A. (2006). Advanced Glycation End Products. *Circulation*, *114*(6), 597–605. <https://doi.org/10.1161/circulationaha.106.621854>
- Gu, Y., Stansfeld, P. J., Zeng, Y., Dong, H., Wang, W., & Dong, C. (2015). Lipopolysaccharide is inserted into the outer membrane through an intramembrane hole, a lumen gate, and the lateral opening of LptD. *Structure (London, England : 1993)*, *23*(3), 496–504. <https://doi.org/10.1016/j.str.2015.01.001>
- Gucinski, G. C., Michalska, K., Garza-Sánchez, F., Eschenfeldt, W. H., Stols, L., Nguyen, J. Y., Goulding, C. W., Joachimiak, A., & Hayes, C. S. (2019). Convergent Evolution of the Barnase/EndoU/Colicin/RelE (BECR) Fold in Antibacterial tRNase Toxins. *Structure (London, England : 1993)*, *27*(11), 1660-1674.e5. <https://doi.org/10.1016/j.str.2019.08.010>
- Hachani, A., Allsopp, L. P., Oduko, Y., & Filloux, A. (2014). The VgrG proteins are “à la carte” delivery systems for bacterial type VI effectors. *The Journal of Biological Chemistry*, *289*(25), 17872–17884. <https://doi.org/10.1074/jbc.M114.563429>
- Hayes, C. S., Bose, B., & Sauer, R. T. (2002). Proline Residues at the C Terminus of Nascent Chains Induce SsrA Tagging during Translation Termination. *Journal of Biological Chemistry*, *277*(37), 33825–33832. <https://doi.org/10.1074/jbc.m205405200>
- Hayes, C. S., & Sauer, R. T. (2003). Cleavage of the A Site mRNA Codon during Ribosome Pausing Provides a Mechanism for Translational Quality Control. *Molecular Cell*, *12*(4), 903–911. [https://doi.org/10.1016/s1097-2765\(03\)00385-x](https://doi.org/10.1016/s1097-2765(03)00385-x)
- Hernandez, R. E., Gallegos-Monterrosa, R., & Coulthurst, S. J. (2020). Type VI secretion system effector proteins: Effective weapons for bacterial competitiveness. *Cellular Microbiology*, *22*(9). <https://doi.org/10.1111/cmi.13241>
- Hespanhol, J. T., Nóbrega-Silva, L., & Bayer-Santos, E. (2023). Regulation of type VI secretion systems at the transcriptional, posttranscriptional and posttranslational level. *Microbiology (Reading, England)*, *169*(8). <https://doi.org/10.1099/mic.0.001376>

- Hipkiss, A. R. (2017). On the Relationship between Energy Metabolism, Proteostasis, Aging and Parkinson's Disease: Possible Causative Role of Methylglyoxal and Alleviative Potential of Carnosine. *Aging and Disease*, 8(3), 334. <https://doi.org/10.14336/ad.2016.1030>
- Holm, L., Laiho, A., Törönen, P., & Salgado, M. (2023). DALI shines a light on remote homologs: One hundred discoveries. *Protein Science : A Publication of the Protein Society*, 32(1), e4519–e4519. <https://doi.org/10.1002/pro.4519>
- Hood, R. D., Singh, P., Hsu, F., Güvener, T., Carl, M. A., Trinidad, R. R. S., Silverman, J. M., Ohlson, B. B., Hicks, K. G., Plemel, R. L., Li, M., Schwarz, S., Wang, W. Y., Merz, A. J., Goodlett, D. R., & Mougous, J. D. (2010). A type VI secretion system of *Pseudomonas aeruginosa* targets a toxin to bacteria. *Cell Host & Microbe*, 7(1), 25–37. <https://doi.org/10.1016/j.chom.2009.12.007>
- Hu, H., Zhang, H., Gao, Z., Wang, D., Liu, G., Xu, J., Lan, K., & Dong, Y. (2014). Structure of the type VI secretion phospholipase effector Tle1 provides insight into its hydrolysis and membrane targeting. *Acta Crystallographica Section D Biological Crystallography*, 70(8), 2175–2185. <https://doi.org/10.1107/s1399004714012899>
- Hu, L., Yu, F., Liu, M., Chen, J., Zong, B., Zhang, Y., Chen, T., Wang, C., Zhang, T., Zhang, J., Zhu, Y., Wang, X., Chen, H., & Tan, C. (2021). RcsB-dependent regulation of type VI secretion system in porcine extra-intestinal pathogenic *Escherichia coli*. *Gene*, 768, 145289. <https://doi.org/10.1016/j.gene.2020.145289>
- Istivan, T. S., & Coloe, P. J. (2006). Phospholipase A in Gram-negative bacteria and its role in pathogenesis. *Microbiology (Reading, England)*, 152(Pt 5), 1263–1274. <https://doi.org/10.1099/mic.0.28609-0>
- Jensen, S. J., Ruhe, Z. C., Williams, A. F., Nhan, D. Q., Garza-Sánchez, F., Low, D. A., & Hayes, C. S. (2023). Paradoxical Activation of a Type VI Secretion System Phospholipase Effector by Its Cognate Immunity Protein. *Journal of Bacteriology*, 205(6), e0011323–e0011323. <https://doi.org/10.1128/jb.00113-23>
- Jiang, F., Wang, X., Wang, B., Chen, L., Zhao, Z., Waterfield, N. R., Yang, G., & Jin, Q. (2016). The *Pseudomonas aeruginosa* Type VI Secretion PGAP1-like Effector Induces Host Autophagy by Activating Endoplasmic Reticulum Stress. *Cell Reports*, 16(6), 1502–1509. <https://doi.org/10.1016/j.celrep.2016.07.012>
- Jiang, F., Waterfield, N. R., Yang, J., Yang, G., & Jin, Q. (2014). A *Pseudomonas aeruginosa* type VI secretion phospholipase D effector targets both prokaryotic and eukaryotic cells. *Cell Host & Microbe*, 15(5), 600–610. <https://doi.org/10.1016/j.chom.2014.04.010>
- Johnson, P. M., Beck, C. M., Morse, R. P., Garza-Sánchez, F., Low, D. A., Hayes, C. S., & Goulding, C. W. (2016). Unraveling the essential role of CysK in CDI toxin activation. *Proceedings of the National Academy of Sciences of the United States of America*, 113(35), 9792–9797. <https://doi.org/10.1073/pnas.1607112113>
- Jones, A. M., Garza-Sánchez, F., So, J., Hayes, C. S., & Low, D. A. (2017). Activation of contact-dependent antibacterial tRNase toxins by translation elongation factors. *Proceedings of*

the National Academy of Sciences of the United States of America, 114(10), E1951–E1957.
<https://doi.org/10.1073/pnas.1619273114>

Jumper, J., Evans, R., Pritzel, A., Green, T., Figurnov, M., Ronneberger, O., Tunyasuvunakool, K., Bates, R., Žídek, A., Potapenko, A., Bridgland, A., Meyer, C., Kohl, S. A. A., Ballard, A. J., Cowie, A., Romera-Paredes, B., Nikolov, S., Jain, R., Adler, J., ... Hassabis, D. (2021). Highly accurate protein structure prediction with AlphaFold. *Nature*, 596(7873), 583–589.
<https://doi.org/10.1038/s41586-021-03819-2>

Kabsch, W. (2010). XDS. *Acta Crystallographica Section D Biological Crystallography*, 66(2), 125–132. <https://doi.org/10.1107/s0907444909047337>

Kapitein, N., Bönemann, G., Pietrosiuk, A., Seyffer, F., Hausser, I., Locker, J. K., & Mogk, A. (2013). ClpV recycles VipA/VipB tubules and prevents non-productive tubule formation to ensure efficient type VI protein secretion. *Molecular Microbiology*, 87(5), 1013–1028.
<https://doi.org/10.1111/mmi.12147>

Khan, F. I., Lan, D., Durrani, R., Huan, W., Zhao, Z., & Wang, Y. (2017). The Lid Domain in Lipases: Structural and Functional Determinant of Enzymatic Properties. *Frontiers in Bioengineering and Biotechnology*, 5. <https://doi.org/10.3389/fbioe.2017.00016>

Kirchberger, P. C., Unterweger, D., Provenzano, D., Pukatzki, S., & Boucher, Y. (2017). Sequential displacement of Type VI Secretion System effector genes leads to evolution of diverse immunity gene arrays in *Vibrio cholerae*. *Scientific Reports*, 7, 45133.
<https://doi.org/10.1038/srep45133>

Ko, J., Kim, I., Yoo, S., Min, B., Kim, K., & Park, C. (2005). Conversion of Methylglyoxal to Acetol by *Escherichia coli* Aldo-Keto Reductases. *Journal of Bacteriology*, 187(16), 5782–5789.
<https://doi.org/10.1128/jb.187.16.5782-5789.2005>

Kold-Christensen, R., & Johannsen, M. (2020). Methylglyoxal Metabolism and Aging-Related Disease: Moving from Correlation toward Causation. *Trends in Endocrinology & Metabolism*, 31(2), 81–92. <https://doi.org/10.1016/j.tem.2019.10.003>

Koskiniemi, S., Garza-Sánchez, F., Edman, N., Chaudhuri, S., Poole, S. J., Manoil, C., Hayes, C. S., & Low, D. A. (2015). Genetic analysis of the CDI pathway from *Burkholderia pseudomallei* 1026b. *PLoS One*, 10(3), e0120265–e0120265.
<https://doi.org/10.1371/journal.pone.0120265>

Koskiniemi, S., Garza-Sánchez, F., Sandegren, L., Webb, J. S., Braaten, B. A., Poole, S. J., Andersson, D. I., Hayes, C. S., & Low, D. A. (2014). Selection of orphan Rhs toxin expression in evolved *Salmonella enterica* serovar Typhimurium. *PLoS Genetics*, 10(3), e1004255–e1004255. <https://doi.org/10.1371/journal.pgen.1004255>

Koskiniemi, S., Lamoureux, J. G., Nikolakakis, K. C., t’Kint de Roodenbeke, C., Kaplan, M. D., Low, D. A., & Hayes, C. S. (2013). Rhs proteins from diverse bacteria mediate intercellular competition. *Proceedings of the National Academy of Sciences of the United States of America*, 110(17), 7032–7037. <https://doi.org/10.1073/pnas.1300627110>

- Kotoujansky, A., Dioloz, A., Boccara, M., Bertheau, Y., Andro, T., & Coleno, A. (1985). Molecular cloning of *Erwinia chrysanthemi* pectinase and cellulase structural genes. *The EMBO Journal*, 4(3), 781–785. <https://doi.org/10.1002/j.1460-2075.1985.tb03697.x>
- Kudryashev, M., Wang, R. Y.-R., Brackmann, M., Scherer, S., Maier, T., Baker, D., DiMaio, F., Stahlberg, H., Egelman, E. H., & Basler, M. (2015). Structure of the type VI secretion system contractile sheath. *Cell*, 160(5), 952–962. <https://doi.org/10.1016/j.cell.2015.01.037>
- Lan, D., Xu, H., Xu, J., Dubin, G., Liu, J., Iqbal Khan, F., & Wang, Y. (2017). Malassezia globosa Mg MDL2 lipase: Crystal structure and rational modification of substrate specificity. *Biochemical and Biophysical Research Communications*, 488(2), 259–265. <https://doi.org/10.1016/j.bbrc.2017.04.103>
- Lazzaroni, J. C., & Portalier, R. C. (1981). Genetic and biochemical characterization of periplasmic-leaky mutants of Escherichia coli K-12. *Journal of Bacteriology*, 145(3), 1351–1358. <https://doi.org/10.1128/jb.145.3.1351-1358.1981>
- Lee, C., Kim, I., Lee, J., Lee, K.-L., Min, B., & Park, C. (2010). Transcriptional Activation of the Aldehyde Reductase YqhD by YqhC and Its Implication in Glyoxal Metabolism of *Escherichia coli*. *Journal of Bacteriology*, 192(16), 4205–4214. <https://doi.org/10.1128/jb.01127-09>
- Lee, C., & Park, C. (2017). Bacterial Responses to Glyoxal and Methylglyoxal: Reactive Electrophilic Species. *International Journal of Molecular Sciences*, 18(1), 169. <https://doi.org/10.3390/ijms18010169>
- Lehman, S. S., Noriea, N. F., Aistleitner, K., Clark, T. R., Dooley, C. A., Nair, V., Kaur, S. J., Rahman, M. S., Gillespie, J. J., Azad, A. F., & Hackstadt, T. (2018). The Rickettsial Ankyrin Repeat Protein 2 Is a Type IV Secreted Effector That Associates with the Endoplasmic Reticulum. *MBio*, 9(3). <https://doi.org/10.1128/mBio.00975-18>
- Leiman, P. G., Basler, M., Ramagopal, U. A., Bonanno, J. B., Sauder, J. M., Pukatzi, S., Burley, S. K., Almo, S. C., & Mekalanos, J. J. (2009). Type VI secretion apparatus and phage tail-associated protein complexes share a common evolutionary origin. *Proceedings of the National Academy of Sciences of the United States of America*, 106(11), 4154–4159. <https://doi.org/10.1073/pnas.0813360106>
- Li, X., Gu, Y., Dong, H., Wang, W., & Dong, C. (2015). Trapped lipopolysaccharide and LptD intermediates reveal lipopolysaccharide translocation steps across the Escherichia coli outer membrane. *Scientific Reports*, 5, 11883. <https://doi.org/10.1038/srep11883>
- Liang, W.-J., Wilson, K. J., Xie, H., Knol, J., Suzuki, S., Rutherford, N. G., Henderson, P. J. F., & Jefferson, R. A. (2005). The gusBC genes of Escherichia coli encode a glucuronide transport system. *Journal of Bacteriology*, 187(7), 2377–2385. <https://doi.org/10.1128/JB.187.7.2377-2385.2005>
- Lopes, J., Gottfried, S., & Rothfield, L. (1972). Leakage of periplasmic enzymes by mutants of Escherichia coli and Salmonella typhimurium: isolation of “periplasmic leaky” mutants. *Journal of Bacteriology*, 109(2), 520–525. <https://doi.org/10.1128/jb.109.2.520-525.1972>

- Lou, Z., Li, M., Sun, Y., Liu, Y., Liu, Z., Wu, W., & Rao, Z. (2010). Crystal structure of a secreted lipase from *Gibberella zeae* reveals a novel “double-lock” mechanism. *Protein & Cell*, *1*(8), 760–770. <https://doi.org/10.1007/s13238-010-0094-y>
- Lu, D., Zheng, Y., Liao, N., Wei, L., Xu, B., Liu, X., & Liu, J. (2014). The structural basis of the Tle4–Tli4 complex reveals the self-protection mechanism of H2-T6SS in *Pseudomonas aeruginosa*. *Acta Crystallographica Section D Biological Crystallography*, *70*(12), 3233–3243. <https://doi.org/10.1107/S1399004714023967>
- Lynch, M., & Conery, J. S. (2000). The evolutionary fate and consequences of duplicate genes. *Science (New York, N.Y.)*, *290*(5494), 1151–1155. <https://doi.org/10.1126/science.290.5494.1151>
- Ma, A. T., McAuley, S., Pukatzki, S., & Mekalanos, J. J. (2009). Translocation of a *Vibrio cholerae* type VI secretion effector requires bacterial endocytosis by host cells. *Cell Host & Microbe*, *5*(3), 234–243. <https://doi.org/10.1016/j.chom.2009.02.005>
- Ma, J., Pan, Z., Huang, J., Sun, M., Lu, C., & Yao, H. (2017). The Hcp proteins fused with diverse extended-toxin domains represent a novel pattern of antibacterial effectors in type VI secretion systems. *Virulence*, *8*(7), 1189–1202. <https://doi.org/10.1080/21505594.2017.1279374>
- Ma, J., Sun, M., Pan, Z., Song, W., Lu, C., & Yao, H. (2018). Three Hcp homologs with divergent extended loop regions exhibit different functions in avian pathogenic *Escherichia coli*. *Emerging Microbes & Infections*, *7*(1), 49. <https://doi.org/10.1038/s41426-018-0042-0>
- Ma, L.-S., Hachani, A., Lin, J.-S., Filloux, A., & Lai, E.-M. (2014). *Agrobacterium tumefaciens* deploys a superfamily of type VI secretion DNase effectors as weapons for interbacterial competition in planta. *Cell Host & Microbe*, *16*(1), 94–104. <https://doi.org/10.1016/j.chom.2014.06.002>
- MacIntyre, D. L., Miyata, S. T., Kitaoka, M., & Pukatzki, S. (2010). The *Vibrio cholerae* type VI secretion system displays antimicrobial properties. *Proceedings of the National Academy of Sciences of the United States of America*, *107*(45), 19520–19524. <https://doi.org/10.1073/pnas.1012931107>
- Majerczyk, C., Brittnacher, M., Jacobs, M., Armour, C. D., Radey, M., Schneider, E., Phattarasokul, S., Bunt, R., & Greenberg, E. P. (2014). Global analysis of the *Burkholderia thailandensis* quorum sensing-controlled regulon. *Journal of Bacteriology*, *196*(7), 1412–1424. <https://doi.org/10.1128/JB.01405-13>
- Majerczyk, C., Schneider, E., & Greenberg, E. P. (2016). Quorum sensing control of Type VI secretion factors restricts the proliferation of quorum-sensing mutants. *ELife*, *5*, e14712. <https://doi.org/10.7554/eLife.14712>
- Mariano, G., Monlezun, L., & Coulthurst, S. J. (2018). Dual Role for DsbA in Attacking and Targeted Bacterial Cells during Type VI Secretion System-Mediated Competition. *Cell Reports*, *22*(3), 774–785. <https://doi.org/10.1016/j.celrep.2017.12.075>

- Michalska, K., Gucinski, G. C., Garza-Sánchez, F., Johnson, P. M., Stols, L. M., Eschenfeldt, W. H., Babnigg, G., Low, D. A., Goulding, C. W., Joachimiak, A., & Hayes, C. S. (2017). Structure of a novel antibacterial toxin that exploits elongation factor Tu to cleave specific transfer RNAs. *Nucleic Acids Research*, *45*(17), 10306–10320. <https://doi.org/10.1093/nar/gkx700>
- Miller, J. H. (1972). *Experiments in molecular genetics*. Cold Spring Harbor Laboratory.
- Monjarás Feria, J., & Valvano, M. A. (2020). An Overview of Anti-Eukaryotic T6SS Effectors. *Frontiers in Cellular and Infection Microbiology*, *10*, 584751. <https://doi.org/10.3389/fcimb.2020.584751>
- Mosavi, L. K., Cammett, T. J., Desrosiers, D. C., & Peng, Z.-Y. (2004). The ankyrin repeat as molecular architecture for protein recognition. *Protein Science : A Publication of the Protein Society*, *13*(6), 1435–1448. <https://doi.org/10.1110/ps.03554604>
- Mougous, J. D., Gifford, C. A., Ramsdell, T. L., & Mekalanos, J. J. (2007). Threonine phosphorylation post-translationally regulates protein secretion in *Pseudomonas aeruginosa*. *Nature Cell Biology*, *9*(7), 797–803. <https://doi.org/10.1038/ncb1605>
- Murakami, M., Taketomi, Y., Sato, H., & Yamamoto, K. (2011). Secreted phospholipase A2 revisited. *Journal of Biochemistry*, *150*(3), 233–255. <https://doi.org/10.1093/jb/mvr088>
- Nazarov, S., Schneider, J. P., Brackmann, M., Goldie, K. N., Stahlberg, H., & Basler, M. (2018). Cryo-EM reconstruction of Type VI secretion system baseplate and sheath distal end. *The EMBO Journal*, *37*(4). <https://doi.org/10.15252/embj.201797103>
- Ostrowski, A., Cianfanelli, F. R., Porter, M., Mariano, G., Peltier, J., Wong, J. J., Swedlow, J. R., Trost, M., & Coulthurst, S. J. (2018). Killing with proficiency: Integrated post-translational regulation of an offensive Type VI secretion system. *PLoS Pathogens*, *14*(7), e1007230. <https://doi.org/10.1371/journal.ppat.1007230>
- Pan, X., Lührmann, A., Satoh, A., Laskowski-Arce, M. A., & Roy, C. R. (2008). Ankyrin repeat proteins comprise a diverse family of bacterial type IV effectors. *Science (New York, N.Y.)*, *320*(5883), 1651–1654. <https://doi.org/10.1126/science.1158160>
- Paradis-Bleau, C., Kritikos, G., Orlova, K., Typas, A., & Bernhardt, T. G. (2014). A genome-wide screen for bacterial envelope biogenesis mutants identifies a novel factor involved in cell wall precursor metabolism. *PLoS Genetics*, *10*(1), e1004056–e1004056. <https://doi.org/10.1371/journal.pgen.1004056>
- Pérez, A., Canle, D., Latasa, C., Poza, M., Beceiro, A., Tomás, M. del M., Fernández, A., Mallo, S., Pérez, S., Molina, F., Villanueva, R., Lasa, I., & Bou, G. (2007). Cloning, nucleotide sequencing, and analysis of the AcrAB-TolC efflux pump of *Enterobacter cloacae* and determination of its involvement in antibiotic resistance in a clinical isolate. *Antimicrobial Agents and Chemotherapy*, *51*(9), 3247–3253. <https://doi.org/10.1128/AAC.00072-07>
- Perkins, B. A., Rabbani, N., Weston, A., Adaikalakoteswari, A., Lee, J. A., Lovblom, L. E., Cardinez, N., & Thornalley, P. J. (2020). High fractional excretion of glycation adducts is

associated with subsequent early decline in renal function in type 1 diabetes. *Scientific Reports*, 10(1), 12709. <https://doi.org/10.1038/s41598-020-69350-y>

- Pietrosiuk, A., Lenherr, E. D., Falk, S., Bönemann, G., Kopp, J., Zentgraf, H., Sinning, I., & Mogk, A. (2011). Molecular basis for the unique role of the AAA+ chaperone ClpV in type VI protein secretion. *The Journal of Biological Chemistry*, 286(34), 30010–30021. <https://doi.org/10.1074/jbc.M111.253377>
- Pissaridou, P., Allsopp, L. P., Wettstadt, S., Howard, S. A., Mavridou, D. A. I., & Filloux, A. (2018). The *Pseudomonas aeruginosa* T6SS-VgrG1b spike is topped by a PAAR protein eliciting DNA damage to bacterial competitors. *Proceedings of the National Academy of Sciences of the United States of America*, 115(49), 12519–12524. <https://doi.org/10.1073/pnas.1814181115>
- Pukatzki, S., Ma, A. T., Revel, A. T., Sturtevant, D., & Mekalanos, J. J. (2007). Type VI secretion system translocates a phage tail spike-like protein into target cells where it cross-links actin. *Proceedings of the National Academy of Sciences of the United States of America*, 104(39), 15508–15513. <https://doi.org/10.1073/pnas.0706532104>
- Pukatzki, S., Ma, A. T., Sturtevant, D., Krastins, B., Sarracino, D., Nelson, W. C., Heidelberg, J. F., & Mekalanos, J. J. (2006). Identification of a conserved bacterial protein secretion system in *Vibrio cholerae* using the *Dictyostelium* host model system. *Proceedings of the National Academy of Sciences of the United States of America*, 103(5), 1528–1533. <https://doi.org/10.1073/pnas.0510322103>
- Qiao, S., Luo, Q., Zhao, Y., Zhang, X. C., & Huang, Y. (2014). Structural basis for lipopolysaccharide insertion in the bacterial outer membrane. *Nature*, 511(7507), 108–111. <https://doi.org/10.1038/nature13484>
- Quentin, D., Ahmad, S., Shanthamoorthy, P., Mougous, J. D., Whitney, J. C., & Raunser, S. (2018). Mechanism of loading and translocation of type VI secretion system effector Tse6. *Nature Microbiology*, 3(10), 1142–1152. <https://doi.org/10.1038/s41564-018-0238-z>
- Rabbani, N., & Thornalley, P. J. (2014). Dicarbonyl proteome and genome damage in metabolic and vascular disease. *Biochemical Society Transactions*, 42(2), 425–432. <https://doi.org/10.1042/bst20140018>
- Rabbani, N., Xue, M., & Thornalley, P. J. (2016). Methylglyoxal-induced dicarbonyl stress in aging and disease: first steps towards glyoxalase 1-based treatments. *Clinical Science*, 130(19), 1677–1696. <https://doi.org/10.1042/cs20160025>
- Reis, P., Holmberg, K., Watzke, H., Leser, M. E., & Miller, R. (2009). Lipases at interfaces: A review. *Advances in Colloid and Interface Science*, 147–148, 237–250. <https://doi.org/10.1016/j.cis.2008.06.001>
- Rojas, C. M., Ham, J. H., Deng, W.-L., Doyle, J. J., & Collmer, A. (2002). HecA, a member of a class of adhesins produced by diverse pathogenic bacteria, contributes to the attachment, aggregation, epidermal cell killing, and virulence phenotypes of *Erwinia chrysanthemi* EC16 on *Nicotiana glauca* seedlings. *Proceedings of the National*

Academy of Sciences of the United States of America, 99(20), 13142–13147.
<https://doi.org/10.1073/pnas.202358699>

- Rojas, C. M., Ham, J. H., Schechter, L. M., Kim, J. F., Beer, S. V., & Collmer, A. (2004). The *Erwinia chrysanthemi* EC16 *hrp/hrc* Gene Cluster Encodes an Active Hrp Type III Secretion System That Is Flanked by Virulence Genes Functionally Unrelated to the Hrp System. *Molecular Plant-Microbe Interactions*[®], 17(6), 644–653. <https://doi.org/10.1094/mpmi.2004.17.6.644>
- Ruhe, Z. C., Low, D. A., & Hayes, C. S. (2020). Polymorphic Toxins and Their Immunity Proteins: Diversity, Evolution, and Mechanisms of Delivery. *Annual Review of Microbiology*, 74, 497–520. <https://doi.org/10.1146/annurev-micro-020518-115638>
- Ruhe, Z. C., Subramanian, P., Song, K., Nguyen, J. Y., Stevens, T. A., Low, D. A., Jensen, G. J., & Hayes, C. S. (2018). Programmed Secretion Arrest and Receptor-Triggered Toxin Export during Antibacterial Contact-Dependent Growth Inhibition. *Cell*, 175(4), 921–933.e14. <https://doi.org/10.1016/j.cell.2018.10.033>
- Ruhe, Z. C., Townsley, L., Wallace, A. B., King, A., Van der Woude, M. W., Low, D. A., Yildiz, F. H., & Hayes, C. S. (2015). CdiA promotes receptor-independent intercellular adhesion. *Molecular Microbiology*, 98(1), 175–192. <https://doi.org/10.1111/mmi.13114>
- Russell, A. B., LeRoux, M., Hathazi, K., Agnello, D. M., Ishikawa, T., Wiggins, P. A., Wai, S. N., & Mougous, J. D. (2013). Diverse type VI secretion phospholipases are functionally plastic antibacterial effectors. *Nature*, 496(7446), 508–512. <https://doi.org/10.1038/nature12074>
- Russell, A. B., Singh, P., Brittnacher, M., Bui, N. K., Hood, R. D., Carl, M. A., Agnello, D. M., Schwarz, S., Goodlett, D. R., Vollmer, W., & Mougous, J. D. (2012). A widespread bacterial type VI secretion effector superfamily identified using a heuristic approach. *Cell Host & Microbe*, 11(5), 538–549. <https://doi.org/10.1016/j.chom.2012.04.007>
- Sampson, B. A., Misra, R., & Benson, S. A. (1989). Identification and characterization of a new gene of *Escherichia coli* K-12 involved in outer membrane permeability. *Genetics*, 122(3), 491–501. <https://doi.org/10.1093/genetics/122.3.491>
- Sana, T. G., Hachani, A., Bucior, I., Soscia, C., Garvis, S., Termine, E., Engel, J., Filloux, A., & Bleves, S. (2012). The second type VI secretion system of *Pseudomonas aeruginosa* strain PAO1 is regulated by quorum sensing and Fur and modulates internalization in epithelial cells. *The Journal of Biological Chemistry*, 287(32), 27095–27105. <https://doi.org/10.1074/jbc.M112.376368>
- Schalkwijk, C. G., & Stehouwer, C. D. A. (2020). Methylglyoxal, a Highly Reactive Dicarbonyl Compound, in Diabetes, Its Vascular Complications, and Other Age-Related Diseases. *Physiological Reviews*, 100(1), 407–461. <https://doi.org/10.1152/physrev.00001.2019>
- Shneider, M. M., Buth, S. A., Ho, B. T., Basler, M., Mekalanos, J. J., & Leiman, P. G. (2013). PAAR-repeat proteins sharpen and diversify the type VI secretion system spike. *Nature*, 500(7462), 350–353. <https://doi.org/10.1038/nature12453>

- Sibbersen, C., & Johannsen, M. (2020). Dicarbonyl derived post-translational modifications: chemistry bridging biology and aging-related disease. *Essays in Biochemistry*, 64(1), 97–110. <https://doi.org/10.1042/ebc20190057>
- Silverman, J. M., Agnello, D. M., Zheng, H., Andrews, B. T., Li, M., Catalano, C. E., Gonen, T., & Mougous, J. D. (2013). Haemolysin coregulated protein is an exported receptor and chaperone of type VI secretion substrates. *Molecular Cell*, 51(5), 584–593. <https://doi.org/10.1016/j.molcel.2013.07.025>
- Singh, R. P., & Kumari, K. (2023). Bacterial type VI secretion system (T6SS): an evolved molecular weapon with diverse functionality. *Biotechnology Letters*, 45(3), 309–331. <https://doi.org/10.1007/s10529-023-03354-2>
- Skubák, P., Araç, D., Bowler, M. W., Correia, A. R., Hoelz, A., Larsen, S., Leonard, G. A., McCarthy, A. A., McSweeney, S., Mueller-Dieckmann, C., Otten, H., Salzman, G., & Pannu, N. S. (2018). A new MR-SAD algorithm for the automatic building of protein models from low-resolution X-ray data and a poor starting model. *IUCr*, 5(2), 166–171. <https://doi.org/10.1107/s2052252517017961>
- Speare, L., Woo, M., Bultman, K. M., Mandel, M. J., Wollenberg, M. S., & Septer, A. N. (2021). Host-Like Conditions Are Required for T6SS-Mediated Competition among *Vibrio fischeri* Light Organ Symbionts. *MSphere*, 6(4), e0128820. <https://doi.org/10.1128/mSphere.01288-20>
- Storey, D., McNally, A., Åstrand, M., Sa-Pessoa Graca Santos, J., Rodriguez-Escudero, I., Elmore, B., Palacios, L., Marshall, H., Hobley, L., Molina, M., Cid, V. J., Salminen, T. A., & Bengoechea, J. A. (2020). *Klebsiella pneumoniae* type VI secretion system-mediated microbial competition is PhoPQ controlled and reactive oxygen species dependent. *PLoS Pathogens*, 16(3), e1007969–e1007969. <https://doi.org/10.1371/journal.ppat.1007969>
- Subedi, K. P., Choi, D., Kim, I., Min, B., & Park, C. (2011). Hsp31 of *Escherichia coli* K-12 is glyoxalase III. *Molecular Microbiology*, 81(4), 926–936. <https://doi.org/10.1111/j.1365-2958.2011.07736.x>
- Taylor, N. M. I., Prokhorov, N. S., Guerrero-Ferreira, R. C., Shneider, M. M., Browning, C., Goldie, K. N., Stahlberg, H., & Leiman, P. G. (2016). Structure of the T4 baseplate and its function in triggering sheath contraction. *Nature*, 533(7603), 346–352. <https://doi.org/10.1038/nature17971>
- Terwilliger, T. C., Grosse-Kunstleve, R. W., Afonine, P. V, Moriarty, N. W., Zwart, P. H., Hung, L.-W., Read, R. J., & Adams, P. D. (2007). Iterative model building, structure refinement and density modification with the *PHENIX AutoBuild*wizard. *Acta Crystallographica Section D Biological Crystallography*, 64(1), 61–69. <https://doi.org/10.1107/s090744490705024x>
- Thornalley, P. J. (2003). Use of aminoguanidine (Pimagedine) to prevent the formation of advanced glycation endproducts. *Archives of Biochemistry and Biophysics*, 419(1), 31–40. <https://doi.org/10.1016/j.abb.2003.08.013>

- Ting, S.-Y., Bosch, D. E., Mangiameli, S. M., Radey, M. C., Huang, S., Park, Y.-J., Kelly, K. A., Filip, S. K., Goo, Y. A., Eng, J. K., Allaire, M., Veessler, D., Wiggins, P. A., Peterson, S. B., & Mougous, J. D. (2018). Bifunctional Immunity Proteins Protect Bacteria against FtsZ-Targeting ADP-Ribosylating Toxins. *Cell*, *175*(5), 1380-1392.e14. <https://doi.org/10.1016/j.cell.2018.09.037>
- Wäneskog, M., Halvorsen, T., Filek, K., Xu, F., Hammarlöf, D. L., Hayes, C. S., Braaten, B. A., Low, D. A., Poole, S. J., & Koskiniemi, S. (2021). Escherichia coli EC93 deploys two plasmid-encoded class I contact-dependent growth inhibition systems for antagonistic bacterial interactions. *Microbial Genomics*, *7*(3), mgen000534. <https://doi.org/10.1099/mgen.0.000534>
- Wang, J., Brackmann, M., Castaño-Díez, D., Kudryashev, M., Goldie, K. N., Maier, T., Stahlberg, H., & Basler, M. (2017). Cryo-EM structure of the extended type VI secretion system sheath-tube complex. *Nature Microbiology*, *2*(11), 1507–1512. <https://doi.org/10.1038/s41564-017-0020-7>
- Wang, J., Yashiro, Y., Sakaguchi, Y., Suzuki, T., & Tomita, K. (2022). Mechanistic insights into tRNA cleavage by a contact-dependent growth inhibitor protein and translation factors. *Nucleic Acids Research*, *50*(8), 4713–4731. <https://doi.org/10.1093/nar/gkac228>
- Wang, L., & Wang, C. (2023). Oxidative protein folding fidelity and redox-taxis in the endoplasmic reticulum. *Trends in Biochemical Sciences*, *48*(1), 40–52. <https://doi.org/10.1016/j.tibs.2022.06.011>
- Wang, Q., Zhong, C., & Xiao, H. (2020). Genetic Engineering of Filamentous Fungi for Efficient Protein Expression and Secretion. *Frontiers in Bioengineering and Biotechnology*, *8*, 293. <https://doi.org/10.3389/fbioe.2020.00293>
- Weigand, R. A., & Rothfield, L. I. (1976). Genetic and physiological classification of periplasmic-leaky mutants of Salmonella typhimurium. *Journal of Bacteriology*, *125*(1), 340–345. <https://doi.org/10.1128/jb.125.1.340-345.1976>
- Whitney, J. C., Beck, C. M., Goo, Y. A., Russell, A. B., Harding, B. N., De Leon, J. A., Cunningham, D. A., Tran, B. Q., Low, D. A., Goodlett, D. R., Hayes, C. S., & Mougous, J. D. (2014). Genetically distinct pathways guide effector export through the type VI secretion system. *Molecular Microbiology*, *92*(3), 529–542. <https://doi.org/10.1111/mmi.12571>
- Whitney, J. C., Chou, S., Russell, A. B., Biboy, J., Gardiner, T. E., Ferrin, M. A., Brittnacher, M., Vollmer, W., & Mougous, J. D. (2013). Identification, structure, and function of a novel type VI secretion peptidoglycan glycoside hydrolase effector-immunity pair. *The Journal of Biological Chemistry*, *288*(37), 26616–26624. <https://doi.org/10.1074/jbc.M113.488320>
- Whitney, J. C., Quentin, D., Sawai, S., LeRoux, M., Harding, B. N., Ledvina, H. E., Tran, B. Q., Robinson, H., Goo, Y. A., Goodlett, D. R., Raunser, S., & Mougous, J. D. (2015). An interbacterial NAD(P)(+) glycohydrolase toxin requires elongation factor Tu for delivery to target cells. *Cell*, *163*(3), 607–619. <https://doi.org/10.1016/j.cell.2015.09.027>

- Yang, Y., & Lowe, M. E. (2000). The open lid mediates pancreatic lipase function. *Journal of Lipid Research*, 41(1), 48–57.
- Zarzycki-Siek, J., Norris, M. H., Kang, Y., Sun, Z., Bluhm, A. P., McMillan, I. A., & Hoang, T. T. (2013). Elucidating the *Pseudomonas aeruginosa* fatty acid degradation pathway: identification of additional fatty acyl-CoA synthetase homologues. *PloS One*, 8(5), e64554–e64554. <https://doi.org/10.1371/journal.pone.0064554>
- Zhai, J. li, Day, L., Aguilar, M.-I., & Wooster, T. J. (2013). Protein folding at emulsion oil/water interfaces. *Current Opinion in Colloid & Interface Science*, 18(4), 257–271. <https://doi.org/10.1016/j.cocis.2013.03.002>
- Zhang, D., de Souza, R. F., Anantharaman, V., Iyer, L. M., & Aravind, L. (2012). Polymorphic toxin systems: Comprehensive characterization of trafficking modes, processing, mechanisms of action, immunity and ecology using comparative genomics. *Biology Direct*, 7, 18. <https://doi.org/10.1186/1745-6150-7-18>
- Zhang, H., Zhang, H., Gao, Z.-Q., Wang, W.-J., Liu, G.-F., Xu, J.-H., Su, X.-D., & Dong, Y.-H. (2013). Structure of the type VI effector-immunity complex (Tae4-Tai4) provides novel insights into the inhibition mechanism of the effector by its immunity protein. *The Journal of Biological Chemistry*, 288(8), 5928–5939. <https://doi.org/10.1074/jbc.M112.434357>
- Zhang, M., Yu, X.-W., Xu, Y., Guo, R.-T., Swapna, G. V. T., Szyperski, T., Hunt, J. F., & Montelione, G. T. (2019). Structural Basis by Which the N-Terminal Polypeptide Segment of *Rhizopus chinensis* Lipase Regulates Its Substrate Binding Affinity. *Biochemistry*, 58(38), 3943–3954. <https://doi.org/10.1021/acs.biochem.9b00462>
- Zheng, J., Shin, O. S., Cameron, D. E., & Mekalanos, J. J. (2010). Quorum sensing and a global regulator TsrA control expression of type VI secretion and virulence in *Vibrio cholerae*. *Proceedings of the National Academy of Sciences of the United States of America*, 107(49), 21128–21133. <https://doi.org/10.1073/pnas.1014998107>
- Zoued, A., Durand, E., Brunet, Y. R., Spinelli, S., Douzi, B., Guzzo, M., Flaugnatti, N., Legrand, P., Journet, L., Fronzes, R., Mignot, T., Cambillau, C., & Cascales, E. (2016). Priming and polymerization of a bacterial contractile tail structure. *Nature*, 531(7592), 59–63. <https://doi.org/10.1038/nature17182>